

Dissertation zur Erlangung des Doktorgrades  
der Fakultät für Chemie und Pharmazie  
der Ludwig-Maximilians-Universität München



**New insights into signaling pathways of  
salicylate and metalloporphyrins**

**Signe Birgitta Blumenthal**

aus München

2005



Erklärung:

Diese Dissertation wurde im Sinne von §13 Abs. 3 bzw. 4 der Promotionsordnung vom 29. Januar 1998 von Prof. Dr. Alexandra K. Kiemer und Prof. Dr. Angelika M. Vollmar betreut.

Ehrenwörtliche Versicherung:

Diese Dissertation wurde selbstständig, ohne unerlaubte Hilfe erarbeitet.

München, 22.03.2005

---

(Signe B. Blumenthal)

Dissertation eingereicht am: 22.03.2005

1. Gutachter: Frau Prof. Dr. Angelika M. Vollmar

2. Gutachter: Herr Prof. Dr. Ernst Wagner

Mündliche Prüfung am: 03.05.2005



dedicated to my family



**1 CONTENTS**



---

<b>1</b>	<b>CONTENTS</b>	<b>I</b>
<b>2</b>	<b>INTRODUCTION</b>	<b>1</b>
<b>2.1</b>	<b>Inflammation</b>	<b>3</b>
<b>2.2</b>	<b>Aim of the study</b>	<b>4</b>
2.2.1	Salicylates and HO-1	4
2.2.2	Metalloporphyrins and caspases	4
<b>2.3</b>	<b>The endothelium</b>	<b>5</b>
<b>2.4</b>	<b>Adhesion molecules</b>	<b>5</b>
2.4.1	Selectins	7
2.4.2	P-selectin in chronic inflammation	8
<b>2.5</b>	<b>Interleukin-4 in chronic inflammation</b>	<b>9</b>
<b>2.6</b>	<b>The heme oxygenase-1</b>	<b>10</b>
2.6.1	The heme oxygenase system	10
2.6.2	Functions of the HO-1 system	13
<b>2.7</b>	<b>Salicylates</b>	<b>14</b>
<b>2.8</b>	<b>Metalloporphyrins</b>	<b>16</b>
<b>2.9</b>	<b>Apoptosis</b>	<b>17</b>
2.9.1	Caspases	19
<b>3</b>	<b>MATERIALS AND METHODS</b>	<b>21</b>
<b>3.1</b>	<b>Materials</b>	<b>23</b>
<b>3.2</b>	<b>Cell culture</b>	<b>24</b>
3.2.1	Primary cells	24
3.2.2	Cell lines	25
3.2.2.1	Jurkat T-lymphocytes	25
3.2.2.2	Human embryonic kidney cell line 293	26
<b>3.3</b>	<b>Animal model</b>	<b>27</b>
3.3.1	Animals	27
3.3.2	Dosage and application routes	27
<b>3.4</b>	<b>Real-time RT-PCR</b>	<b>28</b>

3.4.1	Isolation of total RNA	28
3.4.2	Reverse Transcription	29
3.4.3	Real-time PCR with TaqMan <sup>®</sup> probes	29
<b>3.5</b>	<b>Western blot analysis</b>	<b>31</b>
<b>3.6</b>	<b>Electrophoretic mobility shift assay (EMSA)</b>	<b>34</b>
3.6.1	Extraction of nuclear protein	34
3.6.2	Radioactive labeling of oligonucleotides	35
3.6.3	Binding reaction and electrophoretic separation	36
<b>3.7</b>	<b>Transfection of cells</b>	<b>37</b>
3.7.1	Plasmids	37
3.7.2	Antisense oligonucleotides	38
3.7.3	AP-1 decoy	39
<b>3.8</b>	<b>Reporter gene assay</b>	<b>40</b>
3.8.1	Transfection of HEK 293 cells	40
3.8.2	Luciferase reporter assay	40
<b>3.9</b>	<b>Measurement of caspase activity</b>	<b>41</b>
3.9.1	Caspase-3-like activity	42
3.9.2	Caspase-8-like activity	43
3.9.3	Activity of recombinant caspases	43
<b>3.10</b>	<b>Microscopy</b>	<b>44</b>
3.10.1	Light Microscopy	44
3.10.2	Confocal Laser Scanning Microscopy (CLSM)	44
<b>3.11</b>	<b>Molecular modeling studies</b>	<b>45</b>
<b>3.12</b>	<b>High performance liquid chromatography</b>	<b>47</b>
<b>3.13</b>	<b>Statistical analysis</b>	<b>48</b>
<b>4</b>	<b>RESULTS</b>	<b>49</b>
<b>4.1</b>	<b>Salicylates and HO-1</b>	<b>51</b>
4.1.1	Effect of sodium salicylate on IL-4-induced P-selectin	51
4.1.1.1	Induction of P-selectin by IL-4 independent of NF- $\kappa$ B	51
4.1.1.2	Role of heme oxygenase-1	52

---

4.1.2	HO-1 induction by sodium salicylate	53
4.1.3	HO-1 induction by JNK and AP-1	54
4.1.3.1	Activation of AP-1 by sodium salicylate	54
4.1.3.2	Effect of sodium salicylate on JNK/SAPK	55
<b>4.2</b>	<b>Metalloporphyrins and caspases</b>	<b>57</b>
4.2.1	Porphyryns inhibit caspase-3-like activity	57
4.2.2	Metalloporphyrins inhibit PARP-cleavage	60
4.2.3	Porphyryns inhibit caspase-3-like activity <i>in vivo</i>	61
4.2.4	Porphyryns are direct caspase-3-inhibitors	62
4.2.5	Characterization of the inhibitory action on caspase-3	64
4.2.6	Caspase-3-processing is inhibited by porphyryns	66
4.2.7	Porphyryns inhibit caspase-8-activity	66
4.2.8	Morphologic alterations	68
4.2.9	Molecular modeling studies	69
<b>4.3</b>	<b>TNF-<math>\alpha</math>-induced p38 MAPK and NF-<math>\kappa</math>B activation</b>	<b>71</b>
<b>5</b>	<b>DISCUSSION</b>	<b>73</b>
<b>5.1</b>	<b>Salicylates and HO-1</b>	<b>75</b>
5.1.1	Effect of sodium salicylate on IL-4-induced P-selectin	75
5.1.1.1	Induction of P-selectin by IL-4 independent of NF- $\kappa$ B	75
5.1.1.2	Role of heme oxygenase-1	76
5.1.1.3	Alternative signaling pathways	77
5.1.2	HO-1 induction by sodium salicylate	77
5.1.3	HO-1 induction by JNK and AP-1	78
5.1.3.1	Activation of AP-1 by sodium salicylate	79
5.1.3.2	Effects of sodium salicylate on JNK/SAPK	80
<b>5.2</b>	<b>Metalloporphyrins and caspases</b>	<b>81</b>
5.2.1	Characterization of the inhibitory action	81
5.2.2	Metalloporphyrins as a new class of caspase-inhibitors	82
5.2.3	Physiological relevance	83
5.2.4	HO-independent effects of metalloporphyrins	84

<b>6</b>	<b>SUMMARY</b>	<b>87</b>
6.1	Salicylates and HO-1	89
6.2	Metalloporphyrins and caspases	90
<b>7</b>	<b>BIBLIOGRAPHY</b>	<b>91</b>
<b>8</b>	<b>APPENDIX</b>	<b>107</b>
8.1	Abbreviations	109
8.2	Alphabetical order of companies	113
8.3	Publications	115
8.3.1	Poster presentations	115
8.3.2	Original Publications	115
8.4	Curriculum Vitae	117
8.5	Acknowledgements	119

## 2 INTRODUCTION



## 2.1 Inflammation

Various exogenous and endogenous stimuli can cause cell injury. These stimuli provoke a complex reaction in the vascularized connective tissue called inflammation. Characteristic for any inflammatory process is the reaction of the blood vessels, leading to the accumulation of fluid and leukocytes in extravascular tissue (Cotran *et al.*; 1999).

Inflammation can be divided into acute and chronic forms. Characteristic for an acute progression is the relatively short duration, the exudation of fluid and plasma, and the emigration of leukocytes, predominantly neutrophils. It is the immediate and early response of the organism to an injurious agent. Chronic inflammation is of longer duration and associated with the presence of lymphocytes and macrophages, the proliferation of vascular cells, and tissue necrosis. It develops under persistent infections of certain microorganisms, prolonged exposure to potentially toxic agents, or under certain conditions when immune reactions are set up against the individual's own tissues (autoimmunity) (Cotran *et al.*; 1999).

Basically, inflammation is a protective response to injury aiming to destroy the injurious agent and to simultaneously heal and repair the damaged tissue. However, inflammation and repair may be potentially harmful and are the basis of some common chronic diseases, such as rheumatoid arthritis, atherosclerosis, and lung fibrosis. Thus, it is important to learn about the underlying signaling pathways and to find new targets or ways to control pathological processes of inflammation (Cotran *et al.*; 1999).

During inflammation, specific combinations of cell surface proteins (i.e. adhesion molecules) and certain soluble factors such as cytokines, regulate leukocyte recruitment into extravascular tissues at the site of injury. This is a critical step for the immune response and the repair of damaged tissue. Conversely, uncontrolled extravasation of leukocytes leads to inflammatory disorders (Springer, 1995).

## **2.2 Aim of the study**

### **2.2.1 Salicylates and HO-1**

The adhesion molecule P-selectin has been shown to be a major determinant of inflammatory responses. Different pharmacological agents including salicylate, the active metabolite of acetylsalicylic acid (ASA), have been shown to inhibit IL-4-induced P-selectin expression in endothelial cells. Mechanisms responsible for P-selectin inhibition, however, are as yet not very well known. In the present work we confirmed this finding and aimed to elucidate the events leading to this inhibition.

In the recent past, there has been accumulating evidence that the rate-limiting enzyme in the degradation of heme, heme oxygenase-1 (HO-1) has anti-inflammatory features. Several mechanisms have been postulated which lead to a reduced immune response including the influence on several adhesion molecules such as P-selectin. In accordance with the anti-inflammatory potential of HO-1 we have recently found that ASA induces HO-1 in endothelial cells (Bildner, 2002). This led to the hypothesis that the inhibition of IL-4-induced P-selectin expression by NaSal is mediated *via* an induced HO-1 expression. In the first part of the present work we aimed to prove this hypothesis and tried to clarify the underlying signaling pathway leading to HO-1 induction by NaSal.

### **2.2.2 Metalloporphyrins and caspases**

Apart from the beneficial effects of HO-1 on inflammatory processes, HO-1 is known to provoke anti-apoptotic effects (Maines, 1997). Metalloporphyrins are heme-analogous and are thus able to inhibit the activity of the heme-converting enzyme HO-1. Therefore, they are widely used and accepted tools in research investigating functional aspects of HO-1. In studies concerning the anti-apoptotic features of HO-1, different metalloporphyrins are often employed to either stimulate HO-1-expression or inhibit its activity (Dorman *et al.*; 2004; Sass *et al.*; 2003; Zhang *et al.*; 2004).

Apoptotic cell death is then quantified with various assay methods, such as the measurement of caspase-3-like activity. In an approach to determine potential anti-apoptotic features of ASA-induced HO-1 we observed contradictory results in a respective experimental setting. This led to the hypothesis that metalloporphyrins exert actions other than their well-known HO-1-dependent effects. Therefore, the second part of this work deals with the specificity of metalloporphyrins. Aim of the study was to find the cause for these contradictory results and further investigate a potential effect of the metalloporphyrins on caspase activity.

## **2.3 The endothelium**

The endothelium has an important function in the initial steps of inflammation. In the past, it was considered to be a non-reactive barrier between blood and tissue with its primary function to tightly regulate permeability of the vessel wall in the circulatory system. However, in the recent years it has become obvious that endothelial cells (ECs) are by no means inert. As a gate-keeper between the vessel lumen and the surrounding tissue, they regulate the transfer of small and large molecules, and exert autocrine, paracrine, and endocrine actions on smooth muscle cells and platelets, thereby regulating the vascular tone and coagulation (Cines *et al.*; 1998; Galley *et al.*; 2004). ECs also regulate leukocyte movement into tissues *via* a carefully regulated process involving adhesion molecules that mediate the attachment of leukocytes to the endothelium by binding to specific ligands as well as the process of transmigration (Muller, 2003). Therefore, the endothelium represents a prominent target for numerous inflammatory stimuli released during several inflammatory diseases which demonstrates its important role in inflammatory processes.

## **2.4 Adhesion molecules**

The process of leukocyte infiltration into the inflamed tissue involves several steps including (1) tethering of the immune cell to the vessel wall, (2) rolling, the initial formation of usually reversible

attachments, (3) activation of attached cells and development of stronger, shear-resistant adhesion (sticking), and (4) spreading and migration across the endothelium (diapedesis) (**figure 1**). Each of these steps appears to be necessary for effective leukocyte recruitment, because blocking any of the four can severely reduce leukocyte accumulation in the tissue (Cines *et al.*; 1998).

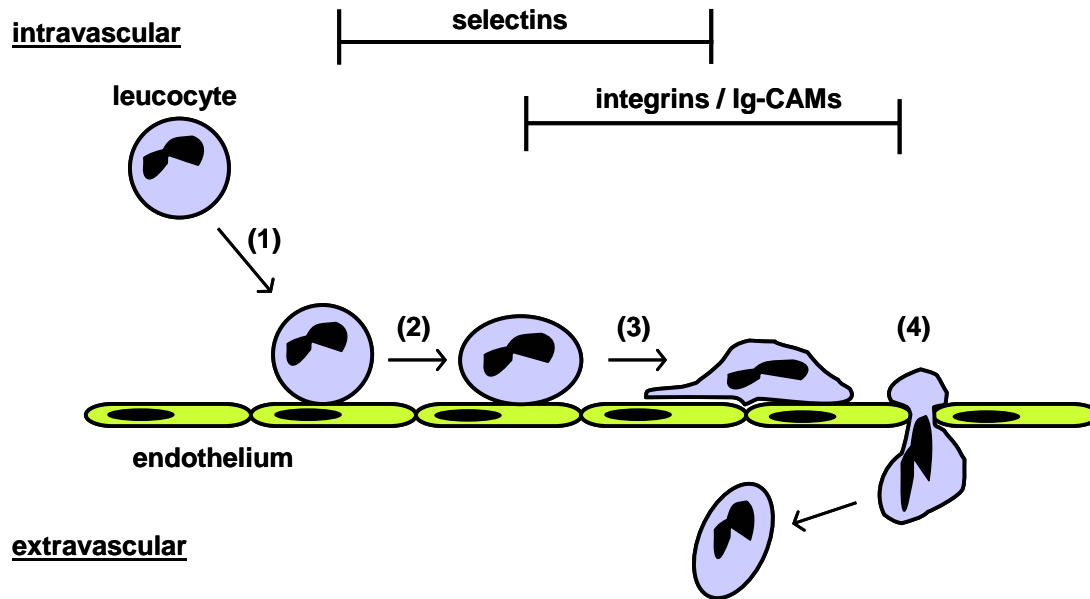


**figure 1: Recruitment of leukocytes to sites of inflammation.** Leukocyte adhesion is a cascade of adhesion and activation events that ends with extravasation of the leukocyte, whereby the cell exerts its effects on the inflamed site. At least four steps are involved: (1) capture (tethering) and (2) rolling of the leukocyte, in which selectins and glyco-conjugated selectin-ligands are involved, (3) activation by chemokines and firm adhesion to the endothelium (sticking), followed by (4) transmigration (diapedesis), both mediated by integrins and immunoglobulin-like cell adhesion molecules (Ig-CAM). Adapted from Cines *et al.* (1998).

Those steps are regulated by different families of cell adhesion molecules, such as selectins, immunoglobulin-like cell adhesion molecules (Ig-CAM), integrins, and cadherins, expressed on endothelial cells and leukocytes. Amongst other things they mediate the binding to counter-receptors on other cells. Specific combinations of chemoattractants and adhesion molecules may control the onset and duration of leukocyte recruitment, as well as the type of leukocytes that are mobilized during acute, chronic, or allergic inflammation. The different inflammatory stimuli activate ECs to express a specific pattern of cell adhesion molecules and chemokines that physically engage circulating leukocytes and promote their adhesion to the vessel wall. Adhesion molecules present on ECs are members of the selectin family, E-selectin and P-selectin, and the Ig-CAMs

intercellular adhesion molecule-1 (ICAM-1) and vascular cell adhesion molecule-1 (VCAM-1). The selectins allow the cells to tether and roll on the vessel wall and the Ig family members subsequently bind to integrins on the leukocyte surface and cause the firm adhesion of the cell (Aplin *et al.*; 1998).

### 2.4.1 Selectins

The selectins mediate the initial tethering and rolling of leukocytes and are essential adhesion molecules for the development of inflammation. They form a family of three lectin-like adhesion receptors composed of three members, L-, E-, and P-selectin (Aplin *et al.*; 1998; Springer, 1995). The structure of a selectin includes an amino-terminal domain that is homologous to calcium-dependent lectins, followed by an epidermal growth factor (EGF)-type domain, two to nine complement regulatory protein repeats, a transmembrane helical segment, and a short cytoplasmic tail (figure 2).

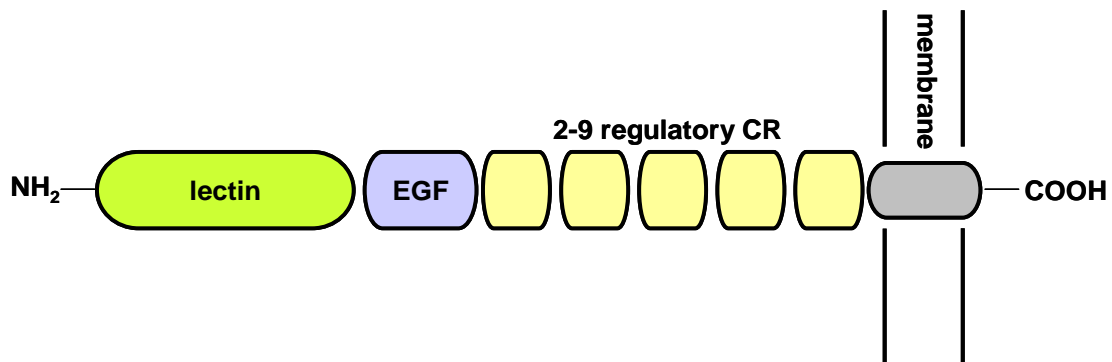


**figure 2:** **Structure of the selectins.** Selectins contain an N-terminal extracellular domain with structural homology to calcium-dependent lectins, followed by a domain homologous to epidermal growth factor (EGF), and two to nine consensus repeats (CR) similar to sequences found in complement regulatory proteins. Each of these adhesion receptors is inserted *via* a hydrophobic transmembrane domain and possesses a short cytoplasmic tail at the carboxy-terminus.

Selectins are glycoproteins and bind, through their lectin domain, to selectin ligands. Selectin ligands are sialylated forms of oligosaccharides, which themselves are covalently bound to various glycoproteins (Menger *et al.*; 1996).

L-selectin (CD62L) is expressed constitutively on leukocytes, but its presentation at the cell surface may be regulated. E-selectin (CD62E) is synthesized and expressed on ECs in response to inflammatory cytokines such as tumor necrosis factor- $\alpha$  (TNF- $\alpha$ ) or interleukin-1 (IL-1). Upregulation of cell surface E-selectin expression is the result of transcriptional activation of the E-selectin gene. P-selectin (CD62P), the largest of the selectins, is stored in the membrane of the  $\alpha$ -granules in platelets and in the membrane of the Weibel-Palade bodies in ECs and is translocated to the cell surface upon cell activation (McEver *et al.*; 1989).

### 2.4.2 P-selectin in chronic inflammation

Former names for P-selectin include platelet activation dependent granule external membrane protein (PADGEM) and granule membrane protein 140 (GMP-140). The existence of preformed P-selectin enables a rapid translocation from the secretory granules to the cell surface upon cell activation by thrombin, histamine, or other agonists (Tedder *et al.*; 1995). This self-limited process occurs within minutes and is particularly important in leukocyte rolling on endothelium in the earliest stages of acute inflammation (Geng *et al.*; 1990; Hattori *et al.*; 1989). Persistent expression of P-selectin on ECs, involving an increase in mRNA and lasting several days, has been observed in human tissues with chronic and allergic inflammation such as allergic rhinitis (Symon *et al.*; 1994), atherosclerotic plaque (Johnson-Tidey *et al.*; 1994), and chronic rheumatoid arthritis (Grober *et al.*; 1993). This suggests that certain inflammatory cytokines induce P-selectin synthesis under some conditions. In fact, augmented expression of P-selectin involving an increase in mRNA is brought about by TNF- $\alpha$  or lipopolysaccharide (LPS) in murine (Gotsch *et al.*; 1994) and bovine ECs (Weller *et al.*; 1992). This increase becomes prominent after 2 to 4 hours and then declines to basal levels within 12 hours (Sanders *et al.*; 1992; Weller *et al.*; 1992). Thus, it remains uncertain whether the effects of these mediators are sufficient to account for the persistent expression of P-selectin observed in human tissues with chronic and allergic inflammation.

Inflammatory mediators, such as TNF- $\alpha$  or LPS, activate transcription of many immediate-early genes, including endothelial cell adhesion molecules. Regulation by the transcription factor nuclear factor  $\kappa$ B (NF- $\kappa$ B), a central mediator of the innate immune response, plays a critical role in activation of these genes (Collins *et al.*; 1995; De Martin *et al.*; 2000; Lentsch *et al.*; 1999). Interestingly, unlike its effects in murine endothelial cells, TNF- $\alpha$  does not increase P-selectin mRNA in human ECs (Yao *et al.*; 1996). Furthermore, the promotor of the human P-selectin gene lacks the recognition element for p65-containing NF- $\kappa$ B heterodimers, the prototypical form of this transcription factor (Pan *et al.*; 1993). This implicates that mediators other than TNF- $\alpha$  and LPS increase the prolonged transcription of endothelial P-selectin independent from NF- $\kappa$ B at sites of chronic or allergic inflammation in humans. In fact, this knowledge led to the discovery of a new category of agonists that induced P-selectin expression with kinetics very different from those induced by the agonists described earlier. Interleukin-3 (IL-3), interleukin-4 (IL-4), and oncostatin M (OSM), cytokines that are present during chronic or allergic inflammation, have been shown to induce a delayed and prolonged accumulation of P-selectin mRNA in human umbilical vein endothelial cells (HUVEC) (Khew-Goodall *et al.*; 1996; Yao *et al.*; 1996).

## 2.5 Interleukin-4 in chronic inflammation

Inflammatory cytokines dramatically and selectively modulate the transcription and expression of the different adhesion molecules and chemoattractants in ECs (Springer, 1995). One such cytokine is IL-4, a glycoprotein secreted by activated T cells, mast cells, and eosinophils. It modulates growth and differentiation of a variety of cell types, including B- and T-lymphocytes, NK cells, mast cells, and bone marrow mast cells and is present at high levels at sites of chronic and allergic inflammation, such as asthma and atopic dermatitis, where it appears to play an important role in disease progression (Bradding *et al.*; 1992; Hamid *et al.*; 1994).

*In vitro*, IL-4 induces HUVEC to synthesize VCAM-1 and P-selectin, but not E-selectin or ICAM-1. VCAM-1 mediates adhesion of mononuclear cells, eosinophils, and basophils, but not neutrophils

to the endothelial surface (Schleimer *et al.*; 1992; Thornhill *et al.*; 1990). These data suggest that IL-4 promotes emigration of mononuclear cells or eosinophils which is a characteristic feature of chronic inflammation and reflects a persistent reaction to injury (Cotran *et al.*; 1999).

## 2.6 The heme oxygenase-1

### 2.6.1 The heme oxygenase system

The ubiquitous heme molecule (**figure 3**) exerts a dual role: in small amounts it acts by itself or as the functional group of many different heme proteins providing diverse and indispensable cellular functions, such as gene transcription, cell differentiation, and proliferation (Ponka, 1999; Sassa *et al.*; 1996). In contrast, excess of free heme, released from heme-containing proteins, constitutes a potentially harmful molecule due to its ability to intercalate into membranes, impair lipid bilayers and organelles, such as mitochondria, and destabilize the cytoskeleton (Balla *et al.*; 1991; Beri *et al.*; 1993). Subsequently, it promotes iron-dependent reactions leading to generation of reactive oxygen species (ROS) and lipid peroxidation (Ryter *et al.*; 2000).

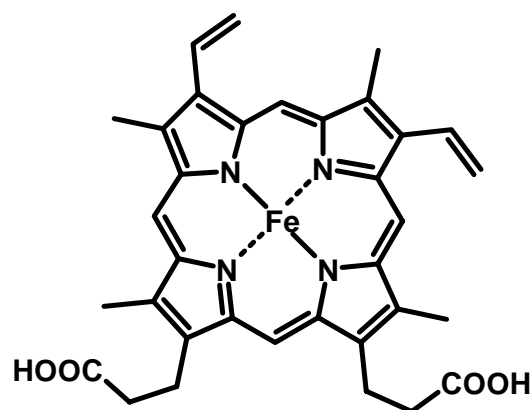
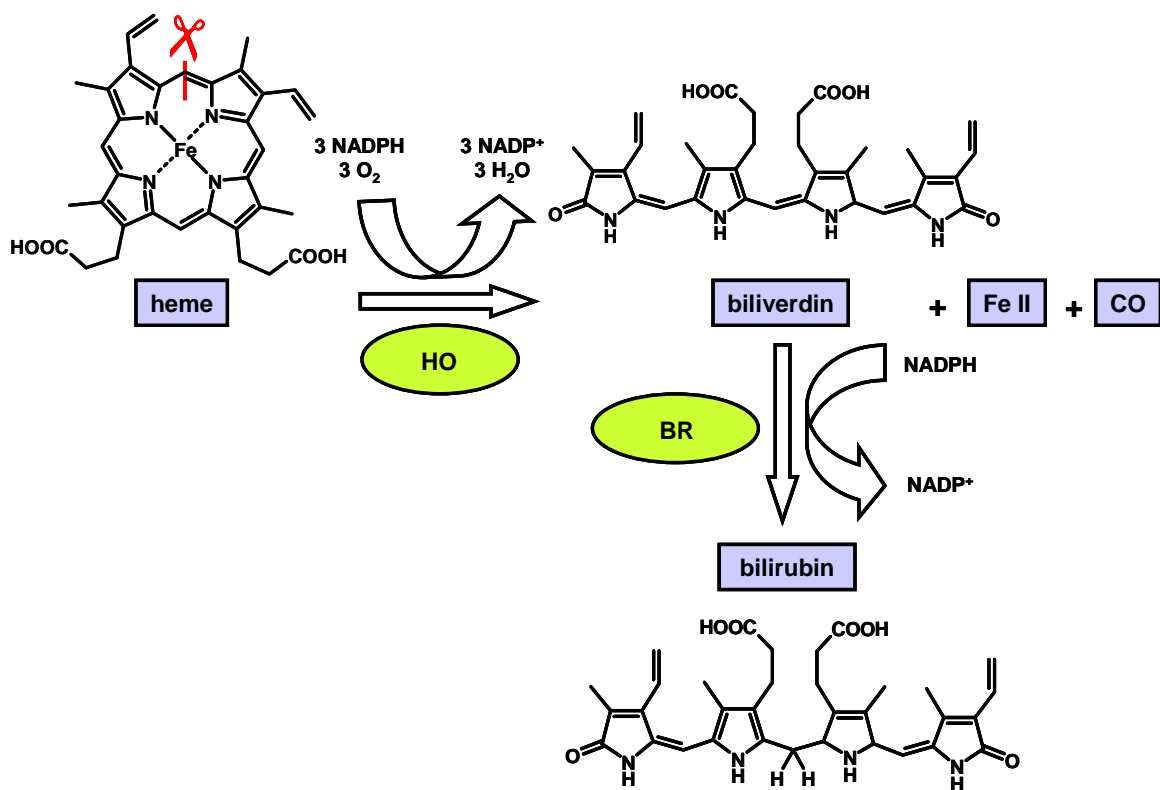


figure 3: Structure of iron(II)-protoporphyrin IX (heme).

Therefore, the amount of free heme must be tightly controlled to maintain cellular homeostasis. One of several defense mechanisms against free heme-mediated oxidative stress and inflammation is the heme oxygenase (HO) system. Heme oxygenase is the rate-limiting enzyme in the degradation of heme and was originally discovered in 1968 (Tenhunen *et al.*; 1968). In concert with NADPH-cytochrome P450 reductase as reducing agent, it catalyzes the oxidative cleavage of heme to yield equimolar amounts of free iron, carbon monoxide (CO), and biliverdin, which is subsequently converted to bilirubin by biliverdin reductase (BR) (**figure 4**).



**figure 4:** **Degradation of heme by heme oxygenase.** Heme is cleaved by heme oxygenase (HO) at the  $\alpha$ -methene carbon bridge to yield equimolar amounts of iron (Fe), carbon monoxide (CO), and biliverdin. Biliverdin is subsequently metabolized to bilirubin by biliverdin reductase (BR). Adapted from Durante (2003).

To date, the HO system is known to include three isoforms of the enzyme. They are products of different genes and their expression differs greatly between cell types, tissue distribution, and regulation. HO-2 is constitutively expressed, mainly in the brain, endothelium, and testes (Maines,

1997). HO-3 has only recently been identified, predominantly in the spleen, liver, thymus, prostate, heart, kidney, brain, and testes, and its protein expression remains to be elucidated (McCoubrey, Jr. *et al.*; 1997). The HO-1 isoform, also termed heat shock protein 32 (Hsp32), is distributed ubiquitously and is strongly induced by a variety of physiological and pathophysiological stimuli, including heme, heavy metals, endotoxins, oxidants, and several inflammatory cytokines (Immenschuh *et al.*; 2000; Maines, 1997). HO-1 has recently been recognized to possess important regulatory properties. It is tightly involved in both physiological as well as pathophysiological processes, such as cytoprotection, apoptosis, and inflammation.

As being highly inducible on the transcriptional level by a multitude of stimuli and involved in diverse signaling pathways, HO-1 is a very important protective strategy of the cell against stress situations (Otterbein *et al.*; 2000). Consistent with the diversity of signaling cascades involved in HO-1 induction, the promotor region of HO-1 contains a variety of regulatory elements including binding sites for NF- $\kappa$ B and AP-1 (Lavrovsky *et al.*; 1994). In the past, the degradation products CO, free iron, and bilirubin were considered as toxic waste (Wagener *et al.*; 2003). Recent insights have provided evidence that this is not the case. Today, the vital function of HO-1 in maintaining cellular homeostasis is ascribed to its breakdown products. Although potentially harmful when present in excessive amounts, all three metabolites have important regulative and protective features:

(i) Free iron(II) is capable of causing severe oxidative stress by generation of reactive oxygen species (ROS) *via* catalyzation of the Fenton reaction. Nevertheless, HO-dependent release of free iron results in up-regulation of the iron storage protein ferritin which subsequently results in cyto-protection (Balla *et al.*; 1992).

(ii) CO is a gaseous messenger with similar functions as nitric oxide (NO). They share the ability to activate the heme protein soluble guanylyl cylcase (sGC), resulting in enhanced generation of the second messenger cGMP and subsequent vasodilatation (Marks *et al.*; 2003).

(iii) Bilirubin has recently been recognized as an important anti-oxidant, and this has been confirmed by several studies in different models of oxidative stress (Otterbein *et al.*; 2000). Thus, the end products of heme catabolism seem to mediate the beneficial effects of HO-1 activation.

## 2.6.2 Functions of the HO-1 system

In the recent years it has become evident that the HO-1 system possesses important regulatory properties in both physiological as well as pathophysiological processes, such as apoptosis, cell proliferation, and inflammation (Maines, 1997). These properties have been demonstrated in numerous *in vitro* and *in vivo* models.

Heme oxygenase and cell proliferation and growth: HO-1 has been demonstrated to stimulate proliferation of numerous cell types, such as keratinocytes and ECs (Clark *et al.*; 1997; Li *et al.*; 2002). The effect of HO-1 on cell proliferation is, however, highly variable and appears to be cell-type-specific. In contrast to its proliferative effects, the enzyme exerts a potent anti-proliferative effect in other cell types, e.g. smooth muscle cells and human T cells (Aizawa *et al.*; 2001; Li *et al.*; 2002; Pae *et al.*; 2004). The importance of HO-1 in growth control is illustrated by observations made in HO-1 deficient (HO-1<sup>-/-</sup>) mice and humans. HO-1<sup>-/-</sup> mice are found to be significantly smaller than wild type animals (Poss *et al.*; 1997) and the first case of human HO-1 deficiency showed severe growth retardation (Yachie *et al.*; 1999).

Heme oxygenase and apoptosis: Expression of HO-1 leads to anti-apoptotic effects in several cell types (Brouard *et al.*; 2000; Petrache *et al.*; 2000; Pileggi *et al.*; 2001; Soares *et al.*; 1998). Elevated HO activity prevents graft rejection through anti-apoptotic pathways as demonstrated in several models (Hancock *et al.*; 1998; Katori *et al.*; 2002). The anti-apoptotic features may be an important mechanism by which HO-1 exerts its cytoprotective function in inflammation, since apoptosis of ECs, such as it occurs during acute and chronic inflammation (Wagener *et al.*; 2003), is highly deleterious.

Heme oxygenase and inflammation: HO-1 has been implicated in modulating the pathogenesis in different models of acute inflammation. The elevated activity of HO-1 is considered to be a protective mechanism that limits the activation level and number of inflammatory cells and the extent of cell death in diseased tissues (Otterbein *et al.*; 1999; Willis *et al.*; 1996). This notion is supported by reports describing exaggerated inflammatory responses in HO-1<sup>-/-</sup> mice (Poss *et al.*; 1997) and by observations made in a case of human HO-1-deficiency (Yachie *et al.*; 1999).

## 2.7 Salicylates

The use of willow bark to reduce pain was already described by Hippocrates. In 1859, the active compound, salicylic acid (SA), was isolated and synthesized. In 1897 Felix Hofmann acetylated the hydroxyl group of SA to eliminate the unpleasant taste and subsequently acetylsalicylic acid (ASA) was introduced as a potent anti-inflammatory and analgesic drug.

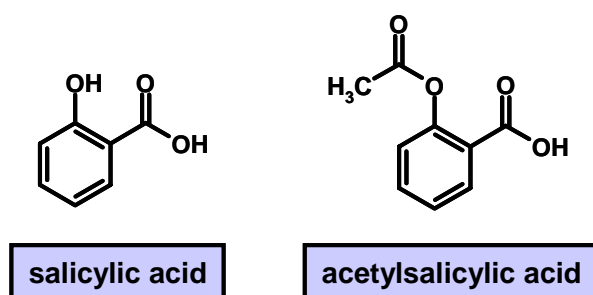


figure 5: Structures of salicylic acid (SA) and acetylsalicylic acid (ASA).

Since then, several other drugs were discovered that share the effects of ASA and SA and were classified as nonsteroidal anti-inflammatory drugs (NSAIDs), to distinguish them from anti-inflammatory glucocorticoids. All these substances have in common to relieve swelling, redness and pain, and to reduce fever and headache. For decades, their therapeutic effects have entirely been attributed to the inhibition of cyclooxygenase (COX) activity and the subsequent reduction of prostaglandin synthesis (Vane, 1971; Vane, 2000). COX catalyzes the first steps of prostaglandin synthesis. Prostaglandins are crucial players in many physiological and pathophysiological

processes. Some of these lipid-derived mediators cause pain, swelling, and redness. In addition, they increase renal blood flow and reduce gastric acid secretion. The majority of therapeutic properties of NSAID can be explained by a reduced level of prostaglandins. However, it has been suggested that additional mechanisms underlie some of their anti-inflammatory actions (Tegeder *et al.*; 2001). For instance, inhibition of the activation of the MAP kinase extracellular signal-regulated kinase (ERK) required for integrin-mediated responses may account for COX-independent effects of salicylates on neutrophil adhesion (Pillinger *et al.*; 1998). Moreover, interference with the activation of transcription factors such as NF- $\kappa$ B has been reported to be relevant (Kopp *et al.*; 1994). A recent study communicated a new pharmacological effect of salicylates *via* an inhibition of NFAT-dependent transcription of several cytokine genes, which play an important role in immune and inflammatory responses (Aceves *et al.*; 2004). Thus, it is plausible that additional unknown targets of salicylates remain to be discovered.

Anti-inflammatory therapy with high-dose ASA (highest daily intake: 5 g) results in plasma salicylate concentrations of 1-2 mM (Amann *et al.*; 2002; Tegeder *et al.*; 2001). After oral administration, about 50 % is rapidly de-acetylated to SA already during and immediately after absorption. Taking into account a plasma protein binding of 80-90 % (Needs *et al.*; 1985), the concentration of free salicylate in the plasma can be expected to be in the range of 250  $\mu$ M (Amann *et al.*; 2002). On the other hand, there are reports suggesting accumulation of acidic NSAIDs such as salicylate in acidic compartments within the body. Salicylate, for example, has been shown to accumulate specifically in inflamed tissue. Therefore, it seems questionable whether plasma salicylate concentrations found in patients are reliable definitions of relevant concentrations in an *in vitro* setting. It is most likely that millimolar concentrations provide a more precise picture of the conditions at sites of inflammation. A lot of studies examining anti-inflammatory properties of these drugs choose concentrations of 2-20 mM of salicylate referring to this point of view (Amann *et al.*; 2002).

## 2.8 Metalloporphyrins

The substrate of HO-1, iron(II)-protoporphyrin IX (FePP, heme, hemin) is a multifunctional molecule in nature, as described in chapter 1.1.3.1. The porphyrin-ring is a tetra dentate ligand that binds metals through two imino nitrogen atoms capable of accepting protons and two pyrrole nitrogens capable of either losing or accepting protons. Several metals, such as Fe, Cu, Zn, Sn, and Co, can form a complex with the porphyrin-ring (Smith *et al.*; 1975). The binding pocket of HO has specificity toward the side chains of the porphyrin-ring and does not recognize the metal moiety of the molecule. In consequence, metalloporphyrins in which the heme-iron has been replaced by other metals, like Zn, Sn and Co, can compete for heme and inhibit the activity of the enzyme because they cannot be degraded to bile pigments (Maines, 1981). On the other hand, heme and other metalloporphyrins are able to induce HO-1-expression, to various degrees though (Sardana *et al.*; 1987; Shan *et al.*; 2000; Shan *et al.*; 2002).

CoPP is often employed as a strong HO-1 inducer in experimental settings aimed to study the functions of HO-1. In fact, CoPP acts as inhibitor of HO-1 activity, like the other metalloporphyrins, as it is able to bind to the catalytic site of the enzyme but cannot be converted to the heme degradation products. On the other hand, CoPP is able to induce the HO-1-expression by a mechanism fundamentally different from that of other stress inducers, possibly *via* a newly identified regulatory region of the HO-1 gene, named metalloporphyrin-responsive element (MPRE) (Shan *et al.*; 2002). Its inducing effect on HO synthesis overweighs its inhibitory effect on the enzyme and thus, results in total in an increased HO-1 activity.

In contrast to CoPP, SnPP and ZnPP are generally viewed as being only weak inducers of HO-1-expression (Shan *et al.*; 2000). However, there are contradictory results that claim ZnPP is the most potent inducer of HO-1-expression (Yang *et al.*; 2001). Nevertheless, it has been proven that tin- and zinc-containing porphyrins decrease HO-1 activity, justifying their usage as potent HO-1-inhibitors.

All these compounds are being widely used in studies performed *in vitro* and *in vivo* to clarify the molecular pathways involved in HO-1 signal transduction (Dorman *et al.*; 2004; Maines, 1981; Pileggi *et al.*; 2001; Sass *et al.*; 2003), to prevent and treat hyperbilirubinemia (Maines *et al.*; 1992), and also to reduce jaundice in the neonates (Kappas, 2004). However, little is known about other biological effects of these inhibitors and inducers.

## 2.9 Apoptosis

Programmed cell death or apoptosis is a major component of both normal development and disease in multicellular organisms. It occurs during physiologic morphogenesis as well as in response to cell damage and is an important mechanism of the organism to eliminate damaged or unwanted cells. The first description of apoptosis was based on morphologic changes of the cell (Kerr *et al.*; 1972). These changes include nuclear condensation, DNA fragmentation, blebbing of the plasma membrane, cell shrinkage, and fragmentation of the cell into apoptotic bodies. These fragments are rapidly phagocytosed by macrophages or neighboring cells. This prevents lysis and induction inflammatory reactions by the cell contents. The crucial components of the apoptotic machinery is a family of proteases, the caspases, which can be divided into initiator and effector caspases (Leist *et al.*; 1997; Nicotera *et al.*; 2004).

Diverse pro-apoptotic stimuli activate the initiator caspases, such as caspase-8 and -9, which in turn cleave the inactive zymogens of the effector caspases, such as caspase-3 and -7. Finally, certain key substrates are cleaved leading to execution, packaging, and disposal of the cell.

Execution of apoptosis can be distinguished into two different pathways: the extrinsic and the intrinsic pathway (**figure 6**). The intrinsic pathway is also known as mitochondrial pathway and is initiated by chemotherapeutic agents, UV radiation, or free radicals. A breakdown of the potential of the mitochondrial membrane leads to release of cytochrome c into the cytoplasm, where it

associates with several other proteins to form the apoptosome. This results in activation of caspase-9 and subsequent activation of effector caspases (Green, 1998).

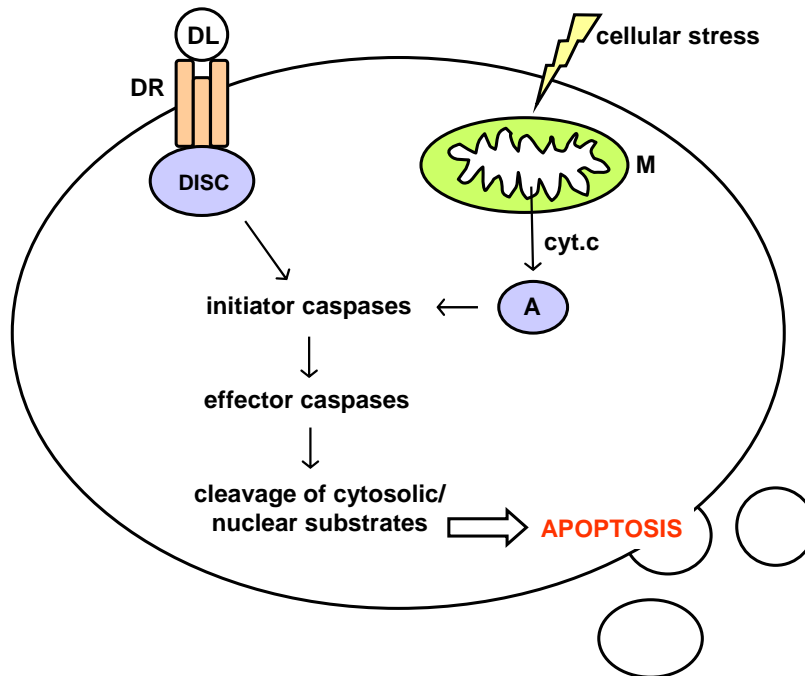


**figure 6: Signaling pathways in apoptosis.** Extrinsic pathway: death ligand (DL) binds to death receptors (DR) such as Fas/CD95. This leads to formation of the death inducing signaling complex (DISC), containing the inactive initiator caspase pro-caspases 8. Intrinsic pathway: cytochrom c (cyt.c) is released from the mitochondrium (M) leading to the formation of the apoptosome (A) containing the initiator caspase pro-caspase 9. Activated initiator caspases in turn cleave the inactive zymogens of effector caspases.

The extrinsic pathway is mediated *via* cell surface receptors, also called death receptors, which belong to the TNF receptor superfamily. Pro-apoptotic ligands such as TNF- $\alpha$  or FasLigand (FasL, CD95L) bind to the corresponding receptor and initiate the formation of a multi-protein complex, also referred to as death inducing signaling complex (DISC). In the DISC, the inactive pro-caspase 8 is autocatalytically cleaved and thereby activated to induce downstream effector caspases, such as caspase-3 and -7. Caspase-8 can also activate the mitochondrial pathway *via* cleavage of Bid, a member of the pro-apoptotic bcl-2 protein family (Green, 1998).

## 2.9.1 Caspases

The caspase family comprises at least 10 cysteine proteases that play a critical role during apoptotic cell death. Their name phrases the active cysteine group and the characteristic cleavage of their targets at aspartate residues. Caspases are expressed as inactive zymogens in the cytoplasm. They consist of an amino-terminal prodomain, a large subunit, and a small subunit at the carboxy-terminus (**figure 7**). The pro-caspases become activated during apoptosis by proteolytic processing at specific sites, followed by assembly of the active form (Denault *et al.*; 2002; Leist *et al.*; 1997; Nicotera *et al.*; 2004). The inactive zymogens are cleaved between the large and the small subunit and the prodomain is removed. The active caspase is derived from association of two pro-caspases. The resulting heterotetrameric enzyme consists of two small and two large subunits and contains two active sites at opposite ends of the molecule (Earnshaw *et al.*; 1999).

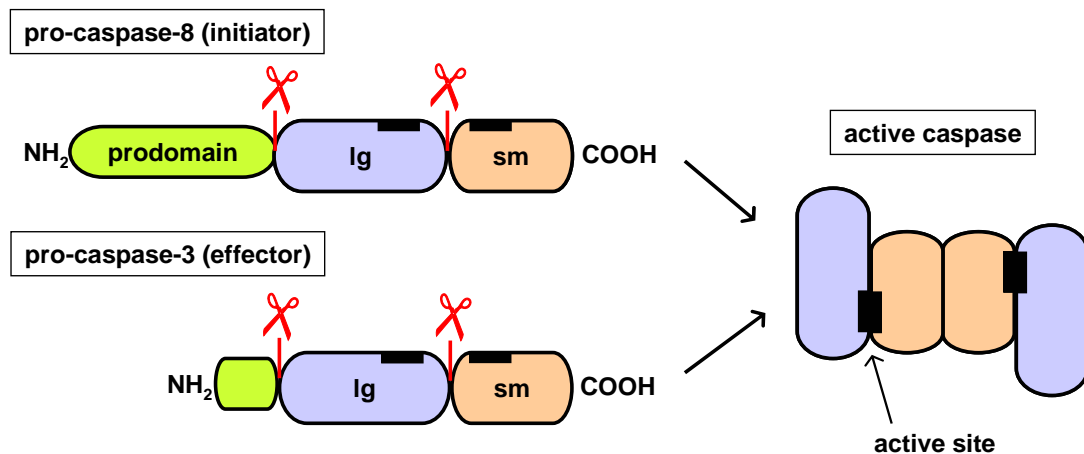


**figure 7:** **Structure of pro-caspase-8 and -3 and the active enzyme.** Pro-caspase-8 and other initiator caspases have a long prodomain containing binding sites for the activating complexes. All effector caspases have a very short prodomain (green). The active enzyme is composed of two large (lg) and two small (sm) subunits. It contains two active sites containing the conserved cleavage motif with the catalytic cysteine group at opposite ends of the molecule. Adapted from Earnshaw *et al.* (1999).

As mentioned above, the apoptotic caspases are generally divided into two classes: the initiator caspases, which include caspase-8, -9, and -10, and the effector caspases, which include

## INTRODUCTION

---

caspase-3, -6, and -7. The active enzyme can in turn cleave a number of defined substrates involved in the biochemical and morphological feature of apoptosis. One example is poly-ADP ribose polymerase (PARP), which is cleaved at a specific Asp-Glu-Val-Asp (DEVD) sequence. Caspase-3 has been identified as the caspase responsible for much of this activity (Nicholson *et al.*; 1995). These findings led to the measurement of caspase-3-like activity as a reliable, simple, and generally accepted method to quantify apoptotic cell death (Gurtu *et al.*; 1997).

### **3 MATERIALS AND METHODS**



### 3.1 Materials

Cell culture media (RPMI 1640, M199), glutamine, penicillin, streptomycin, and amphotericin B were from PAN Biotech (Aidenbach, Germany) and endothelial cell growth medium (ECGM) was from Promocell (Heidelberg, Germany). Endothelial Medium Supplement and tumor necrosis factor- $\alpha$  (TNF- $\alpha$ ) were purchased from Sigma-Aldrich Chemie GmbH (Taufkirchen, Germany). Dulbecco's Modified Eagle Medium (DMEM) was from Cambrex (Verviers, Belgium). Fetal calf serum (FCS) was from Biochrom (Berlin, Germany), FCS gold was from PAA Laboratories (Cölbe, Germany), and human recombinant Fas Ligand (FasL), cobalt(III)-, tin-, and zinc(II)-protoporphyrin were from Alexis (Grünberg, Germany). Sodium salicylate (NaSal) was from Fluka (Buchs, Switzerland). The caspase-inhibitor z-VAD-fmk, the MAPK p38-inhibitor SB203580, the human recombinant caspases-3 and -8, and the anti-PARP antibody were from Calbiochem (Schwalbach, Germany). The ECL Plus Western Blotting Detection Reagent was from Amersham Biosciences (Freiburg, Germany). The protease inhibitor cocktail Complete<sup>®</sup> and Collagenase A were from Roche (Mannheim, Germany). CAPS was from USB (Cleveland, USA). Anti-hsp32 (HO-1) and HRP-conjugated anti-CPP32 (caspase-3) were from BD Transduction Laboratories (Heidelberg, Germany). Anti-phospho-JNK and HRP-conjugated goat anti-mouse antibody were from Cell Signaling/New England Biolabs (Frankfurt/Main, Germany). HRP-conjugated goat anti-rabbit was from Dianova (Hamburg, Germany). Anti-p65 was from Santa Cruz (Heidelberg, Germany) and AlexaFluor633 goat anti-mouse antibody for immunocytochemistry was from Molecular Probes/Invitrogen (Karlsruhe, Germany). Double-stranded AP-1 and NF- $\kappa$ B-oligonucleotides for EMSA were from Promega (Mannheim, Germany). The plasmids pNF- $\kappa$ B-Luc and pFC-MEKK were from Stratagene (Heidelberg, Germany) and pEGFP-N1 was from Clontech (Palo Alto, CA, USA). The plasmid pSV- $\beta$ -Gal and salmon sperm DNA were kindly provided by Genzentrum (University of Munich, Germany). Dominant negative (dn) p38 MAPK plasmid and empty vector plasmid were a kind gift from Dr. Stephan Ludwig (University of Würzburg, Germany). Primers for P-selectin and GAPDH were from Invitrogen (Karlsruhe, Germany). TaqMan<sup>®</sup> probes for P-selectin and GAPDH were from PE Applied Biosystems (Warrington, United Kingdom). All other materials

were purchased from Sigma-Aldrich (Taufkirchen, Germany), Carl-Roth GmbH (Karlsruhe, Germany), or Merck-Eurolab (Munich, Germany). If not stated otherwise, all solutions were prepared with double-distilled water.

## 3.2 Cell culture

### Solutions:

#### PBS (pH 7.4):

Na <sub>2</sub> HPO <sub>4</sub>	10.4 mM
KH <sub>2</sub> PO <sub>4</sub>	3.16 mM
NaCl	132.2 mM

#### Trypsin/EDTA (T/E):

Trypsin (1:250 in PBS)	0.05 g
EDTA	0.20 g
PBS	ad 100 ml

#### PBS+:

NaCl	137 mM
KCl	2.68 mM
Na <sub>2</sub> HPO <sub>4</sub>	8.10 mM
KH <sub>2</sub> PO <sub>4</sub>	1.47 mM
MgCl <sub>2</sub>	0.5 mM
CaCl <sub>2</sub>	0.68 mM

All cells were routinely tested for contamination of mycoplasma with the PCR detection kit VenorGeM (Minerva Biolabs, Berlin, Germany).

### 3.2.1 Primary cells

Human umbilical vein endothelial cells (HUVEC) were prepared by digestion of umbilical veins with 0.1 g/l of collagenase A (37°C, 45 min) (Marin *et al.*; 2001) and were grown in a humidified atmosphere at 5 % CO<sub>2</sub> and 37°C in an incubator (Heraeus, Hanau, Germany). For experiments investigating the HO-1 induction by NaSal, cells were cultured in endothelial cell growth medium (ECGM) supplemented with 100 U/ml penicillin and 100 µg/ml streptomycin. For experiments

regarding the relationship of TNF- $\alpha$ -induced NF- $\kappa$ B-activation and p38 MAPK, cells were cultured in Medium 199 (M199) supplemented with 20 % heat-inactivated FCS, 2 % endothelial medium supplement, 2 mM glutamine, 100 U/ml penicillin, 100  $\mu$ g/ml streptomycin, and 2.5  $\mu$ g/ml amphotericin B. In order to compensate inter-individual differences, cells of at least two umbilical cords were combined for each cell preparation.

After reaching a confluent state, cells were either sub-cultured 1:3 in culture flasks or seeded in plates for experiments. For passaging, medium was removed and cells were washed with phosphate buffered saline (PBS) before they were incubated with 1-2 ml trypsin/EDTA (T/E) for 1-2 min at 37°C. The cells were gradually detached and the digestion was stopped with M199 containing 10 % heat-inactivated FCS, 100 U/ml penicillin, 100  $\mu$ g/ml streptomycin, and 2.5  $\mu$ g/ml amphotericin B. After centrifugation at 218 x *g*, 4°C for 10 min the pellet was resuspended in normal growth medium. All experiments were performed with cells of passage number three grown until confluence in 6-, 12-, 24- or 96-well plates (TPP, Trasadingen, Switzerland).

For long-term storage, confluent HUVEC were trypsinized, centrifuged at 218 x *g*, 4°C for 10 min, and resuspended in 1.5 ml freezing medium, containing M199 supplemented with 20 % FCS, 2 % endothelial medium supplement, 100 U/ml penicillin, 100  $\mu$ g/ml streptomycin, 2.5  $\mu$ g/ml amphotericin B and 10 % dimethylsulfoxide (DMSO). The cell suspension was transferred to cryovials and frozen at -20°C for one day, afterwards at -86°C for one week, and finally stored at -196°C in liquid nitrogen. This procedure was maintained in order to ensure gradual freezing of the cells. For thawing, the content of a cryovial was gently dissolved in pre-warmed Medium 199. To remove DMSO from the cells, they were centrifuged at 218 x *g*, 4°C for 10 min and resuspended in complete culture medium and transferred to a 75 cm<sup>2</sup> culture flask.

## **3.2.2 Cell lines**

### **3.2.2.1 Jurkat T-lymphocytes**

The subclone J16 of the Jurkat cell line, derived from an acute lymphatic leukemia, was graciously provided by Dr. S. Eichhorst (Klinikum Großhadern, Munich, Germany). This subclone is

particularly sensitive to CD95-induced apoptosis. Jurkat T cells were cultured in RPMI 1640, supplemented with 10 % FCS gold, 100 U/ml penicillin, 100 µg/ml streptomycin, and 0.1 M pyruvate in a humidified atmosphere at 5 % CO<sub>2</sub> and 37°C. For experiments, cells of passage numbers 3 to 15 were used at a density of 6 to 7 x 10<sup>5</sup> cells/ml.

Due to the fact that the genome of Jurkat cells is quite unstable and mutations occur frequently when cell density is too high, cultures must not be grown over 1.5 x 10<sup>6</sup> cells/ml. For the determination of the cell concentrations 1 ml of cell suspension was analyzed with Cell Viability Analyzer Vi-Cell™ (Beckman Coulter, Krefeld, Germany). The concentration required was achieved by dilution with pre-warmed medium.

Freezing and thawing was performed as described in chapter 4.1. Jurkat cells were frozen at a concentration of 5 x 10<sup>5</sup> in 1.5 ml freezing medium (RPMI 1640, supplemented with 20 % FCS gold and 10 % DMSO). After defrosting cells were grown for at least five days before any experiments.

### **3.2.2.2 Human embryonic kidney cell line 293**

Human embryonic kidney 293 (HEK 293) cells were originally generated by transformation of human embryonic kidney cell culture with sheared adenovirus 5 DNA, and were described by Graham *et al.* (1977).

HEK 293 from the German Collection of Microorganisms and Cell Cultures (DSMZ, Braunschweig, Germany) were grown as monolayer in DMEM supplemented with 10 % FCS (Biochrom, Berlin, Germany), 2 mM glutamine, 100 U/ml penicillin, and 100 µg/ml streptomycin in a humidified atmosphere at 5 % CO<sub>2</sub> and 37°C. After reaching ~85-90 % confluence, the cells were sub-cultured 1:10 in culture flasks or seeded in plates for experiments.

### **3.3 Animal model**

The following experiments were kindly performed by Stefan Seyfried and Dr. Gisa Tiegs (Department of Experimental Pharmacology and Toxicology, University of Erlangen-Nuremberg, Germany).

#### **3.3.1 Animals**

BALB/c-mice (age: 6-8 weeks; weight range: 18-22 g) were obtained from the animal facilities of the Institute of Experimental and Clinical Pharmacology and Toxicology of the University of Erlangen-Nuremberg, Germany. All mice received human care according to the guidelines of the National Institute of Health as well as to the legal requirements in Germany. They were maintained under controlled conditions (22°C, 55 % humidity and 12 h day/night rhythm) and fed a standard laboratory chow.

#### **3.3.2 Dosage and application routes**

Activating anti-CD95 Ab (Jo2; BD/Pharmingen, Heidelberg, Germany) was administered intravenously at 125 µg/kg in 200 µl pyrogen-free saline. CoPP (i.p.; 10 mg/kg) and SnPP (i.p.; 25 mg/kg) were dissolved in sterile 0.2 M NaOH and pH was adjusted to 7.9 by 1 M HCl (stock concentrations: CoPP 1 mg/ml, SnPP 2.5 mg/ml). The porphyrins were administered 2 h after induction of liver injury by anti-CD95 Ab. Animals were killed 6 h after administration of anti-CD95 Ab and the isolated livers were frozen in liquid nitrogen.

## **3.4 Real-time RT-PCR**

Real-time polymerase chain reaction (PCR) is the ability to monitor the progress of the PCR as it occurs. Data is therefore collected throughout the PCR process, rather than at the end of it as in conventional RT-PCR. A fluorescent reporter is used to visualize the increasing amount of PCR product in a reaction. By recording the amount of fluorescence emission at each cycle, it is possible to monitor the PCR reaction during exponential phase where the first significant increase in the amount of PCR product correlates to the initial amount of target template (for review see Bustin (2002)).

### **3.4.1 Isolation of total RNA**

Extraction of mRNA was performed with RNeasy<sup>®</sup> Mini Kit (Quiagen, Hilden, Germany) according to the manufacturers description. The RNeasy<sup>®</sup> procedure uses a silica-gel-based membrane and a specialized high-salt buffer system, which allows RNA longer than 200 bases to bind to the RNeasy<sup>®</sup> membrane. This procedure provides an enrichment for mRNA since most RNA <200 nucleotides, such as rRNA and tRNA, are selectively excluded. Cells are first lysed and homogenized in the presence of a highly denaturing guanidine isothiocyanate (GITC)-containing buffer, which immediately inactivates ribonucleases (RNases) to ensure isolation of intact RNA. Ethanol is added to provide appropriate binding conditions for the attachment of RNA to the silica-gel membrane. The size distribution of the isolated RNA is comparable to that obtained by the classical RNA isolation method of centrifugation through a CsCl cushion. Since the method of real-time PCR is sensitive to very small amounts of DNA, DNA-digestion was performed during the isolation procedure.

#### **Experimental procedure:**

Cells were grown in 6-well plates until confluence. Total RNA was prepared using the RNA isolation RNeasy<sup>®</sup> Mini Kit. The cells were lysed and homogenized in a buffer containing

$\beta$ -mercaptoethanol and GITC. Subsequently, 70 % ethanol was added and the samples were applied on to the RNeasy<sup>®</sup> mini columns. All other cellular components were removed by washing procedures with two different washing buffers. After the first washing step, RNase-free DNase was applied for DNase digestion (RNase-free DNase Set, Quiagen, Hilden Germany). Samples were incubated for 15 min and washing steps were continued. The purified RNA was eluted from the column with water under low salt conditions.

The obtained amount of RNA was determined from spectrophotometric optical density measurement (Lambda Bio 20 Photometer, PerkinElmer, Überlingen, Germany). Absorption was measured at 260 nm ( $A_{260}$ ) and 280 nm ( $A_{280}$ ). The RNA concentration was calculated from the  $A_{260}$  value. The ratio  $A_{260}/A_{280}$  was used for characterizing the purity of RNA (optimum: 1.8-2.0). Strong absorption at 280 nm points to protein contamination.

### 3.4.2 Reverse Transcription

#### Experimental procedure:

Reverse Transcription was carried out using the RNA PCR Core Reagent Kit (PE Applied Biosystems, Hamburg, Germany). Each reaction tube contained 400 ng of total RNA in a volume of 20  $\mu$ l containing 5.5 mM  $MgCl_2$ , 1x RT buffer, 500  $\mu$ M of each dNTP, 2.5  $\mu$ M of random hexamers, 0.4 U/ $\mu$ l RNase inhibitor, 1.25 U/ $\mu$ l MultiScribe reverse transcriptase and water to volume. RT-reactions were carried out in a GeneAmp PCR system 9700 (PE Applied Biosystems, Hamburg, Germany) at 25°C for 10 min and 48°C for 30 min. The reaction was stopped at 95°C for 5 min. cDNA was stored at -20°C.

### 3.4.3 Real-time PCR with TaqMan<sup>®</sup> probes

PCR amplifying P-selectin cDNA was performed with a Taq DNA polymerase from *Thermophilus aquaticus*. For real-time detection the TaqMan<sup>®</sup> assay system was used. This assay uses a probe technology that exploits the 5'  $\rightarrow$  3' -nuclease activity of the Taq polymerase. The probe is an oligonucleotide with the reporter dye 6-carboxyfluorescein (FAM) at the 5' end and the quencher

dye 6-carboxytetra-methylrhodamine (TAMRA) at the 3' end. When the probe is intact the quencher dye absorbs the fluorescence of the reporter dye due to the close proximity of the two. By the exo-nuclease activity of the Taq polymerase, the probe is cleaved (**figure 8**) allowing an increase in fluorescence emission. The cDNA sequence for P-selectin was obtained from the National Center for Biotechnology Information (NCBI). PCR primers and TaqMan<sup>®</sup> fluorogenic probes were designed using the Primer Express<sup>®</sup> 2.0 software program. Forward primer P-selectin: 5'-TGAAGGAAGGTTTTCTCCACTTTG-3'; reverse primer P-selectin: 5'-AGACTCCAGAAGATGCTACAGGAATT-3'. By using glyceraldehyde-3-phosphate dehydrogenase (GAPDH) as a housekeeping gene, results are quantified based on the relative expression of the target gene vs. the reference gene GAPDH using the mathematical model for relative quantification according to Pfaffl (2001). Forward primer GAPDH: 5'-GGGAAGGTGAAGGTCGGAGT-3'; reverse primer GAPDH: 5'-TCCACTTTACCAGAGTTAAAAGCAG-3'.

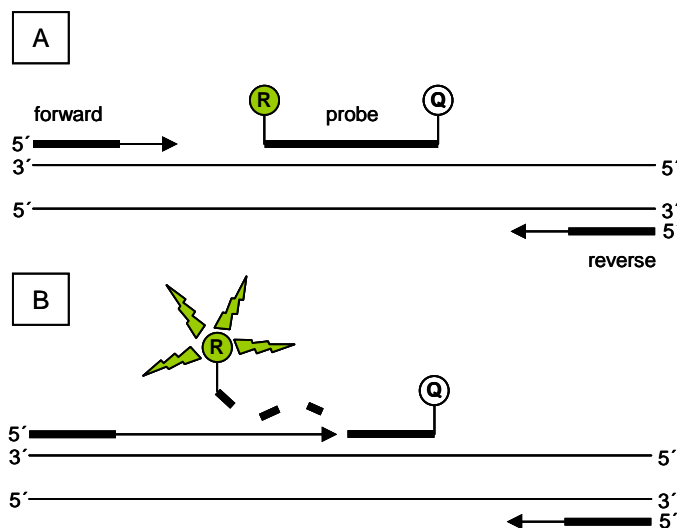


**figure 8:** TaqMan<sup>®</sup> system. After denaturation, primers and probes anneal to the target (**A**). Fluorescence does not occur because of the proximity between fluorophore (F) and quencher (Q). During extension, the probe is cleaved (**B**), allowing fluorescence of the reporter dye.

**Experimental procedure:**

Real-time PCR was performed using the TaqMan<sup>®</sup> PCR Core Reagent Kit. Each reaction tube contained 50 ng of cDNA, 10x TaqMan<sup>®</sup> buffer A, 5.5 mM MgCl<sub>2</sub>, 0.2 mM of dATP, dCTP, and

dGTP, 0.4 mM of dUTP, 0.01 U/ $\mu$ l of AmpErase UNG, 0.025 U/ $\mu$ l of AmpliTaq Gold Polymerase, 600 nM of forward and reverse primer, and 200 nM of the respective TaqMan<sup>®</sup> probe. All samples were run in duplicates. Standard curves were constructed on a 1:10 serial dilution of total RNA. Amplification conditions on the GeneAmp 5700 (PE Applied Biosystems, Hamburg, Germany) included 2 min 50°C for activation of the AmpErase Uracil N-glycoylase (UNG) to cleave the dU-containing PCR-products that are carried over from an earlier PCR, followed by 10 min 95°C for activation of the Hot Start AmpliTaq Gold Polymerase. Afterwards 40 cycles at 95°C for 15 sec and 60°C for 1 min are carried out for amplification of the target sequence. During the exponential phase of the increase in amplification products a fluorescence signal threshold is determined by the software at which point the signal generated from a sample is significantly greater than background fluorescence and all samples can be compared.

### 3.5 Western blot analysis

#### Solutions:

##### Modified RIPA buffer (lysis buffer):

NaCl	150 mM
Tris-HCl (pH 7.4)	50 mM
Nonidet P-40	1.0 %
sodium deoxycholate	0.25 %
SDS	0.10 %

##### Laemmli sample buffer (3x):

Tris-HCl (pH 8.8)	187.5 mM
SDS	6.0 %
glycerol	30 %
bromphenol blue	0.015 %
$\beta$ -mercaptoethanol	12.5 %

##### Added freshly before use:

Complete <sup>®</sup>	4 %
PMSF	1 mM

For protection of phosphorylated proteins:

NaF	1 mM
activated Na <sub>3</sub> VO <sub>4</sub>	1 mM

**Separation gel 10%:**

Rotiphorese™ Gel 30	40 %
Tris (pH 8.8)	375 mM
SDS	0.1 %
TEMED	0.1 %
APS	0.5 %

**Stacking gel:**

Rotiphorese™ Gel 30	17 %
Tris (pH 6.8)	125 mM
SDS	0.1 %
TEMED	0.2 %
APS	1 %

**Electrophoretic buffer (5x):**

Tris	24.6 mM
glycine	192 mM
SDS	0.1 %

**TBS-T (pH 8.0):**

Tris	24.6 mM
NaCl	188 mM
Tween 20	0.2 %

**Anode buffer:**

Tris	12 mM
CAPS	8 mM
methanol	15 %

**Cathode buffer:**

Tris	12 mM
CAPS	8 mM
SDS 10 %	0.1 %

**Antibodies:****Primary antibodies:**

- Anti-hsp32 (HO-1) monoclonal mouse anti-human
- Anti-phospho-p38 MAPK polyclonal rabbit anti-human
- Anti-phospho-JNK/SAPK monoclonal mouse anti-human
- Anti-PARP monoclonal mouse anti-human
- Peroxidase-conjugated anti-CPP-32 (caspase-3) monoclonal mouse anti-human

**Secondary antibodies:**

- Peroxidase-conjugated goat anti-rabbit IgG
- Peroxidase-conjugated goat anti-mouse IgG

**Experimental procedure:**

Cell samples: For detecting proteins in whole cell lysates, cells were cultured in 6-well plates until confluence and were either left untreated or stimulated as indicated in the respective figure legend. Briefly, cells were washed with PBS and lysed in modified RIPA buffer. Cells were homogenized and centrifuged. In the supernatant, protein concentrations were determined with the bicinchoninic

acid method (BC assay reagents, Iteadim, Montluçon, France) using a BSA standard (Pierce, Rockford, USA). Samples were adjusted to the same protein content. The separation of proteins was carried out by denaturing SDS-polyacrylamide gel electrophoresis (SDS-PAGE) according to Laemmli (1970). Laemmli sample buffer was added and the samples were boiled at 95°C for 5 min in order to let the SDS-protein-complexes develop. The identical charge densities on the surface of the complexes allow the separation of proteins according to their size. For gel preparation an acrylamide 30 % / bis-acrylamide 0.8 % stock solution (Rotiphorese™ Gel 30 from Roth, Karlsruhe, Germany) was applied. Electrophoresis was carried out with a Mini-Protean 3 Cell (BioRad, Munich, Germany).

Subsequently, the separated proteins were transferred to a polyvinylidene fluoride (PVDF) membrane (Immobilon-P, Millipore, Schwalbach, Germany) by semi-dry electro-blotting between two horizontal plate electrodes (BioRad, Munich, Germany) with a discontinuous buffer system. Blotting was performed with 1.5 mA per cm<sup>2</sup> of blotting surface for 60 min. Unspecific binding sites on the membrane were saturated by blocking in a 5 % solution of non-fat dry milk powder (Blotto, BioRad, Munich, Germany) in TBS-T. Antibody solutions were prepared 1:1,000 or 1:10,000 in 1 % Blotto in TBS-T and the membranes were incubated with the indicated primary antibody overnight at 4°C under constant shaking. After washing with TBS-T the appropriate HRP-conjugated secondary antibody was applied for 60 min at room temperature. Immunoreactive bands were visualized with a chemiluminescent detection kit (ECL Plus™, Amersham, Freiburg, Germany) and subsequent exposure to a medical x-ray film (Super RX, Fuji, Düsseldorf, Germany). Films were developed with an AGFA Curix 60 (AGFA, Cologne, Germany) and scanned for digital analysis.

Tissue samples: Western blot analysis of *in vivo* samples was kindly performed by Stefan Seyfried and Dr. Gisa Tiegs (Department of Experimental Pharmacology and Toxicology, University of Erlangen-Nuremberg, Germany). Mice were treated as described in chapter 2.3. Livers were stored on dry ice during the preparation of tissue homogenates. Livers were homogenized in lysis buffer containing 0.5 % Nonidet P-40 (NP40), 137 mM NaCl, 2 mM EDTA, 50 mM Tris-HCl pH 8.0, 10 % glycerol. Following centrifugation supernatants were stored at -85°C. 30 µg of protein were fractionated by 12.5 % SDS-PAGE and blotted onto a nitrocellulose membrane. Western blots were developed using an enhanced chemiluminescence system (Amersham, Freiburg, Germany)

according to the manufacturers' instructions. Semi-quantitative evaluation was done using the Gel Doc 2000 System (BioRad, Munich, Germany).

### **3.6 Electrophoretic mobility shift assay (EMSA)**

Experiments investigating the HO-1 induction by NaSal were kindly performed by Cornelia Niemann. Experiments regarding the relationship of TNF- $\alpha$ -induced NF- $\kappa$ B-activation and p38 MAPK were kindly performed by Brigitte Weiss.

The interaction of proteins with DNA is central to the control of many cellular processes including transcription. One well established technique to studying gene regulation and determining protein-DNA interactions is the electrophoretic mobility shift assay (EMSA). Nuclear extracts, containing the protein of interest e.g. a transcription factor, are incubated with linear DNA fragments consisting of the corresponding binding sequence. The EMSA technique is based on the observation that protein-DNA complexes migrate more slowly than free DNA molecules when subjected to non-denaturing polyacrylamide gel electrophoresis.

#### **3.6.1 Extraction of nuclear protein**

**Solutions:**

**Buffer A:**

HEPES (pH 7.9)	10 mM
KCl	10 mM
EDTA	0.1 mM
EGTA	0.1 mM
DTT	1 mM
PMSF	0.5 mM
Complete <sup>®</sup>	1 %

**Buffer B:**

HEPES (pH 7.9)	20 mM
NaCl	400 mM
EDTA	1 mM
EGTA	0.5 mM
glycerol	25 %
DTT	1 mM
PMSF	1 mM
Complete <sup>®</sup>	2 %

**Experimental procedure:**

HUVEC were cultured in 6-well plates until confluence and were treated as indicated. Nuclear extracts were prepared as described by Schreiber *et al.* (1989) as follows: briefly, cells were washed with ice-cold PBS, scraped off in PBS with a rubber cell scraper, centrifuged, and resuspended in ice-cold hypotonic buffer A. Cells were incubated on ice for 15 min. NP40 (10 %, 25  $\mu$ l) was added to the cells followed by 10 sec of vigorous vortexing and centrifugation of the homogenate at 12,000 x *g* for 30 sec. The supernatant, containing the cytosolic proteins, was removed. The nuclear pellet was resuspended by vigorous shaking for 15 min at 4°C in hypertonic buffer B. The nuclear extract was centrifuged at 12,000 x *g* for 5 min and the supernatant containing nuclear proteins was frozen at -80°C. The protein concentrations were determined by the method of Bradford (Bradford, 1976).

**3.6.2 Radioactive labeling of oligonucleotides****Solutions:****STE buffer (pH 7.5):**

Tris-HCl	10 mM
NaCl	100 mM
EDTA	1 mM

**Experimental procedure:**

Double-stranded oligonucleotide probes containing the consensus sequence either for AP-1 (5'-CGCTTGATGAGTCAGCCGGAA-3') or for NF- $\kappa$ B (5'-AGTTGAGGGGACTTTCCCAGGC-3') were 5'-end-labeled with adenosine 5'-[ $\gamma$ -<sup>32</sup>P]triphosphate (3,000 Ci/mmol) (Amersham, Freiburg, Germany) by using the T4 polynucleotide kinase (PNK) (USB, Cleveland, USA), which catalyzes the transfer of the terminal phosphate of ATP to the 5'-hydroxyl termini of DNA. The oligonucleotides were incubated with T4 PNK for 10 min at 37°C and the reaction was stopped by adding EDTA-solution (0.5 M). The radiolabeled DNA was separated from unlabeled remnants by

using NucTrap probe purification columns (Stratagene, La Jolla, USA). Radiolabeled DNA was eluted from the column by STE buffer.

### 3.6.3 Binding reaction and electrophoretic separation

#### Solutions:

##### Binding buffer (5x) (pH 7.5):

glycerol	20 %
MgCl <sub>2</sub>	5 mM
EDTA	2.5 mM
NaCl	250 mM
Tris-HCl	50 mM

##### Loading buffer (pH 7.5):

Tris-HCl	250 mM
bromphenol blue	0.2 %
glycerol	40 %

##### Reaction buffer:

DTT	2.6 mM
binding buffer (5x)	90 %
loading buffer	10 %

##### TBE buffer (10x) (pH 8.3):

Tris	0.89 M
boric acid	0.89 M
EDTA	0.02 M

##### Non-denaturing PAA-gel (4.5 %):

TBE (10x)	5.3 %
Rotiphorese™ Gel 30	15.8 %
glycerol	2.6 %
TEMED	0.05 %
APS	0.08 %

#### Experimental procedure:

Equal amounts of nuclear protein (approx. 2 µg) were incubated for 5 min at room temperature in a total volume of 14 µl containing 2 µg poly(dIdC) and 3 µl reaction buffer. Subsequently, 1 µl of the radiolabeled oligonucleotide probe (approx. 300,000 cpm) was added. After incubation for 30 min (RT), the nucleoprotein-oligonucleotide complexes were resolved by electrophoresis (Mini-Protean

3, Bio-Rad, Munich, Germany) on non-denaturing polyacrylamide gels (4.5 %). TBE was used as electrophoresis buffer. Bands were visualized by applying the gels to Cyclone Storage Phosphor Screens (Canberra-Packard, Dreieich, Germany) and analysis by a phosphor imager (Cyclone Storage Phosphor System, Canberra-Packard, Dreieich, Germany).

## 3.7 Transfection of cells

### 3.7.1 Plasmids

For reporter gene assays human embryonic kidney 293 (HEK 293) cells were transiently transfected by using the calcium phosphate co-precipitation method originally described by Graham *et al.* (1973) and modified by Jordan *et al.* (1996) for the transfection of HEK 293 cells. The uptake of DNA by cells in culture is markedly enhanced by presenting the nucleic acid as a co-precipitate of calcium phosphate and DNA. After entering the cell by endocytosis, some of the co-precipitate escapes from endosomes or lysosomes and enters the cytoplasm, from where it is transferred to the nucleus. Depending on the cell type, up to 50 % of a population of cells then express transfected genes in a transient fashion.

name	promoter	reporter gene
pNF- $\kappa$ B-Luc	NF- $\kappa$ B (5x)	firefly - luciferase
pFC-MEKK	CMV	MEKK
pEGFP-N1	CMV	green fluorescent protein
pSV- $\beta$ -Gal	SV40	lacZ
kRSPA-Flag-p38 (AF)	RSV-LTR	dn p38
kRSPA	RSV-LTR	empty expression vector as control

**table 1: List of plasmids**

### Solutions:

#### HBS (2x):

NaCl	280 mM
KCl	10 mM
Na <sub>2</sub> HPO <sub>4</sub>	1.5 mM
glucose	12 mM
HEPES	50 mM

### Experimental procedure:

1 x 10<sup>6</sup> cells were seeded in 100 mm or 60 mm dishes the day before transfection and grown at 37°C, 5 % CO<sub>2</sub> overnight. On the following day appropriate amounts of plasmid DNA were mixed with 2.8 µg salmon sperm DNA serving as carrier, 750 µl of sterile 250 mM CaCl<sub>2</sub>-solution, and 750 µl of sterile HEPES buffered saline (HBS) (2x) with an adjusted pH at 7.07 and incubated for 30 min at room temperature. The precipitate was added to the cells in the 100 mm dish and then incubated for 8 h at 37°C, 5 % CO<sub>2</sub>. In 60 mm dishes, cells were similarly transfected with plasmid DNA and 1 µg salmon sperm DNA, mixed with 250 µl of CaCl<sub>2</sub>-solution and 250 µl of HBS-buffer. Afterwards the medium was aspirated and cells were washed twice with ice-cold PBS+ and then fed with fresh medium. On the next day, transfected cells were seeded in 24-well plates at a concentration of 1.5 x 10<sup>5</sup> cells/well and grown for another 16 h. Transfection efficiency was judged by fluorescence microscopy evaluating GFP-transfected HEK-cells.

### 3.7.2 Antisense oligonucleotides

In order to silence the expression of certain genes human umbilical vein endothelial cells (HUVEC) were transiently transfected with antisense oligodesoxynucleotides (ODN) by using jetPEI<sup>TM</sup>-RGD transfection reagent (Poly transfection/Biomol, Hamburg, Germany). The ODN sequences for HO-1 were 5'-CGCCTTCATGGTgcc-3' (antisense) and 5'-GGCACCATGAAGgcg-3' (sense) (Wagener *et al.*; 1999). jetPEI<sup>TM</sup>-RGD is an Arg-Gly-Asp (RGD) peptide-conjugated polyethylenimine. It allows efficient transfection of endothelial cells expressing integrins. The short synthetic peptides mimic

the natural ligands of integrins, therefore integrin-mediated cell entry can be triggered by using RGD-conjugated jetPEI<sup>TM</sup> (Erbacher *et al.*; 1999). This transfection reagent is based on the property of linear cationic polyethylenimine (PEI) molecules (Mislick *et al.*; 1996). The DNA is compacted into positively charged particles capable of interacting with anionic proteoglycans on the cell surface and enters by endocytosis. In the cell it acts as a proton sponge that buffers the endosomal pH and protects the DNA from degradation. At the same time it induces endosomal osmotic swelling and rupture which provides an escape mechanism for DNA particles to the cytoplasm (Boussif *et al.*; 1995).

**Experimental procedure:**

HUVEC were grown in 6-well plates until they reached ~80 % confluence. For each well 5 µg DNA and 10 µl jetPEI<sup>TM</sup>-RGD were used. The DNA was incubated with jetPEI<sup>TM</sup>-RGD for 30 min at room temperature. Cells were treated with the jetPEI<sup>TM</sup>-RGD/DNA mixture for 4 h. To ensure sufficient silencing of the targeted protein, further experiments were done 24 h after transfection.

**3.7.3 AP-1 decoy**

Similar to the antisense approach described above, the decoy approach is also working with oligonucleotides. It uses ODN containing an enhancer element, to bind to sequence-specific DNA-binding proteins and therefore interferes with transcription (Tomita *et al.*; 2003). An AP-1 decoy consists of the consensus sequence of the transcription factor AP-1. It is able to catch the activated form of the transcription factor leading to an inactivation of the AP-1 response. The sequences of the ODN were 5'-cgctTGATGACTCAGCCgga-3' (decoy) and 5'-cgctTGATGACTTGGCCgga-3' (scrambled decoy) (Jan *et al.*; 2000). Lower case letters represent phosphorothioate modifications. AP-1 decoys were transfected into HUVEC with JetPEI<sup>TM</sup> according to chapter 2.8.2. Experiments were performed 3-4 h after transfection.

## 3.8 Reporter gene assay

### 3.8.1 Transfection of HEK 293 cells

Transfection of human embryonic kidney 293 cells (HEK 293) was performed as described in chapter 7.1. Cells were co-transfected with the luciferase reporter construct pNF- $\kappa$ B-Luc and the  $\beta$ -galactosidase gene pSV- $\beta$ -Gal. The plasmid pNF- $\kappa$ B-Luc contains the Simian virus 40 (SV40) promoter driving the firefly luciferase gene. For the experiments with the dominant negative (dn) version of p38, cells were additionally transfected with kRSPA-Flag-p38 (AF) mutant or the empty expression vector (kRSPA). In order to rule out interactions of the different plasmids, control cells were transfected with pNF- $\kappa$ B-Luc, pSV- $\beta$ -Gal or salmon sperm alone. Cells co-transfected with pNF- $\kappa$ B, pSV- $\beta$ -Gal, pFC-MEKK and salmon sperm served as a positive control.

### 3.8.2 Luciferase reporter assay

Firefly luciferase is widely used as a reporter to study gene expression. Light is produced by converting the chemical energy of luciferin oxidation through an electron transition, forming the product molecule oxyluciferin. The enzyme catalyzes the luciferin oxidation using ATP and  $Mg^{2+}$  as co-substrate and the generated light can be measured. For normalization, cells are co-transfected with the gene encoding  $\beta$ -galactosidase. This *E.coli*-derived enzyme catalyzes the cleavage of the synthetic substrate chlorophenolred- $\beta$ -D-galactopyranoside (CPRG) releasing chlorophenolred which is measured by spectrophotometry.

#### Solutions:

##### Z-buffer:

$Na_2HPO_4$	60 mM
$NaH_2PO_4$	40 mM
KCl	10 mM
MgCl	10 mM

##### Substrate solution:

CPRG (50 mM)	100 $\mu$ l
$\beta$ -mercaptoethanol	10 $\mu$ l
z-buffer	10 ml

**Experimental procedure:**

Cells were pre-incubated for 2 h with various substances and subsequently stimulated with 1 ng/ml TNF- $\alpha$  for 6 h. Then cells were washed with PBS+ and lysed with the provided passive lysis buffer (Promega, Heidelberg, Germany). To ensure complete and even coverage of the cells with passive lysis buffer, the plates were placed on a rocking platform for 15 min at room temperature and frozen at -85°C until measurement. Nuclear factor (NF)- $\kappa$ B activity was measured by the luciferase assay system (Promega, Heidelberg, Germany), according to the manufacturers description, with an AutoLumat Plus (Berthold, Pforzheim, Germany). Galactosidase activity was assayed by adding the substrate solution to 10  $\mu$ l of each sample and measuring the absorbance at 550 nm at 37°C in a SpectraFluor Plus microplate reader (Tecan, Crailsheim, Germany).

### 3.9 Measurement of caspase activity

The activation of caspase-3, a member of the caspase family thought to mediate apoptosis in most mammalian cell types (Hengartner, 2000), can be measured with the help of a synthetic peptide substrate DEVD (Asp-Glu-Val-Asp) labeled with a fluorescent molecule, 7-amino-4-trifluoromethyl coumarin (AFC). Activated caspases cleave the substrate after the aspartate residue releasing the fluorophore (**figure 9**). This results in a shift from blue to green fluorescence, measured at an extinction wavelength of 400 nm and an emission wavelength of 505 nm.



figure 9: Liberation of AFC by caspase-3-cleavage of Ac-DEVD-AFC.

The reaction has a linear progression over at least 2 h at substrate saturation. Since caspases need a thiol group for their catalytic activity, they are susceptible to changes of redox potential by agents such as air oxygen or traces of metal ions. Therefore, the substrate buffer contains dithiothreitol (DTT) as a reducing agent.

### **3.9.1 Caspase-3-like activity**

DEVD has been identified as the consensus cleavage site for caspase-3 (Nicholson *et al.*; 1995), as well as other closely related family proteases, such as caspase-6 and -7. Therefore, the activity which is assayed with this method within whole cell lysates or tissue homogenates has to be termed “caspase-3-like activity” regarding caspase-3 as the major effector caspase.

#### **Solutions:**

##### **Lysis buffer:**

MgCl <sub>2</sub>	5 mM
EGTA	1 mM
Triton <sup>®</sup> X-100	400 µl
HEPES (pH 7.5)	25 mM

##### **Substrate buffer:**

HEPES (pH 7.5)	50 mM
sucrose	1 %
CHAPS	0.1 %

##### **Added freshly before use:**

Ac-DEVD-AFC	50 µM
DTT	10 mM

#### **Experimental procedure:**

Cell samples: Cells were cultured in 12-well plates, treated as indicated, and washed with ice-cold PBS, followed by addition of 70 µl cold lysis buffer. Subsequently, the plates were frozen at -85°C until measurement. The frozen plates were allowed to thaw on ice, cells were scraped and cell lysates were collected, followed by centrifugation at 21,910 x g, 4°C for 10 min. Supernatants were transferred to microtiter plates (Greiner, Frickenhausen, Germany) and caspase-3-like activity was measured according to the method originally described by Gurtu *et al.* (1997).

Tissue samples: Mice were treated as described in chapter 2.3. Livers were stored on dry ice during the preparation of tissue homogenates. 1 ml of ice-cold lysis buffer was added to 100 mg of liver tissue. After homogenization with a Potter S device (Braun Biotech, Melsungen, Germany), lysates were cleared by centrifugation. The obtained supernatants were stored in aliquots at -85°C. Caspase activity was measured as described above.

### 3.9.2 Caspase-8-like activity

Similarly to the assessment of caspase-3-like activity, the activity of other caspases can be determined, by changing the cleavage site of the substrate. By using the consensus cleavage site IETD (Ile-Glu-Thr-Asp), enzyme activity of caspase-8 and other closely related family proteases, such as caspase-9, becomes detectable. Activities in cell lysates and tissue homogenates were determined as described in chapter 2.10.1 by using Ac-IETD-AFC as caspase substrate.

### 3.9.3 Activity of recombinant caspases

#### **Solutions:**

#### **Buffer A (pH 7.4):**

HEPES	50 mM
NaCl	100 mM
CHAPS	0.1 %
EDTA	1 mM
glycerol	10 %

#### **Experimental procedure:**

Human recombinant caspase-3 and -8 were supplied in buffer A additionally containing 10 mM dithiothreitol (DTT). Before each experiment, the stock solutions were diluted to 2 U/ $\mu$ l with buffer A plus 400  $\mu$ M DTT. Activity of the enzymes (final concentration: 40 U/ml) was measured at 37°C in 100  $\mu$ l buffer A (without addition of DTT) containing 50  $\mu$ M caspase substrate, in microtiter plates following the generation of free AFC from the synthetic substrate Ac-DEVD-AFC for caspase-3 or

Ac-IETD-AFC for caspase-8 respectively. The activities measured in wells containing diluted recombinant caspase and substrate only were taken as 100 %.

### **3.10 Microscopy**

#### **3.10.1 Light Microscopy**

To detect changes in morphology of cells undergoing apoptosis, certain characteristic changes like blebbing, shrinking and formation of apoptotic bodies can be visualized in a light microscope. After incubation of the cells as indicated in the respective figure, they were viewed with a Zeiss Axiovert 25 microscope (Zeiss, Oberkochen, Germany) and pictures were taken with the connected reflex camera.

#### **3.10.2 Confocal Laser Scanning Microscopy (CLSM)**

Confocal Laser Scanning Microscopy (CLSM) offers a higher optical resolution compared to conventional microscopy. By two conjugated pinholes, one illumination pinhole through which only a disk-shaped area is lit and one in front of the detector which is focused on the same focal plane as the illumination pinhole, out-of-focus blurs are cut off and image definition is enhanced.

#### **Experimental procedure:**

Collagen-coated (1 % collagen in PBS) glass cover slips ( $\varnothing$  12 mm) were prepared in 24-well plates. HUVEC were grown until confluence and were treated as indicated. After treatment cells were washed with PBS+ and were fixed with a buffered formaldehyde solution (4 %). Cells were washed with PBS and were permeabilized with Triton X-100 (0.2 %). After further wash steps with PBS, unspecific binding was blocked by incubation with 0.2 % bovine serum albumin (BSA) solution. This was done in order to minimize non-specific adsorption of antibodies. Cells were

incubated with the primary antibody anti-p65 (1  $\mu\text{g/ml}$ ) for 1 h, washed with PBS, and incubated with AlexaFluor633 goat anti-mouse antibody (5  $\mu\text{g/ml}$ ) for 30 min. Again, cells were washed with PBS. The cover slips were embedded in fluorescent mounting medium (DakoCytomation, Hamburg, Germany) and put onto glass objective slides. Images were obtained using a Zeiss LSM 510 Meta confocal laser scanning microscope (Zeiss, Oberkochen, Germany).

### 3.11 Molecular modeling studies

The experiments described in this chapter were kindly performed by Dr. Monika Höltje, Birte Brandt, and Prof. Dr. Hans-Dieter Höltje (Institute of Pharmaceutical Chemistry, Heinrich-Heine-University Düsseldorf).

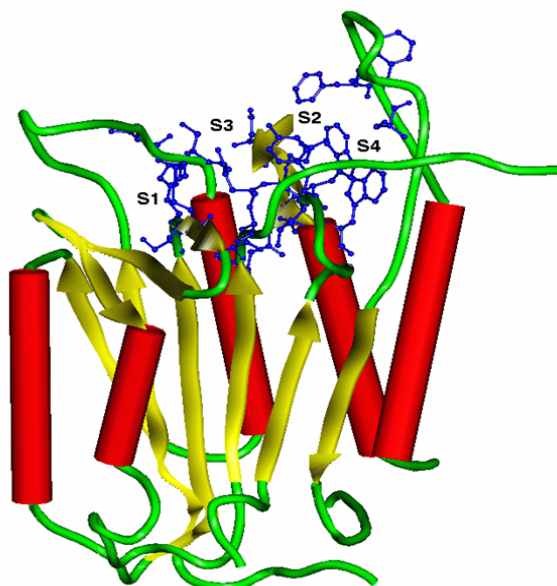


**figure 10:** **Crystal structure of caspase-3.** Amino acids of the active site regions S1-S4 are displayed in blue balls and sticks.

Automated docking analysis was carried out by using AutoDock 3.0 (Morris *et al.*; 1999). The crystal structure of caspase-3 was obtained from the Brookhaven Protein Databank (code: 1QX3). Several x-ray crystal structures reveal how specific peptidic and non peptidic inhibitors bind to caspase-3 (Erlanson *et al.*; 2003; Lee *et al.*; 2000a; Riedl *et al.*; 2001; Rotonda *et al.*; 1996). The

ligands occupy the active site of the caspase in the S1-S4 regions (**figure 10**). To identify potential ligand locations, a protoporphyrin molecule (without metal ligand, **figure 11**) was docked in the active site of the enzyme. Protoporphyrin was taken due to the fact that standard force field methods can not calculate physico-chemical properties of metal ions adequately. The ligand was kept flexible so that it could adjust to the positions of the protein side chains. 50 independent docking runs were carried out. For each calculation, similar ligand geometries were clustered and represented by the one with the most favorable interaction energy. The obtained complexes were energetically minimized by using a conjugate gradient algorithm permitting the ligand side chain atoms to relax. Energy minimizations were carried out by using the PRGEN program (Zbinden *et al.*; 1998). To validate the results obtained by the docking procedure, a series of GRID calculations was performed.

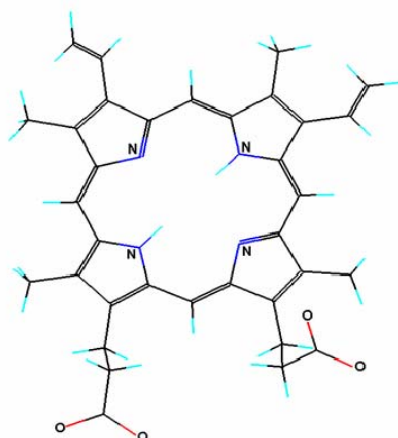


**figure 11: Molecular structure of protoporphyrin**

The program predicts favorable interactions between a molecule of known three-dimensional structure (i.e. caspase-3) and different probes representing characteristic chemical features of a ligand molecule. Unlike the docking studies, the complete structure of caspase-3 was investigated here, in order to search for possible protoporphyrin binding sites in addition to the known active site.

### 3.12 High performance liquid chromatography

For the use in different experiments with cultured cells, stability of acetylsalicylic acid (ASA) in aqueous solutions was tested by high performance liquid chromatography (HPLC).

#### Experimental procedure:

Separation of acetylsalicylic acid (ASA) and salicylic acid (SA) was carried out on a Merck/Hitachi HPLC system (pump L6200A, autosampler AS-2000A, diode array detector L-4500A). A LiChrospher® 60 RP-select B 5 µm column (Merck/Hitachi, Darmstadt, Germany) was used at room temperature and a flow rate of 1.2 ml/min. The elution solvent was 40 % acetonitrile. For detection a spectrum of absorption from 200 to 400 nm was acquired. Chromatograms were recorded 3 h (A), 6 days (B), and 12 months (C) after solution of ASA in Medium 199 (M199). As can be seen in **figure 12**, hydrolyzation of ASA occurred already after 3 h. The second peak with a retention time of about 3 min could be identified as salicylic acid (SA). After 6 days the amount of SA was exceeding the amount of ASA and no ASA was left after 12 months of storage.

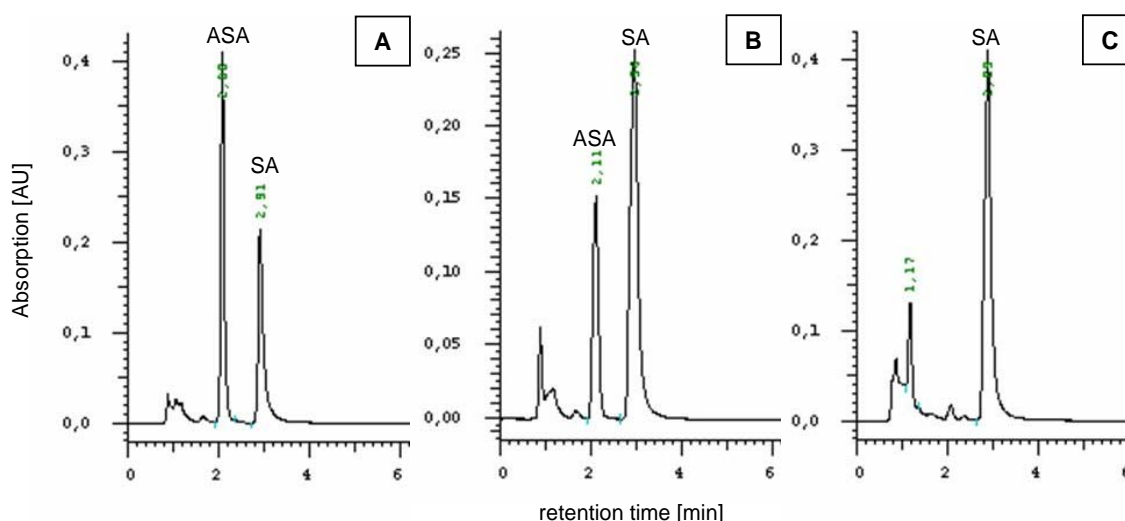


**figure 12:** Representative chromatograms of solutions of acetylic salicylic acid in cell culture medium. Chromatograms were recorded 3 hours (A), 6 days (B), and 12 months (C) after solution of the substance in M199.

### **3.13 Statistical analysis**

All experiments were done from at least two to three different cell preparations. Each experiment was performed at least in duplicates. Data is expressed as mean  $\pm$  SEM. Statistical analysis was performed with GraphPad Prism<sup>®</sup> (Version 3.02, GraphPad Software Inc., San Diego, USA). Statistical significance between groups was determined by one sample t-test or student's t-test. A p-value  $< 0.05$  was considered to be statistically significant.

## 4 RESULTS



## 4.1 Salicylates and HO-1

### 4.1.1 Effect of sodium salicylate on IL-4-induced P-selectin

The cytokine interleukin-4 (IL-4) is known to induce prolonged expression of the adhesion molecule P-selectin in human endothelial cells. It has been shown that salicylates are able to inhibit this induction. We aimed to confirm this fact in our cell system. Treatment of HUVEC with IL-4 resulted in an increase of P-selectin mRNA up to 15-fold (**figure 13A**). This induction was abrogated by pre-treatment with NaSal, as shown in **figure 13B**.

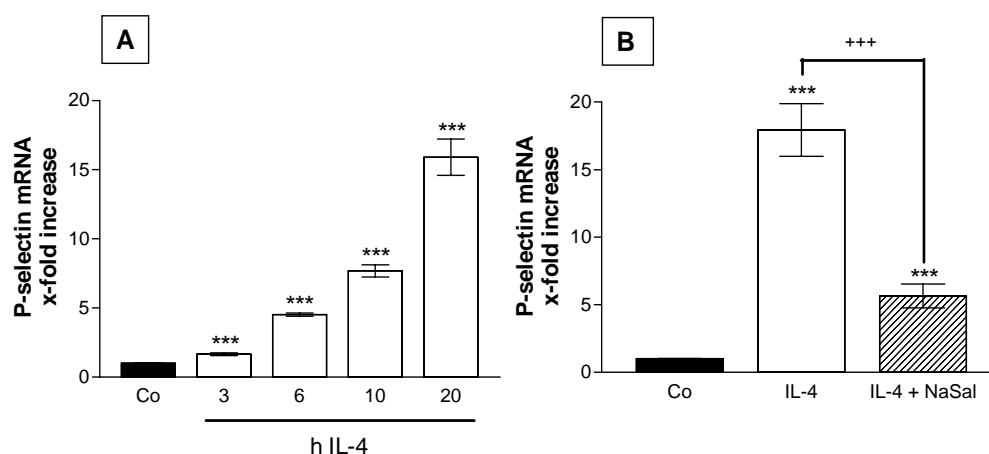


**figure 13:** IL-4-induced P-selectin mRNA is decreased by NaSal. HUVEC were either left untreated (Co) or were treated with Interleukin-4 (IL-4, 10 ng/ml) for the indicated times (**A**). Cells were either left untreated (Co) or were treated with IL-4 (10 ng/ml) for 20 h with or without pre-treatment with sodium salicylate (NaSal, 10 mM) for 60 min (**B**). Levels of P-selectin mRNA were determined by real-time RT-PCR as described in chapter 2.4. Values of untreated cells were set as 1. \*\*\* $p < 0.001$  vs. Co. +++ $p < 0.001$  vs. IL-4.

#### 4.1.1.1 Induction of P-selectin by IL-4 independent of NF- $\kappa$ B translocation

Salicylates are known to mediate some of their anti-inflammatory effects *via* an inhibition of the transcription factor NF- $\kappa$ B. However, the delayed and prolonged accumulation of P-selectin mRNA induced by IL-4 is postulated to be independent of NF- $\kappa$ B-activation and translocation. Our findings

shown in **figure 14** supported this assumption. In fact, there was no visible nuclear translocation of the NF- $\kappa$ B subunit p65 after IL-4 treatment in HUVEC compared to untreated cells. In contrast, TNF- $\alpha$ -treated cells showed a marked NF- $\kappa$ B-translocation into the nucleus.

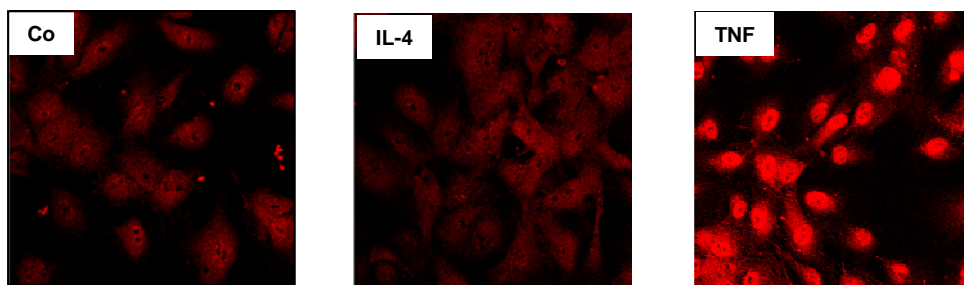


**figure 14:** IL-4 does not induce p65-translocation in HUVEC. Cells were either left untreated (Co) or were treated with IL-4 (10 ng/ml) for 4 h. Treatment with TNF- $\alpha$  (10 ng/ml, 4 h) served as a positive control. Immunocytochemistry for p65 and confocal laser scanning microscopy were performed as described in chapter 2.11.

#### 4.1.1.2 Role of heme oxygenase-1

Salicylates have been shown to induce heme oxygenase-1 (HO-1). Furthermore, a role of HO-1 in inhibition of different adhesion molecules including P-selectin expression had been suggested. In order to elucidate whether HO-1 participates in the NaSal-mediated abrogation of the IL-4-induced P-selectin levels, we used the HO-1-inhibitor tin-protoporphyrin IX (SnPP). In addition, we transfected HUVEC with antisense ODN in order to inhibit the NaSal-induced HO-1 expression. The functionality of the antisense approach, i.e. the ability of the ODN to reduce the HO-1 protein content, is shown in **figure 15**.

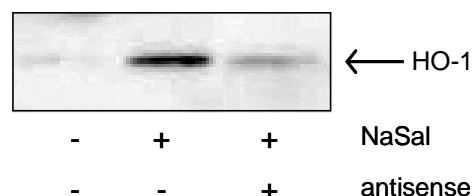


**figure 15:** Prove of functionality of the HO-1 antisense oligonucleotides. Cells were transfected with HO-1 antisense as described in chapter 2.8. Cells were treated with NaSal (10 mM, 60 min). For detection of HO-1 protein contents Western blot was performed as described in chapter 2.5.

As can be seen in **figure 16**, SnPP treatment as well as the antisense-approach revealed that HO-1 is partly involved in this inhibitory action of NaSal.

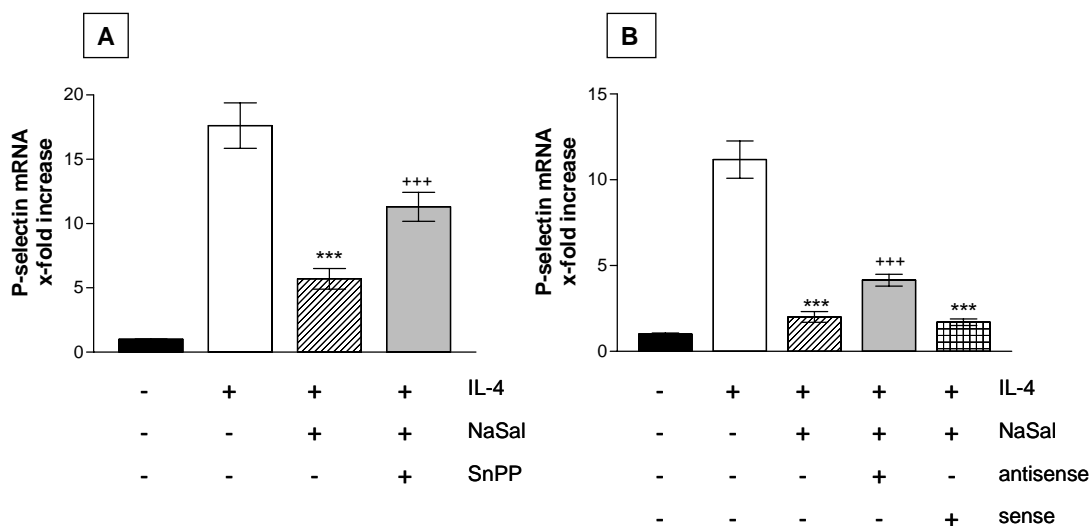


**figure 16: HO-1 is involved in the NaSal-mediated inhibition of P-selectin mRNA expression by IL-4.** Cells were either left untreated or were treated with IL-4 (10 ng/ml) for 20 h with or without pre-treatment with NaSal (10 mM) for 60 min. SnPP was employed 30 min before NaSal (**A**). For antisense experiments (**B**), cells were transfected with HO-1 antisense or sense as described in chapter 2.8. Levels of P-selectin mRNA were determined by real-time RT-PCR as described in chapter 2.4. Values of untreated cells were set as 1. \*\*\* $p < 0.001$  vs. IL-4. +++ $p < 0.001$  vs. IL-4- and NaSal-treated cells.

#### 4.1.2 HO-1 induction by sodium salicylate

The induction of HO-1 by acetylsalicylic acid (ASA) in HUVEC has previously been shown by Dr. Nicole Bildner (Bildner, 2002). ASA is not very stable in aqueous environment like it occurs during treatment of cells (as described in chapter 3.12) and is rapidly de-acetylated to salicylic acid (SA). It has been demonstrated that after oral administration of an analgesic dose of ASA, about 50 % is de-acetylated to SA already during and immediately after absorption (Amann *et al.*; 2002).

To confirm the HO-1-inducing effect of ASA for its degradation product SA, we performed time- and concentration-courses with sodium salicylate (NaSal). As shown in **figure 17A**, NaSal (10 mM) lead to elevated levels of HO-1 protein in a time-dependent manner with maximum induction

between 30-90 min after treatment. We also confirmed the dose-dependency of this effect. Concentrations ranging from 10  $\mu$ M to 10 mM induced HO-1 protein expression (**figure 17B**).

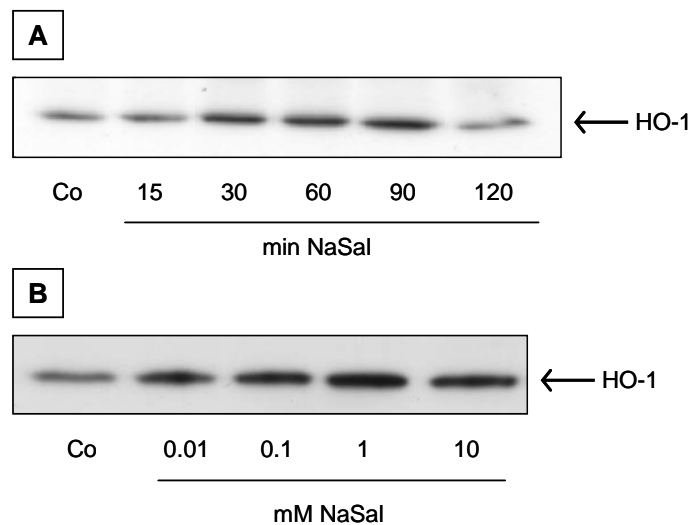


**figure 17:** Time- and concentration-course of NaSal-induced HO-1 expression. Cells were either left untreated (Co) or were treated with NaSal (10 mM) for the indicated times (**A**) or with different concentrations of NaSal for 60 min (**B**). For detection of HO-1 protein expression Western blot was performed as described in chapter 2.5.

### 4.1.3 HO-1 induction by JNK and AP-1

Since we found that NaSal is able to induce HO-1 expression similar to ASA, we wanted to confirm the proposed molecular mechanisms mediating the up-regulation of HO-1 protein expression by NaSal. Recent studies revealed that the transcription factor activator protein-1 (AP-1) is likely to be involved in HO-1 gene transcription in different cell types including endothelial cells. This has been shown by ourselves for the ASA-induced HO-1 expression in HUVEC (Bildner, 2002).

#### 4.1.3.1 Activation of AP-1 by sodium salicylate

To investigate the influence of NaSal on the DNA-binding activity of AP-1, cells were treated with sodium salicylate for different periods of time and EMSA was performed. In fact, treatment of HUVEC with NaSal (10 mM) resulted in a pronounced time-dependent activation of AP-1 DNA-binding activity (**figure 18**). This effect was maximal after 40 min.

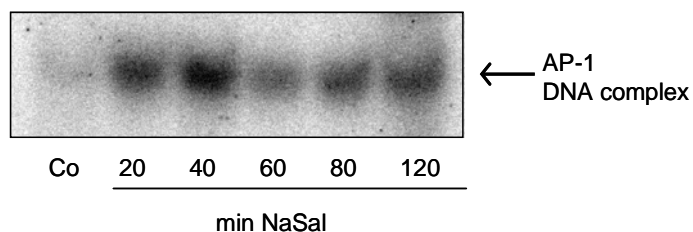


**figure 18: Time-course of NaSal-induced AP-1 DNA-binding activity.** HUVEC were either left untreated (Co) or were treated with NaSal (10 mM) for the indicated times. AP-1 DNA-binding activity was assessed by electrophoretic mobility shift assay (EMSA) as described in chapter 2.7.

To causally link AP-1 to the induction of HO-1, we performed AP-1 decoy experiments. Functionality of this approach was confirmed in our lab by Dr. Robert Fürst (Fürst, 2005). HUVEC were transfected with AP-1 decoy oligonucleotides and treated with NaSal. The decoy completely abrogated the increase of HO-1 expression by NaSal (**figure 19**), suggesting that AP-1 is crucial for the NaSal-induced up-regulation of HO-1. These findings clearly corroborated the suggested signaling pathway of ASA.

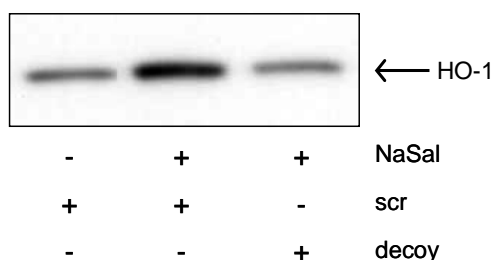


**figure 19: Involvement of AP-1 in the NaSal-induced HO-1 expression.** HUVEC were transfected with AP-1 decoy or scrambled decoy (scr) as described in chapter 2.8.3. After transfection cells were either left untreated or were treated with NaSal (10 mM) for 60 min. HO-1 protein expression was determined by Western blot as described in chapter 2.5.

#### 4.1.3.2 Effect of sodium salicylate on JNK/SAPK

It is well known that transcriptional activity of AP-1 is activated *via* the MAP kinase c-jun N-terminal kinase (JNK) and it has previously been shown that JNK also mediates the induction of HO-1 by ASA. To confirm these findings for the present setting, we examined the ability of high-dosed NaSal to activate JNK. In fact, the phosphorylated form of JNK became detectable after 15 min (**figure 20A**).

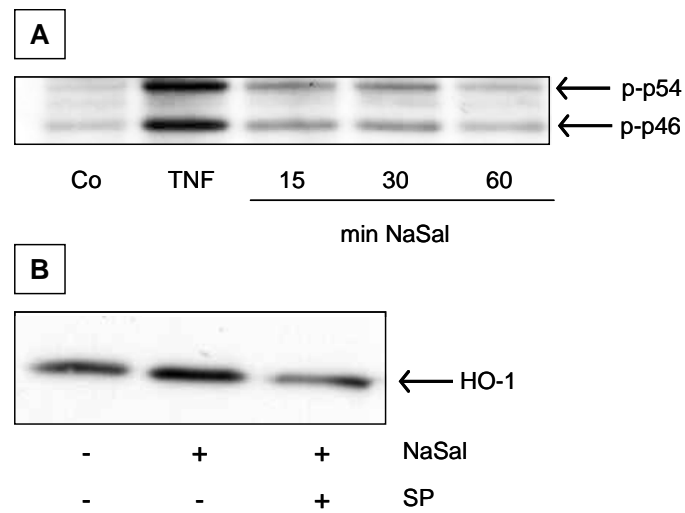


**figure 20: JNK mediates the NaSal-induced HO-1 expression.** Cells were either left untreated (Co), were treated with TNF- $\alpha$  (10 ng/ml) for 30 min, or were treated with NaSal (10 mM) for the indicated times (**A**). Cells were either left untreated or were pre-treated with the JNK-inhibitor SP600125 (SP, 10  $\mu$ M, 60 min). NaSal was added to the cells for 60 min (**B**). Phospho-JNK (p-p46/54) and HO-1 protein levels were determined by Western blot as described in chapter 2.5.

The participation of JNK in the signaling of NaSal was confirmed by employing the JNK inhibitor SP600125. As shown in **figure 20B**, the inhibitor completely blocks the induction of HO-1 protein by NaSal.

## 4.2 Metalloporphyrins and caspases

### 4.2.1 Porphyrins inhibit caspase-3-like activity

As shown in chapter 3.1, NaSal induces heme oxygenase (HO-1). In order to investigate whether HO-1, described as a cytoprotective protein, protects human umbilical vein endothelial cells (HUVEC) from apoptosis, cells were treated with NaSal and apoptosis was induced by different cytotoxic substances. Employing different metalloporphyrins as HO-1-inhibitors surprisingly showed contradictory results during assessment of caspase-3-like activity. As an inhibitor of HO-1, tin-protoporphyrin IX (SnPP) had been suggested to lead to an increase in caspase-3-like activity by inhibiting the cytoprotective features of HO-1. In our experiments, however, we observed the opposite effect of SnPP on caspase activity (**figure 21**).

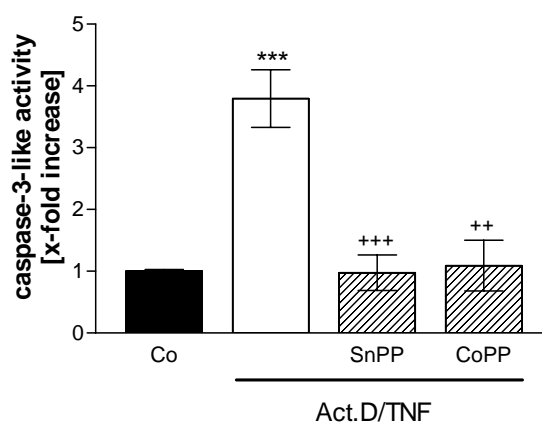


**figure 21: SnPP inhibits Actinomycin D/TNF- $\alpha$ -induced caspase-3-like activity.** Cells were either left untreated or treated with a combination of Actinomycin D (1  $\mu$ g/ml) and TNF- $\alpha$  (10 ng/ml) alone (Act.D/TNF, 3 h) or pre-treated with the HO-1-inhibitor tin-protoporphyrin IX (SnPP, 10  $\mu$ M, 30 min) or the HO-1-inducer cobalt(III)-protoporphyrin IX (CoPP, 10  $\mu$ M, 30 min). Caspase-3-like activity was determined as described in chapter 2.10. Values of untreated cells were set as 1. \*\*\*p<0.001 vs. Co. \*\*\*p<0.001 vs. Act.D/TNF. \*\*p<0.01 vs. Act.D/TNF.

These results led to the assumption that SnPP, or possibly metalloporphyrins in general, might have a direct influence on caspase-3-like activity. In order to answer this question we were looking

## RESULTS

---

for a system independent of the HO system. A classical model for investigating apoptosis are Jurkat T-lymphocytes treated with Fas ligand (FasL).

Metalloporphyrins, as well as FasL, have been demonstrated to affect HO-1 expression in different cell types including Jurkat cells (Pae *et al.*; 2004; Sardana *et al.*; 1987). However, Western blot analysis assured that in our experimental setting HO-1 was neither induced by FasL nor by porphyrins (**figure 22**).

Different times of treatment with these substances, as indicated in further experiments, did not result in an increased HO-1 expression either (data not shown). Therefore, the effect on caspase activity by the metalloporphyrins seems to be HO-1 independent.

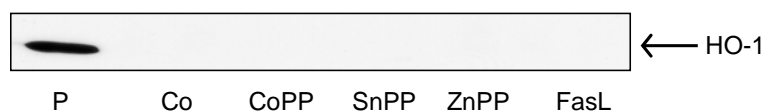


**figure 22:** **FasL and metalloporphyrins do not influence HO-1 expression in Jurkat cells.** Cells were either left untreated (Co) or treated with FasL (100 ng/ml, 16 h) or with the different porphyrins (CoPP, ZnPP, SnPP, 10  $\mu$ M each, 30 min). Human umbilical vein endothelial cells (HUVEC) treated with CoPP (10  $\mu$ M) served as a positive control (P) for induction of HO-1 protein. For detection of HO-1 protein expression Western blot was performed as described in chapter 2.5.

We tested the inhibition of caspase-3-like activity by different metalloporphyrins in Jurkat cells treated with FasL (100 ng/ml, 16 h). Since we suspected a direct inhibition of the enzyme by the porphyrins, they were added to the FasL-treated cells 30 min before the cells were lysed. Both the HO-1-inducer cobalt(III)-protoporphyrin IX (CoPP) and the HO-1-inhibitor SnPP showed a similar effect as observed in HUVEC after Actinomycin D/TNF- $\alpha$  treatment. Also zinc(II)-protoporphyrin IX (ZnPP), another potent HO-1-inhibitor like SnPP, showed the same inhibition (**figure 23**). As all three of the porphyrins were able to inhibit caspase-3-like activity we only used CoPP for further experiments.

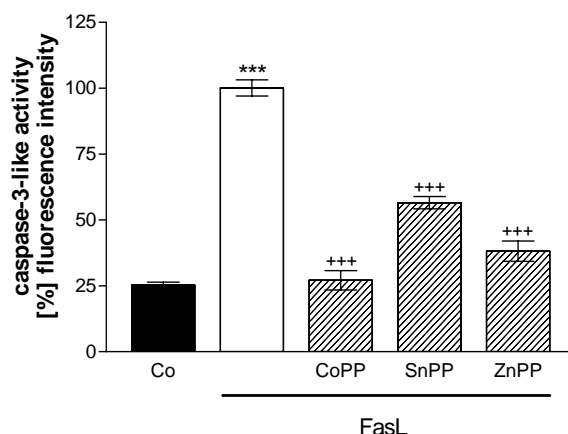


**figure 23: Different metalloporphyrins are able to inhibit FasL-induced caspase-3-like activity in Jurkat T-lymphocytes.** Cells were either left untreated (Co) or treated with FasL (100 ng/ml) for 16 h. CoPP, SnPP, and ZnPP (10  $\mu$ M each) were added 30 min before the cells were lysed. Caspase-3-like activity was measured as described in chapter 2.10. Values of FasL-treated cells were set as 100 %. \*\*\* $p$ <0.001 vs. Co. \*\*\* $p$ <0.001 vs. FasL

Morphological studies showed that after 16 h of treatment with FasL the cells are in a very late stage of apoptosis (data not shown). Therefore, we looked for an earlier time point where caspase-3-like activity would become detectable. Incubation with FasL for 2 h already resulted in a marked induction of caspase activity with a maximum at 6 h (**figure 24**).

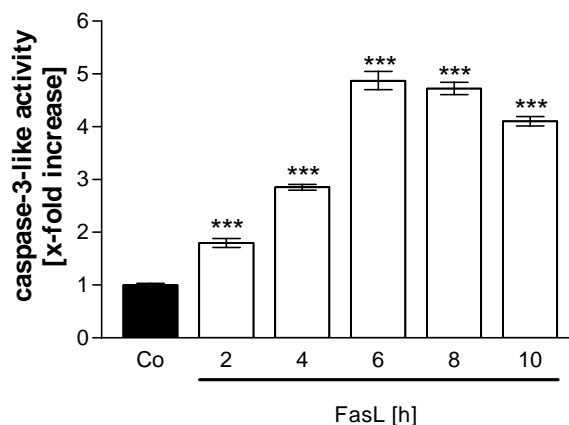


**figure 24: Time-dependent induction of caspase-3-like activity by Fas ligand.** Cells were treated with FasL (100 ng/ml) for the indicated times. Caspase-3-like activity was measured as described in chapter 2.10. Values of untreated cells were set as 1. \*\*\* $p$ <0.001 vs. Co.

For the following experiment we chose a FasL treatment for 6 h and observed that CoPP (10  $\mu$ M) inhibited enzyme activity induced by FasL also at this early time point (**figure 25**).

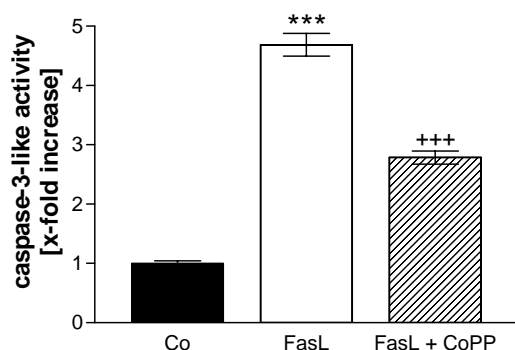


**figure 25: CoPP inhibits FasL-induced caspase-3-like activity.** Cells were either left untreated (Co) or treated with FasL (100 ng/ml) alone or together with CoPP (10  $\mu$ M) for 6 h. Caspase-3-like activity was measured by the release of free AMC after cleavage of the caspase-3-substrate as described in chapter 2.10. Values of untreated cells were set as 1. \*\*\* $p$ <0.001 vs. Co. +++ $p$ <0.001 vs. FasL.

#### 4.2.2 Metalloporphyrins inhibit PARP-cleavage

In order to rule out that the effects of the porphyrins on caspase activity are in any way related to the method of determining caspase activity, we aimed to determine effects of metalloporphyrins on a physiological substrate. Poly-ADP ribose polymerase (PARP) is known to be a prominent substrate of caspase-3 during apoptosis. In fact, Western blot analysis (**figure 26**) of Jurkat T-lymphocytes revealed a reduction of the 85 kDa cleavage product of PARP in CoPP-treated cells compared to Jurkat-cells treated with FasL alone.

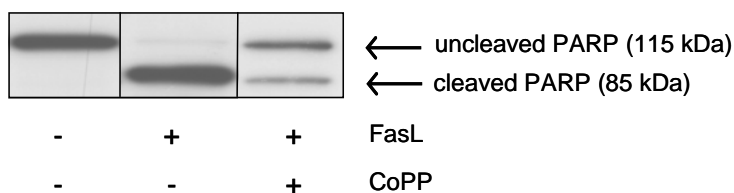


**figure 26: CoPP inhibits FasL-induced PARP-cleavage in Jurkat cells.** Cells were either left untreated (Co) or treated with FasL (100 ng/ml) alone or together with CoPP (10  $\mu$ M) for 6 h. For detection of PARP-cleavage Western blot was performed as described in chapter 2.5.

### 4.2.3 Porphyrins inhibit caspase-3-like activity *in vivo*

We aimed to clarify whether the inhibitory effect of metalloporphyrins on caspase-3-like activity is also relevant *in vivo*. Therefore we used a mouse model of Anti-CD95 (FasL) antibody (anti-CD95 Ab)-induced apoptotic liver injury as described in chapter 2.3. Mice were treated with activating anti-CD95 Ab for 6 h resulting in high caspase-3-like activity. CoPP and SnPP were administered 2 h after anti-CD95 Ab in order to make sure that no considerable HO-1 expression occurred yet (figure 27).

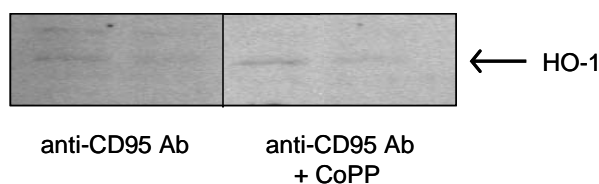


**figure 27: CoPP does not influence HO-1 protein expression in our *in vivo* setting.** Mice were treated with CoPP (10 mg/kg) 2 h after induction of caspase activity by activating anti-CD95 Ab (10 mg/kg). Animals were killed after 6 h and HO-1 protein expression was determined by Western blot as described in chapter 2.5.

Measurement of caspase-3-like activity in liver homogenates clearly showed that metalloporphyrins are able to inhibit this enzyme also *in vivo* (figure 28).

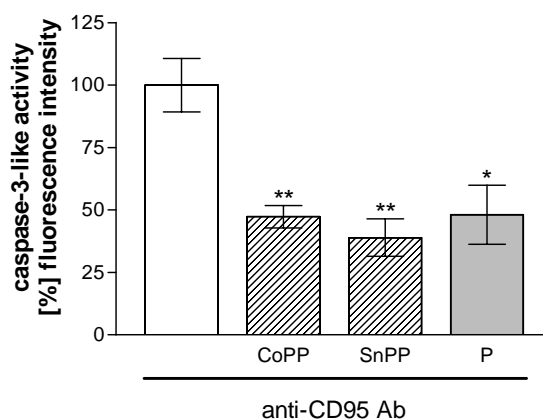


**figure 28: Porphyrins influence caspase-3-like activity *in vivo*.** Mice were treated with CoPP (10 mg/kg) or SnPP (25 mg/kg) 2 h after induction of caspase activity by activating anti-CD95 Ab (10 mg/kg). At 6 h after challenge caspase-3-like activity was measured as described in chapter 2.10. SnPP was also added to liver homogenates of mice treated with anti-CD95 Ab immediately before the measurement of caspase activity serving as a positive control (P). Values of anti-CD95 Ab-treated mice were set as 100 %. \*\* $p < 0.01$  vs. anti-CD95 Ab. \* $p < 0.05$  vs. anti-CD95 Ab.

#### 4.2.4 Porphyrins are direct caspase-3-inhibitors

To elucidate the mechanism of caspase inhibition, porphyrins were added directly to lysates of FasL-treated Jurkat cells containing activated caspases. Activities as shown in **figure 29** suggest that the mode of inhibition may occur in a direct manner. CoPP and the other metalloporphyrins showed a stronger inhibitory effect on caspase-3-like activity than in whole cells.

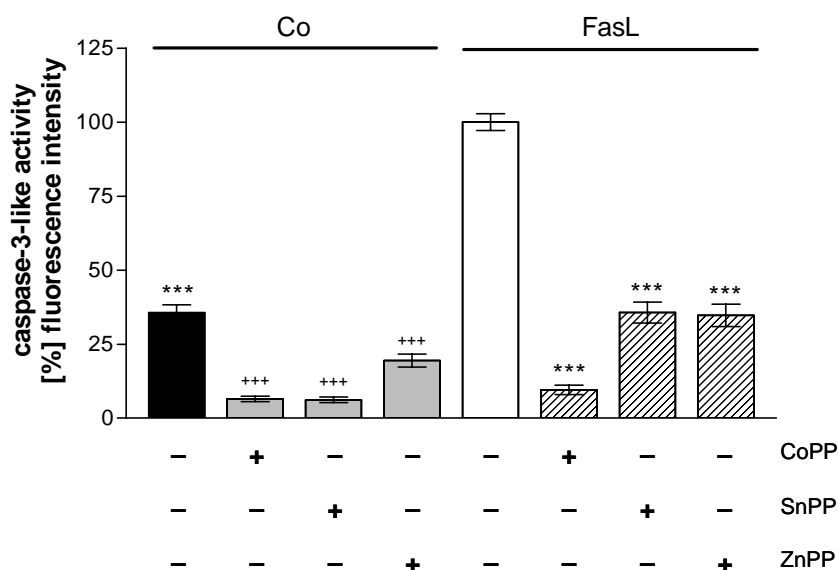


**figure 29: Metalloporphyrins inhibit caspase-3-like activity in cell lysates of FasL-induced Jurkat T-lymphocytes.** Cells were either left untreated (Co) or treated with FasL (100 ng/ml) for 16 h. CoPP, SnPP and ZnPP (10  $\mu$ M each) were added to the cell lysates immediately before the measurement of caspase activity as described in chapter 2.10. Values of FasL-treated cells were set as 100 %. \*\*\* $p$ <0.001 vs. FasL. +++ $p$ <0.001 vs. Co.

To confirm a direct inhibition of caspase activity by porphyrins, recombinant caspase-3 was employed. As can be seen in **figure 30**, the porphyrins were able to inhibit the activity of the isolated enzyme.

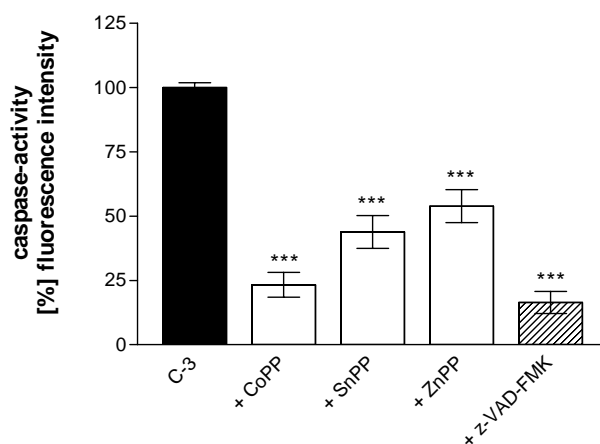


**figure 30: Metalloporphyrins inhibit activity of recombinant caspase-3.** Recombinant caspase-3 (C-3) was incubated with CoPP, SnPP, and ZnPP (10  $\mu$ M each). The caspase-inhibitor z-VAD-fmk served as a positive control (z-VAD-fmk, 25  $\mu$ M). Caspase activity was measured as described in chapter 2.10. Activity of caspase-3 in the absence of any porphyrin was taken as 100 %. \*\*\* $p < 0.001$  vs. C-3.

The  $IC_{50}$ -values of the three metalloporphyrins, as assessed by activity measurement with isolated caspase-3, demonstrate that the inhibitory potency of CoPP ( $IC_{50} \sim 10$  nM) clearly exceeds that of the two other porphyrins ( $IC_{50} \sim 2.5$   $\mu$ M) (**figure 31**).

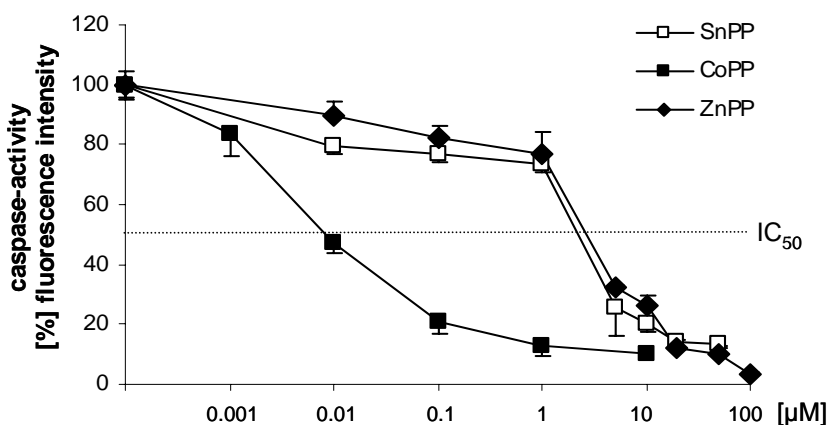


**figure 31: Dose-dependent inhibition of recombinant caspase-3 by metalloporphyrins.** CoPP (0.001  $\mu$ M - 10  $\mu$ M), SnPP, or ZnPP (0.001 - 100  $\mu$ M each) were added to recombinant caspase-3 immediately before the measurement of caspase activity as described in chapter 2.10. Activity of caspase-3 in the absence of any porphyrin was taken as 100 %.

## 4.2.5 Characterization of the inhibitory action on caspase-3

In order to clarify the mode of action of the metalloporphyrins on caspase-3-activity, we tested if the effect was reversible by adding an excess of caspase substrate. Further experiments were performed in order to elucidate the possible molecular mechanism of inhibition.

Employing increasing amounts of the caspase-3-substrate revealed that the inhibitory effect of the porphyrins is not reversible at substrate concentrations of up to 1 mM, as shown in **figure 32**.

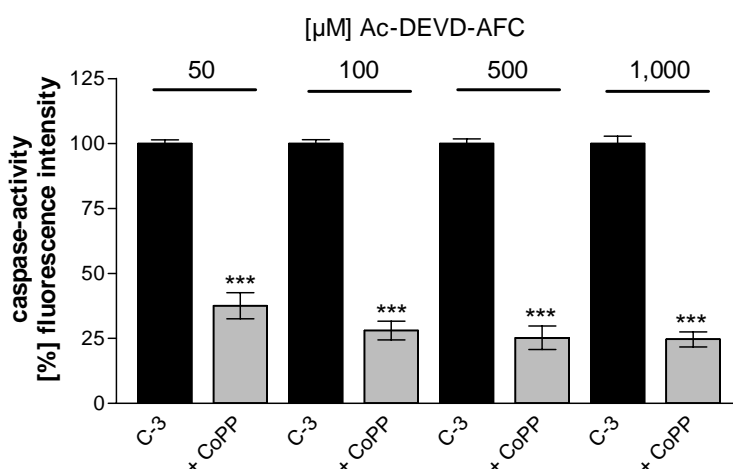


**figure 32:** Increasing amounts of caspase-3-substrate is not able to abrogate the inhibition of caspase activity. CoPP (10  $\mu$ M) was added to recombinant caspase-3 (C-3) and caspase activity was assessed with varying concentrations of caspase-3-substrate Ac-DEVD-AFC (50 - 1,000  $\mu$ M). Activity of caspase-3 in the absence of the porphyrin was taken as 100 %. \*\*\* $p < 0.001$  vs. C-3.

To clarify the possible molecular mechanism of inhibition we examined which part of the metalloporphyrin-complex is responsible for the inhibitory effect on caspase activity. One approach was the application of the corresponding metals as salts to recombinant caspase-3. Different concentrations were used starting from equimolar amounts (10  $\mu$ M) going down to 25 nM of the salts. All metal salts used showed no significant inhibition of caspase activity. The results for the experiments with  $ZnCl_2$  are shown in **figure 33**. The other salts used were  $CoCl_2$  and  $SnCl_2$  (data not shown).

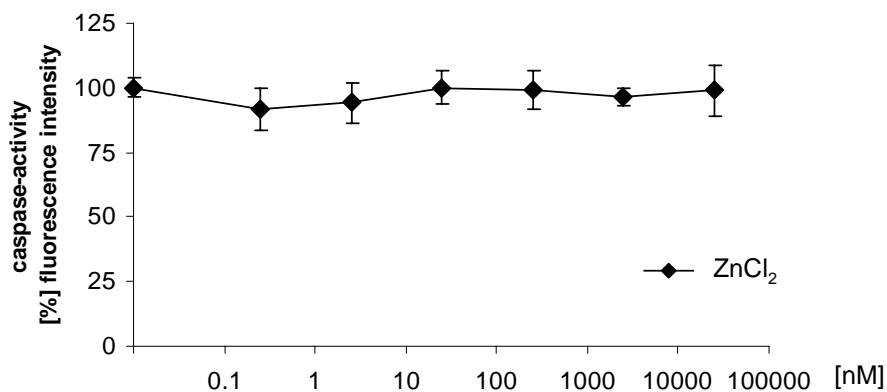


**figure 33:** **ZnCl<sub>2</sub> is not able to inhibit recombinant caspase-3.** Increasing amounts of ZnCl<sub>2</sub> (0.25 nM – 25 μM) were added to recombinant caspase-3 and caspase activity was assessed as described in chapter 2.10. Activity of recombinant caspase-3 in the absence of the metal salt was set as 100 %.

The fact that protoporphyrin IX lacking the metal moiety was also able to inhibit caspase-3-activity (**figure 34**) points to the protoporphyrin-ring as responsible structural element for the caspase-3-inhibition. Molecular modeling data confirmed this assumption.

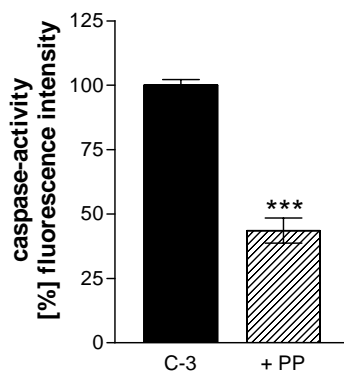


**figure 34:** **Protoporphyrin sodium salt influences the activity of recombinant caspase-3.** Equimolar amounts of protoporphyrin IX sodium salt (PP, 10 μM) was added to recombinant caspase-3 (C-3) and enzyme activity was assessed as described in chapter 2.10. Activity of caspase-3 in the absence of PP was set as 100 %. \*\*\*p<0.001 vs. C-3.

#### 4.2.6 Caspase-3-processing is inhibited by porphyrins

Active caspase-3 is cleaved from its inactive zymogen procaspase-3 by initiator-caspases such as caspase-8. As shown in **figure 35**, treatment with FasL leads to a decrease of the uncleaved procaspase-3. In the presence of CoPP the processing of procaspase-3 is blocked. The same effect could be seen for SnPP (data not shown). This suggests that porphyrins also interfere with caspases upstream of caspase-3.

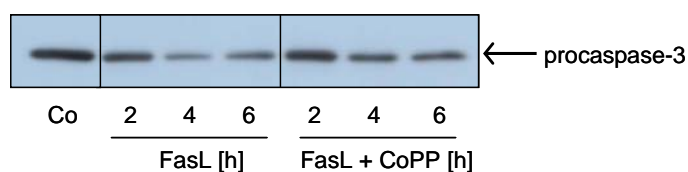


**figure 35: Procaspase-3-processing is inhibited by CoPP in Jurkat T-lymphocytes.** Cells were either left untreated (Co) or treated with FasL (100 ng/ml) in the presence or absence of CoPP (10  $\mu$ M) for the indicated times. Cellular levels of uncleaved procaspase-3 were examined by Western blot as described in chapter 2.5.

#### 4.2.7 Porphyrins inhibit caspase-8-activity

The data presented so far clearly demonstrates that metalloporphyrins directly inhibit caspase-3. The question arises whether this inhibitory effect of the porphyrins is specific for caspase-3 or if other caspases are equally affected.

To address this question we chose caspase-8, being a representative of the initiator caspases, as opposed to caspase-3 which is an executor caspase. To find out at which time point caspase-8-activation becomes detectable, we performed a time course. After 3 h of incubation with FasL, we observed a significant increase in caspase-8-like activity (**figure 36**).

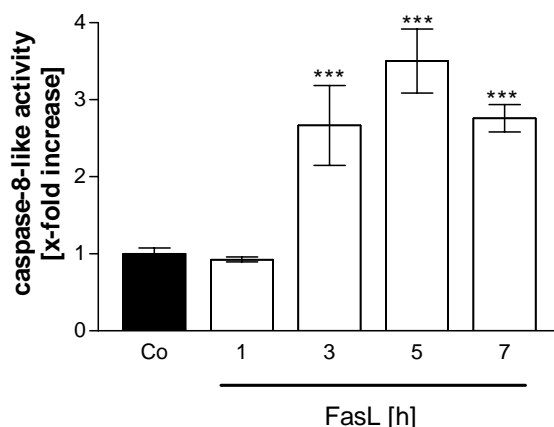


**figure 36: Time-dependent induction of caspase-8-like activity by FasL.** Cells were treated with FasL (100 ng/ml) for the indicated times. Caspase-8-like activity was measured as described in chapter 2.10. Values of untreated cells were set as 1. \*\*\* $p < 0.001$  vs. Co.

Importantly, we found that in whole cells (**figure 37A**) as well as in cell lysates (**figure 37B**) metalloporphyrins had a similarly inhibitory action on caspase-8-like activity as we had observed for caspase-3.

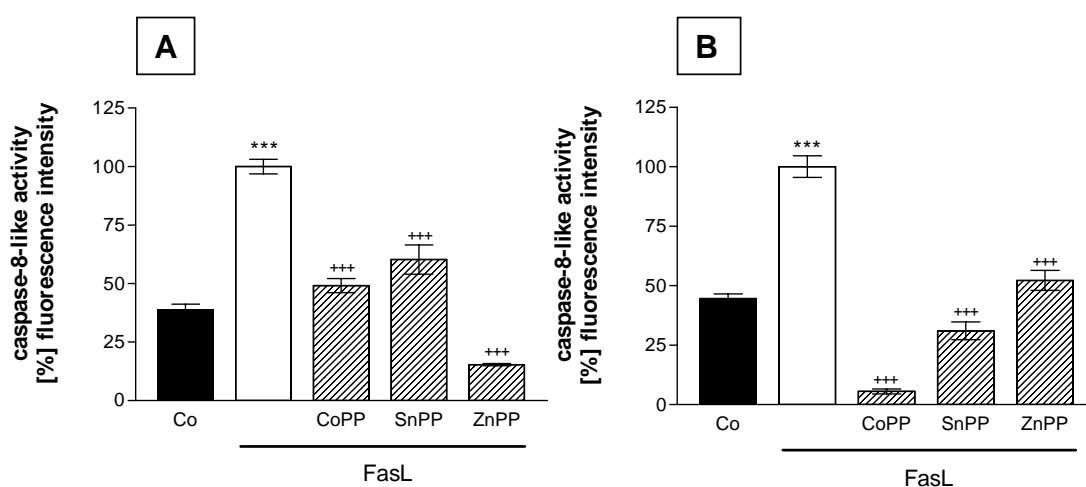


**figure 37: Metalloporphyrins inhibit FasL-induced caspase-8-like activity in Jurkat T-lymphocytes.** Cells were either left untreated (Co) or treated with FasL (100 ng/ml, 5 h). CoPP, SnPP or ZnPP (10  $\mu$ M each) were added either 30 min before the cells were lysed (**A**) or immediately before the measurement of caspase-8-like activity (**B**). Caspase-3-like activity was measured as described in chapter 2.10. Values of FasL-treated cells were set as 100 %. \*\*\* $p < 0.001$  vs. Co. \*\*\* $p < 0.001$  vs. FasL.

The metalloporphyrins were also tested with recombinant caspase-8 and as can be seen in **figure 38A** caspase-8-activity was inhibited to the same extent as recombinant caspase-3. Caspase-8 was similarly inhibited in the *in vivo* model (**figure 38B**).

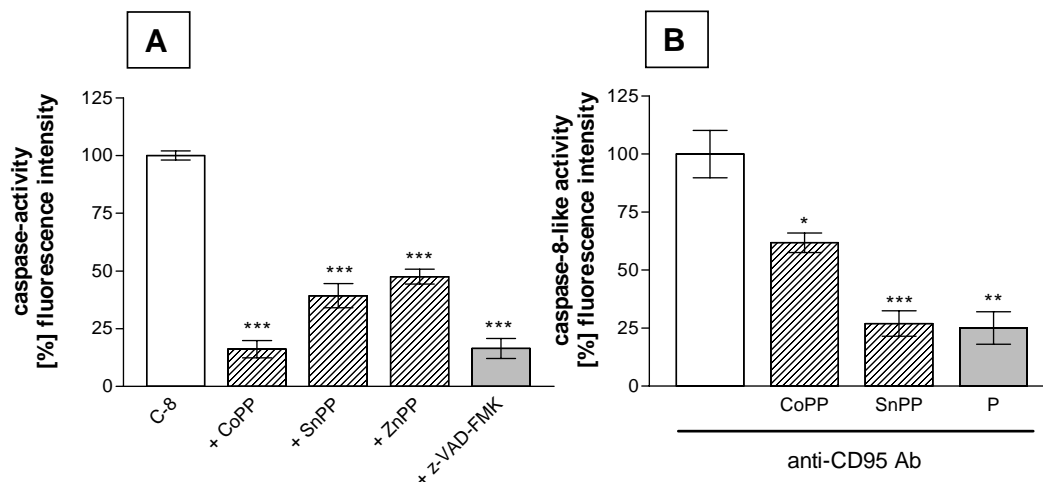


**figure 38: Metalloporphyrins inhibit isolated caspase-8 (A) and caspase-8-like activity *in vivo* (B).** Recombinant caspase-8 (C-8) was incubated with CoPP, SnPP, and ZnPP (10  $\mu$ M each) (A). Z-VAD-fmk (25  $\mu$ M) served as a positive control. Caspase activity was measured as described in chapter 2.10. Activity of caspase-8 alone was taken as 100 %. \*\*\* $p$ <0.001 vs. C-8. Mice were treated with CoPP (10 mg/kg) or SnPP (25 mg/kg) 2 h after induction of caspase activity by anti-CD95 Abs (anti-CD95 Ab, 10 mg/kg) (B). Activity of caspase-8 was detected 6 h after challenge as described in chapter 2.10. SnPP was also added to liver homogenates of mice treated with anti-CD95 Ab immediately before the measurement of caspase activity serving as a positive control (P). Values of anti-CD95 Ab-treated mice were set as 100 %. \*\*\* $p$ <0.001, \*\* $p$ <0.01, \* $p$ <0.05 vs. anti-CD95 Ab.

## 4.2.8 Morphologic alterations

During apoptosis, cells undergo distinct morphologic changes such as cell shrinkage and the formation of apoptotic bodies. FasL treatment induces the formation of apoptotic bodies as indicated in **figure 39**. The treatment of CoPP clearly reduced the formation of apoptotic bodies as observed by light microscopic analysis.

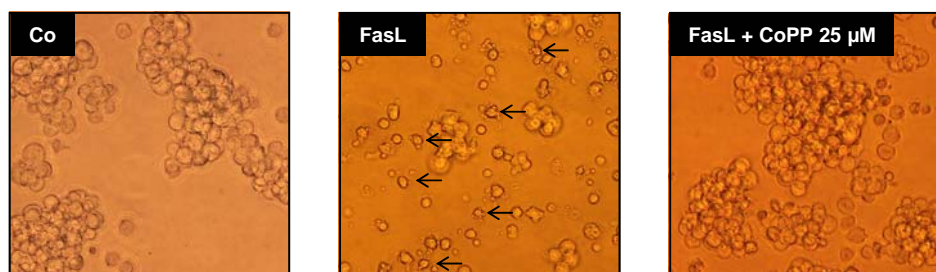


**figure 39: Influence of CoPP on FasL-induced formation of apoptotic bodies.** Jurkat cells were either left untreated (Co) or treated with FasL (10 ng/ml) alone or together with CoPP (10  $\mu$ M) for 6 h. Images were obtained as described in chapter 2.11.1.

## 4.2.9 Molecular modeling studies

Molecular modeling studies confirmed the biochemical data suggesting a direct interaction of metalloporphyrins with caspase-3. Protoporphyrin fits well into the active site of caspase-3, as can be seen from the molecular superposition of the binding conformations extracted from the AutoDock results (**figure 40**).

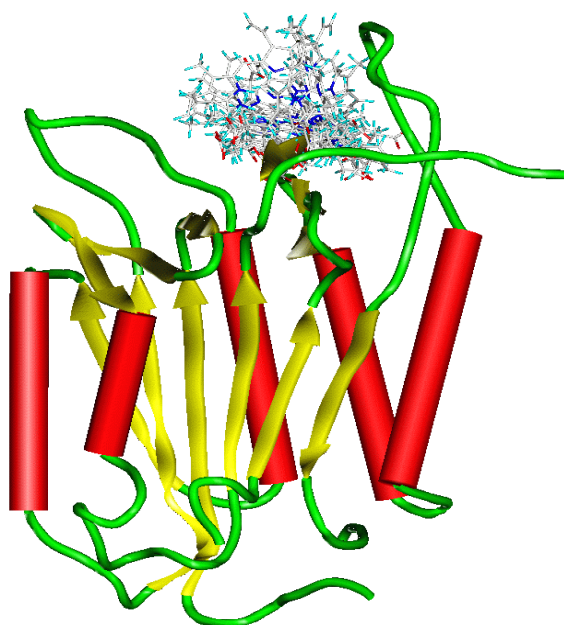


**figure 40: Auto-Dock results.** Caspase-3 together with 10 putative binding conformations of protoporphyrin.

In **figure 41**, the most energetically favorable interaction complex can be viewed in detail: one carboxylate group of the protoporphyrin forms a bidentate salt bridge to the guanidinium group of Arg-341. Moreover, one of the carboxylate oxygens forms a hydrogen bond with the backbone NH of Ser-180. The second carboxylate group acts as a hydrogen bond acceptor for the backbone NH of Arg-341 and for the -OH of Tyr-338. The -OH group of Ser-343 points in the direction of the N/NH atoms of the protoporphyrin in a way that either hydrogen bonds or interactions with a central metal cation can occur.

## RESULTS

---

The protoporphyrin carbon skeleton makes some hydrophobic contacts with Thr-177, Trp-340, and Phe-381B. The program "GRID" was used to test the complete protein for areas that offered energetically favorable interactions with a ligand molecule.

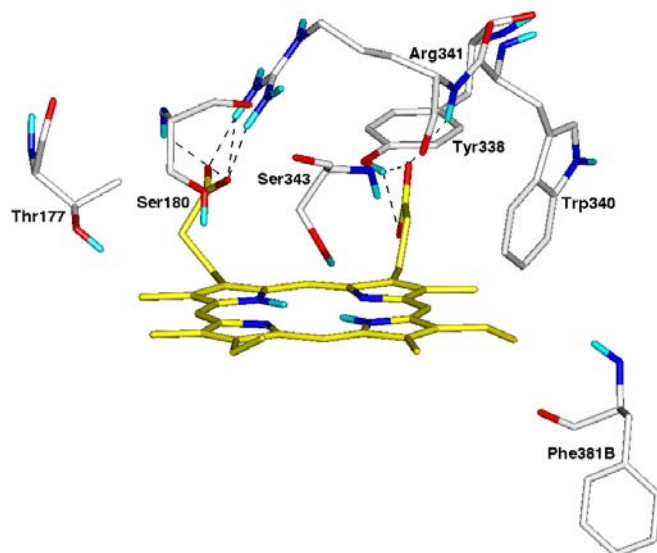


**figure 41: Auto-Dock results.** Representation of the most energetically favorable caspase-3/protoporphyrin-complex showing the major protein-ligand interactions.

Since the protoporphyrin molecule exhibits mainly carbons and carboxylate groups which may act as binding partners for a protein, we selected a hydrophobic probe and a  $\text{CO}^-$  probe as representatives. The calculations suggest that the most favored region of interactions for the probes is located in the active site of the enzyme which is in agreement with our docking procedure. However, from the GRID results one further potential binding region was detected. In order to evaluate its suitability to act as a specific binding site for the protoporphyrin, subsequent AutoDock investigations were performed (data not shown). No energetically favorable binding mode was detected by AutoDock since the protoporphyrin molecule is too bulky to fit well into this pocket. As previously mentioned in chapter 2.12, metal ion properties and influences cannot be estimated reliably with force field methods. To investigate the differences seen in the various metalloporphyrins on caspase-3-activity, extensive quantum chemical computations have to be performed.

### 4.3 TNF- $\alpha$ -induced p38 MAPK and NF- $\kappa$ B activation

In a third part of this work, we aimed to clarify the relationship of TNF- $\alpha$ -induced p38 MAPK and NF- $\kappa$ B activation. The atrial natriuretic peptide (ANP) has previously been shown as an inhibitor of NF- $\kappa$ B activity and p38 MAPK in HUVEC (Kierner *et al.*; 2002). Both p38 MAPK as well as NF- $\kappa$ B have been suggested as a regulator of MCP-1 induction (Roebuck *et al.*; 1999). In this framework we aimed to clarify a potential interplay between these two inflammatory signaling pathways.

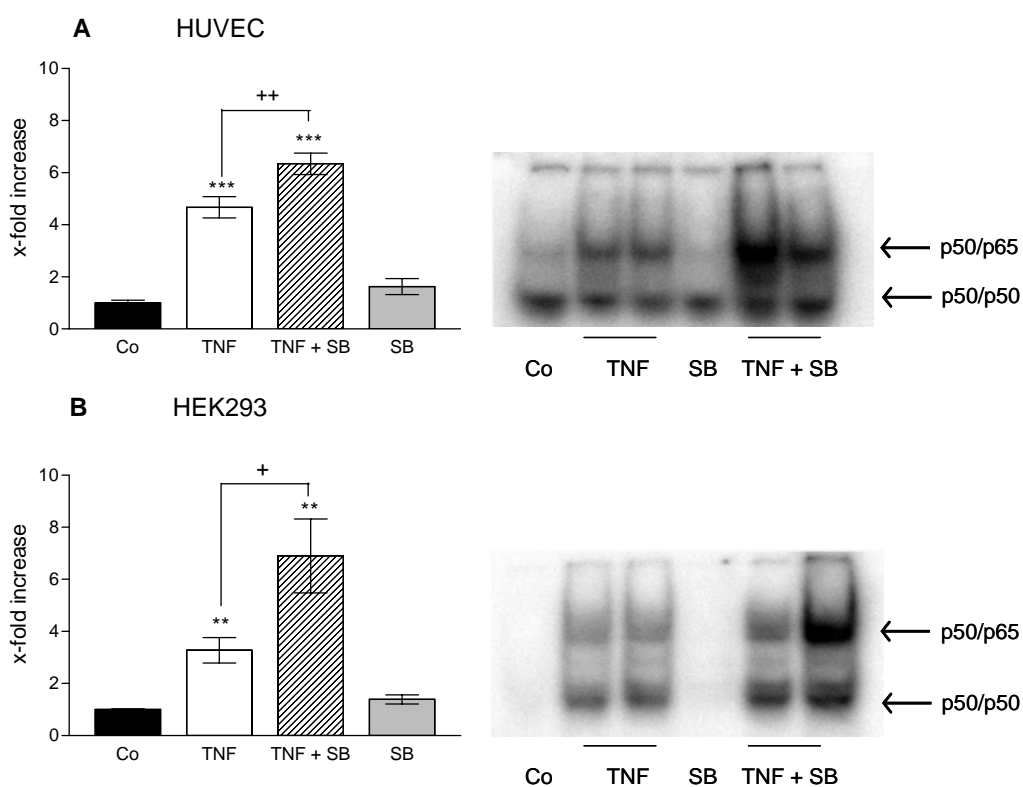


**figure 42: Involvement of p38 in TNF- $\alpha$ -induced NF- $\kappa$ B DNA-binding activity.** HUVEC (A) or HEK 293 (B) were either left untreated (Co) or were treated with TNF- $\alpha$  (60 min, HUVEC: 10 ng/ml; HEK 293: 1 ng/ml) with or without pre-treatment with the p38-inhibitor SB203580 (SB, 5  $\mu$ M) for 60 min. NF- $\kappa$ B-binding activity was assessed by electrophoretic mobility shift assay (EMSA) as described in chapter 2.7. The histograms show phosphoimaging analysis of EMSA experiments. Values of untreated cells were set as 1. \*\*\* $p$ <0.001, \*\* $p$ <0.01 vs. Co. \*\* $p$ <0.01, \* $p$ <0.05 vs. TNF.

In order to investigate the relationship between p38 MAPK and TNF- $\alpha$ -induced NF- $\kappa$ B activity, we performed EMSA employing the chemical p38 MAPK inhibitor, SB203580. These experiments

## RESULTS

were performed in HUVEC as well as in HEK 293. As **figure 42** clearly shows, both TNF- $\alpha$ -stimulated HUVEC and HEK 293 showed a significantly increased NF- $\kappa$ B DNA-binding activity after pre-treatment with SB203580, suggesting an inhibitory action of p38 on NF- $\kappa$ B DNA-binding activity.

Due to potential unspecific effects by the use of chemical kinase inhibitors, we additionally performed Luciferase reporter gene assay using cells transfected with a dominant negative p38 MAPK mutant (Ludwig *et al.*; 1998). Due to the difficulty of efficient HUVEC transfection (Teifel *et al.*; 1997) we used HEK 293 for reporter gene assay. Our observations from EMSA experiments were supported by the results of Luciferase reporter gene assay. As **figure 43** clearly demonstrates, the dominant negative p38 mutant led to a significant increase in NF- $\kappa$ B transcriptional activity compared to TNF- $\alpha$ -treated cells.

These findings reveal that the inhibition of p38 MAPK leads to significant activation of NF- $\kappa$ B transcriptional activity in TNF- $\alpha$ -pre-treated HUVEC and HEK 293. For more details reference is made to the publication by Weber *et al.* (2003).

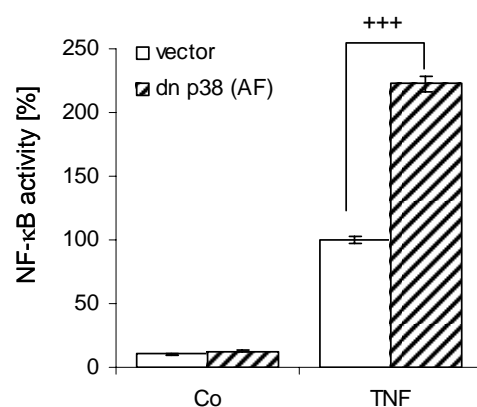


**figure 43: Involvement of p38 in TNF- $\alpha$ -induced NF- $\kappa$ B transcriptional activity.** HEK 293 cells were transfected with pNF- $\kappa$ B-Luc and pSV- $\beta$ Gal plus dn p38 or empty vector as described in chapter 2.9.1. Plasmid-transfected cells were either left untreated (Co) or were treated with TNF (1 ng/ml, 6 h). Luciferase activity was measured as described in chapter 2.9.2. Values of TNF-treated cells transfected with the empty vector were set as 100 %. +++p<0.001 vs. TNF-treated cells transfected with empty vector plasmid.

## 5 DISCUSSION



## 5.1 Salicylates and HO-1

### 5.1.1 Effect of sodium salicylate on IL-4-induced P-selectin

P-selectin on endothelial cells (ECs) has been shown to be a major determinant of inflammatory responses. Two mechanisms to control cell-surface P-selectin expression have been characterized: one that results in rapid up-regulation within minutes after stimulation lasting only several hours and utilizing only preformed protein stored in Weibel-Palade bodies (Geng *et al.*; 1990; Hattori *et al.*; 1989). The other takes several hours to increase P-selectin expression through a sustained increase in gene transcription lasting several hours or even days (Gotsch *et al.*; 1994; Khew-Goodall *et al.*; 1996). The latter mechanism seems to be involved in processes of chronic and allergic inflammation and is mediated by a number of cytokines including interleukin-4 (IL-4) (Khew-Goodall *et al.*; 1999; Yao *et al.*; 1996). Different pharmacological agents, including sodium salicylate (NaSal), have been shown to inhibit IL-4-induced P-selectin expression in ECs (Xia *et al.*; 1998). In the present work we confirmed this finding in our experimental setting and aimed to elucidate the events leading to this inhibition.

#### 5.1.1.1 Induction of P-selectin by IL-4 independent of NF- $\kappa$ B

The transcription factor nuclear factor  $\kappa$ B (NF- $\kappa$ B) is a central mediator of the innate immune response and plays a critical role in the regulation of gene expression of many genes in inflammatory processes, including adhesion molecules. In murine ECs inflammatory mediators such as tumor necrosis factor  $\alpha$  (TNF- $\alpha$ ) and lipopolysaccharide (LPS) increase persistent expression of P-selectin thus implicating a role in chronic inflammation (Gotsch *et al.*; 1994). These mediators mobilize heterodimeric NF- $\kappa$ B proteins from the cytoplasm to the nucleus, where they bind to  $\kappa$ B elements of responsive genes encoding different proteins such as adhesion molecules. In contrast, these mediators do not increase P-selectin expression in human ECs (Yao *et al.*;

1996), which can be explained by the lack of the classical NF- $\kappa$ B binding site for NF- $\kappa$ B heterodimers in the promotor of the human P-selectin gene. In addition, IL-4 was able to induce P-selectin expression in ECs independent of NF- $\kappa$ B DNA-binding as observed by electrophoretic mobility shift assay (EMSA) (Xia *et al.*; 1998). In consistence with the latter results, we found that IL-4 does not induce p65 translocation. This suggests the existence of alternative signaling pathways for the induction of P-selectin expression in human endothelial cells.

Salicylates are known to impair activation of NF- $\kappa$ B (Kopp *et al.*; 1994; Pierce *et al.*; 1996), presumably by inhibiting the phosphorylation of inhibitory protein  $\kappa$ B (I $\kappa$ B) that is required for its degradation and the subsequent release of NF- $\kappa$ B (Bayon *et al.*; 1999; Yin *et al.*; 1998; Yoo *et al.*; 2001). They have been shown to inhibit the ability of inflammatory mediators, such as TNF- $\alpha$  or LPS, to induce expression of E-selectin, VCAM-1, or ICAM-1 in ECs (Weber *et al.*; 1995). This inhibition is mainly attributed to their ability to block activation of NF- $\kappa$ B. However, as mentioned above, the induction of P-selectin expression by IL-4 in human ECs seems to be completely independent of NF- $\kappa$ B activation. Thus, the abrogation of this effect by salicylate cannot be explained by its ability to block NF- $\kappa$ B activation.

### 5.1.1.2 Role of heme oxygenase-1

Several studies have shown that HO-1 has anti-inflammatory features (Otterbein *et al.*; 1999; Willis *et al.*; 1996). Those findings are supported by observations made in cases of murine (Poss *et al.*; 1997) and human (Yachie *et al.*; 1999) HO-1-deficiency.

In the recent years a role of HO-1 in regulating the expression of different adhesion molecules had been suggested by several groups. Interestingly, an inhibition of P-selectin expression by HO-1 had been observed in rodents. Induction by hemin exerted a significant regulatory influence on the expression of P-selectin and E-selectin in different vascular beds in LPS-treated rats (Vachharajani

*et al.*; 2000), in the mesenteric tissue of rats under oxidative stress (Hayashi *et al.*; 1999), and also in an *in vivo* thrombosis model in mice (Lindenblatt *et al.*; 2004). In addition, decreased endothelial expression of P-selectin and ICAM-1 was demonstrated in an ischemia/reperfusion injury model after treatment with the HO-1 product biliverdin (Fondevila *et al.*; 2004). Data regarding a similar inhibition by HO-1 in human cells, however, has as yet been lacking. The question arises whether HO-1 is able to inhibit P-selectin expression also in human cells.

### **5.1.1.3 Alternative signaling pathways**

Induction of P-selectin transcription in HUVEC by IL-4 seems to involve activation of signal transducer and activator of transcription 6 (STAT6) (Khew-Goodall *et al.*; 1999). On the other hand it has been shown that in fibroblasts ASA and NaSal inhibit IL-4-induced activation of STAT6 *via* Src kinase (Perez *et al.*; 2002). However, the causal connection between salicylate-conducted STAT6 inhibition and P-selectin inhibition remains to be elucidated. Moreover, in the study of Perez *et al.* the IL-4-induced STAT6 is not completely abolishable by the same concentration of salicylate as used by us. Therefore, it can be speculated that there is an alternative pathway, involving HO-1, leading to attenuation of P-selectin expression by salicylate.

## **5.1.2 HO-1 induction by sodium salicylate**

In accordance with the anti-inflammatory and cytoprotective potential of HO-1, we have recently found that acetylsalicylic acid (ASA) induces HO-1 expression in ECs (Bildner, 2002). This has also been shown by others (Grosser *et al.*; 2003), who postulated a new site of action for ASA in anti-thrombotic therapy.

Simultaneously, numerous observations were made revealing that nonsteroidal anti-inflammatory drugs (NSAIDs), such as salicylates, cause anti-inflammatory effects mostly independently of

cyclooxygenase (COX) activity and prostaglandin synthesis inhibition. This becomes apparent regarding the doses of ASA necessary to treat chronic inflammatory diseases which are much higher than those required to inhibit COX activity (Abramson *et al.*; 1989). In addition, ASA inhibits COX activity by acetylating the enzyme, whereas salicylate, the active metabolite, lacks the acetyl group and is ineffective as a COX inhibitor at therapeutic doses but is nevertheless able to reduce inflammation (April *et al.*; 1990; Chiabrando *et al.*; 1989; Preston *et al.*; 1989). Therefore, the question as to the mode of action of salicylate becomes central for the understanding of the pharmacology of ASA in anti-inflammatory therapy.

Taken together, these observations led to the question whether NaSal in anti-inflammatory concentrations may be able to abrogate IL-4-induced P-selectin expression in HUVEC *via* an induction of HO-1. In fact, we found that NaSal time- and dose-dependently induces HO-1 protein. Moreover, blocking the HO-1 induction leads to a significant reduction of the inhibitory effect by NaSal, suggesting a participation of HO-1.

These findings implicate a new signal transduction mechanism of salicylate and may provide a better understanding of the anti-inflammatory features of this drug. Therefore, it was of highest interest to elucidate the underlying signaling pathway leading to HO-1 induction.

### 5.1.3 HO-1 induction by JNK and AP-1

The transcription factor activator protein-1 (AP-1) has been reported to play a crucial role in the induction of HO-1 expression by several different stimuli such as atrial natriuretic peptide (ANP), hyperoxia, cholecystokinin-octapeptide (CCK-8), TNF- $\alpha$ , and IL-1 $\alpha$  (Huang *et al.*; 2004; Kiemer *et al.*; 2003; Lee *et al.*; 2000b; Terry *et al.*; 1998). This is consistent with the finding that the human HO-1 gene contains AP-1 binding sites (Lavrovsky *et al.*; 1994). AP-1 activity is known to be

regulated by members of the mitogen activated protein kinase (MAPK) family, predominantly by c-jun N-terminal kinase (JNK) (Widmann *et al.*; 1999).

The recent findings that high-dosed NaSal was able to induce HO-1 expression raised the question whether the JNK/AP-1 pathway might also be involved in the signaling in this experimental setting. In fact, NaSal enhanced phosphorylation of JNK and subsequently AP-1 DNA-binding in HUVEC.

We then aimed to approve the causal relationship between an increased HO-1 expression and an activation of the JNK/AP-1 pathway by NaSal. By inhibiting either AP-1 DNA-binding by decoy ODNs or JNK phosphorylation by employing the JNK inhibitor SP600125, we were able to abrogate the NaSal-induced HO-1 expression. This suggests that the JNK/AP-1 pathway plays a crucial role in the signaling events responsible for an increased HO-1 expression after NaSal treatment.

#### **5.1.3.1 Activation of AP-1 by sodium salicylate**

Our finding that NaSal induces AP-1 DNA-binding differs from the data published on this subject by other investigators (Flescher *et al.*; 1995; Vartiainen *et al.*; 2003). Only two other publications report about stimulatory effects on the transcription factor AP-1 by aspirin-like drugs so far. One paper reports the increase in AP-1-binding activity by salicylates, though only after activation of the spinal cord cultures in a hypoxia/reoxygenation model (Vartiainen *et al.*; 2003). In human T-lymphocytes other nonsteroidal anti-inflammatory drugs such as indomethacin, diclofenac, and flurbiprofen, but not including ASA or NaSal itself, were tested and shown to activate AP-1 (Flescher *et al.*; 1995).

On the other hand, publications about an inhibitory effect of salicylates on AP-1 DNA-binding activity after activation by different stimuli are numerous. In mouse epidermal cells, ASA and NaSal have been shown to inhibit epidermal growth factor-induced AP-1 activation and also basal AP-1 levels (Dong *et al.*; 1997) as well as arsenite-induced AP-1 transactivation (Chen *et al.*; 2001).

Furthermore, salicylates were able to block UV-induced AP-1 activity in transgenic mice (Huang *et al.*; 1997). In human cell systems, salicylates have also shown inhibitory action on AP-1, for instance in human cervical cancer cells after Epstein-Barr virus (EBV) treatment (Muroso *et al.*; 2000).

All this stands in contrast to our findings, but it must be mentioned that all these opposing studies show inhibitory effects of the salicylates only in settings where the cells have been activated by diverse stimuli. Only one of these groups is also looking at the basal effects of ASA and NaSal observing reduced AP-1 levels in mouse epidermal cells (Dong *et al.*; 1997) though lower concentrations of the salicylates were used than implicated in our experiments. Thus, investigations on the basal effects of salicylates on different cell systems are very few, and there is no data whatsoever about the effects of salicylates on AP-1 in ECs.

### 5.1.3.2 Effects of sodium salicylate on JNK/SAPK

In conformity with our findings about the relationship of NaSal and JNK are the findings of Wong *et al.* and Schwenger *et al.* who reported that salicylate treatment leads to activation of JNK in human blood eosinophils (Wong *et al.*; 2000) and in HO-29 colon cancer and COS-1 cells, respectively (Schwenger *et al.*; 1999). On the other hand, the same group had shown earlier that salicylate inhibits the TNF- $\alpha$ -induced activation of JNK in human fibroblasts but fails to elicit JNK activation after treatment with salicylate alone (Schwenger *et al.*; 1997). In mouse epidermal cells salicylates were able to block JNK after UV-radiation (Huang *et al.*; 1997). The contradictory results on this issue suggest that the effects of salicylate on JNK depend on the cellular context.

In conclusion, we elucidated the signaling pathway of NaSal leading to the induction of HO-1 protein expression. The presented data demonstrates that JNK and AP-1 are crucially involved.

## 5.2 Metalloporphyrins and caspases

In the present work we demonstrate that different metalloporphyrins can inactivate caspases *in vitro* as well as *in vivo*. This inactivation could be seen when adding the porphyrins to cells or tissue where the caspases had been activated during apoptosis, to cell lysates containing the activated enzymes, and also to recombinant caspase-3 and -8. This strongly suggests that the observed inhibitory effect is a direct one.

### 5.2.1 Characterization of the inhibitory action

To clarify the possible molecular mechanism of inhibition we examined which part of the metalloporphyrin-complex is responsible for the inhibitory effect on caspase-3-like activity. In fact, we saw a similar effect by using protoporphyrin IX disodium salt on isolated caspase-3. Employing the corresponding metal salts did not mimic the inhibitory action on caspase activity by the different metalloporphyrins.

In this context it has been shown that heavy metals like zinc at micromolar concentrations are able to influence activity of the isolated caspase-3, possibly by coordinating with one or two amino acids of the active site of the enzyme (Truong-Tran *et al.*; 2001). The effects of  $Zn^{2+}$  were investigated on apoptotic events in leukemia cells (Perry *et al.*; 1997) and in a cell-free model (Stennicke *et al.*; 1997), revealing caspase-3 and others as a target of zinc inhibition in apoptosis. Kown *et al.* demonstrated that zinc suppresses caspase-3-activity and apoptosis *in vivo* using rats transplanted in the abdomen with allogeneic hearts (Kown *et al.*; 2000). On the other hand, stimulating effects of cobalt ions on caspase activity and expression in macrophages were the results of the work by Petit *et al.* (Petit *et al.*; 2004). However, the findings of this and another study showing similar effects after  $CoCl_2$  treatment in PC12 cells (Zou *et al.*; 2002) were attained with quite high

concentrations and after long-term treatments. Therefore, mechanisms different from the direct ones observed in this work are likely to be involved in the latter findings.

Taken together, the data presented here implicates that the inhibition of caspase activity by the metalloporphyrins is mainly accountable to the porphyrin-ring.

Therefore, it is especially interesting to note that there are differences in the potency of the different metalloporphyrins in inhibiting caspase activity. CoPP is the most efficient inhibitor of the three metalloporphyrins that were examined. In summary, this still remains a controversial issue and considering the complex stabilities of typical metalloporphyrins which allow free metal to occur in the attomolar ( $10^{-18}$  M) range (Bonnett, 2003), it is most unlikely that enough free metal is available to account for the differences seen in the various metalloporphyrins. Detailed molecular modeling studies are under way to investigate the molecular basis of this matter as well as the effects on other caspases.

### 5.2.2 Metalloporphyrins as a new class of caspase-inhibitors

Our work identifies metalloporphyrins as a novel class of irreversible caspase inhibitors. So far, known inhibitors are members of the family of inhibitors of apoptosis protein (IAP) and the two virus-derived proteins cowpox serpin CrmA and p35 from baculovirus (Riedl *et al.*; 2004; Stennicke *et al.*; 2002). Besides these naturally occurring compounds, well established and widely used caspase inhibitors have been generated by synthetically coupling caspase-specific peptide-sequences to certain aldehyde (CHO), chloromethylketone (CMK), fluoroacyloxymethylketone (FAOM), or fluoromethylketone (FMK) compounds (Cohen, 1997).

Several x-ray crystal structures reveal how specific peptidic and non-peptidic inhibitors bind to caspase-3 (Erlanson *et al.*; 2003; Lee *et al.*; 2000a; Riedl *et al.*; 2001; Rotonda *et al.*; 1996). The ligands occupy the active site of the caspase in the S1-S4 regions. The interactions between the

ligands and the protein mainly result from hydrophobic contacts and hydrogen bonds. A free carboxyl acid seems to play an important role in the ligand structure since it is critical for the binding of the inhibitors to the caspase enzyme. Our investigations demonstrate that the protoporphyrin can occupy the active site of caspase-3 energetically favorable and in a binding mode similar to that of known inhibitors. This postulated binding mode is consistent with crystal data of caspase-3, in which the inhibitors occupy similar parts of the active site. The very potent peptidic inhibitor XIAP-BIR2 exhibits an Asp-148 residue that is essential for the inhibiting effect (mutations of Asp-148 lead to a complete loss of inhibitory activity). Asp-148 forms hydrogen bonds *via* its backbone and its side chain atoms to Arg-341 and Ser-343. The protoporphyrin seems to meet the structural requirements for caspase-inhibitors well since it is able to form (among hydrophobic contacts) the important interactions between its free carboxylic acids and the corresponding amino acids in the catalytic center of the enzyme.

### 5.2.3 Physiological relevance

Metalloporphyrins as inhibitors of caspase-3 and -8 raise the question of the physiological function of these compounds. A possible *in vivo* relevance may be discussed using zinc protoporphyrin as an example. Research concerning ZnPP as a naturally occurring metabolite of heme biosynthesis has dramatically increased in the past decade. So far, proposed physiological functions are the control of heme catabolism until bilirubin conjugation becomes activated in neonates and a possible modulation of CO production in brain metabolism (Labbe *et al.*; 1999). In addition, the therapeutic potential of ZnPP and other metalloporphyrins has attracted interest in the treatment of hyperbilirubinemia (Kappas, 2004; Maines *et al.*; 1992). As yet, all of these suggested functions have been connected to the inhibitory effect of ZnPP on the HO system. Our data introduces a direct inhibitory effect on caspase activity as an additional mechanism of action of ZnPP. This knowledge may provide a better understanding of the role of this metabolite in physiology as well as in pathophysiology.

### 5.2.4 HO-independent effects of metalloporphyrins

Our data, demonstrating that metalloporphyrins directly inhibit caspases, indicates that these substances have additional effects to their HO-dependent actions. This information therefore largely contributes to the controversial topic concerning the selectivity of pharmacologic inhibitors. In fact, several studies have raised concern that these porphyrins may have substantial effects on other heme-dependent proteins. In this context Ignarro *et al.* revealed inhibitory effects on isolated guanylate cyclase by different metalloporphyrins. Interestingly, metal-free protoporphyrin IX itself was found to activate soluble guanylate cyclase (sGC) and metallation of the protoporphyrin IX converted the potent activator into an inhibitor of the isolated enzyme (Ignarro *et al.*; 1984). Another study conclusively demonstrated that the HO-1 inhibitors tin-protoporphyrin (SnPP) and zinc(II)-protoporphyrin (ZnPP) have a blocking effect on purified sGC *in vitro* and pointed out that studies using metalloporphyrins as inhibitors of HO must be carried out and interpreted with care (Serfass *et al.*; 1998). Luo *et al.* demonstrated in an *in vivo* setting a direct inhibition of sGC by ZnPP and SnPP (Luo *et al.*; 1994).

The non-selectivity of some metalloporphyrins was further emphasized by Meffert *et al.* by demonstrating an inhibition of hippocampal nitric oxide synthase (NOS) by ZnPP and other porphyrins (Meffert *et al.*; 1994). Jozkowicz *et al.* found differential effects of metalloporphyrins in vascular smooth muscle cells (VSMCs) and macrophages and thus postulated that the influence of the inhibition of the HO-1 enzymatic activity is masked by HO-1-independent effects of metalloporphyrins on NOS (Jozkowicz *et al.*; 2003). However, both NOS and sGC are heme-containing proteins and interestingly the target enzymes identified in the present work, the caspases, do not contain heme. Thus, the outcome of this study shows a novel mode of action for metalloporphyrins and introduces them as a new class of caspase-inhibitors.

Further effects have been shown for ZnPP, which led to an irreversible attenuation of Ca<sup>2+</sup> current in pituitary cells (Linden *et al.*; 1993). Likewise, ZnPP significantly inhibited hematopoiesis in rabbit

and human bone marrow (Lutton *et al.*; 1997) and modulated the viability of cells (Jozkowicz *et al.*; 2003; Lutton *et al.*; 1997). The mechanisms for these effects are not well examined and it remains to be elucidated whether they do involve heme-dependent enzymes or not. Yet, all these observations are clearly not fully explicable by their modulating action on the HO system and thus support the hypothesis that these heme-analogues exert quite a range of HO-independent actions. The observed increase in cell viability in different cell types (Jozkowicz *et al.*; 2003; Lutton *et al.*; 1997), for instance, which was observed for SnPP, may be explicable by the inhibitory effect on caspase activity.

Based on our findings, the usage of CoPP as HO-1 inducer is not helpful when examining anti-apoptotic effects of HO-1. As shown by the presented data, direct effects of porphyrins on caspases could occur time dependently, independent of HO-1 expression. Furthermore, employing SnPP and ZnPP as HO-1 inhibitors in order to prove anti-apoptotic functions of HO-1 should lead to contradictory results depending on the time frame.

However, a huge number of studies employing HO-1-inducers or -inhibitors other than metallo-porphyrins and reporting cytoprotective features of HO-1, certainly justify the assumption of cytoprotective features of HO-1. Induction of the enzyme by other well established methods such as sodium arsenite (Fauconneau *et al.*; 2002), tetracycline-regulated expression systems (Petrache *et al.*; 2000), adenoviral gene transfer (Sass *et al.*; 2003), or doxorubicin (Ito *et al.*; 2000), and furthermore, inhibition of the HO system by antisense (Choi *et al.*; 2004) or siRNA approaches (Zhang *et al.*; 2004) clearly showed HO-1-dependent reduction of apoptotic cell death in different cell types *in vitro* and *in vivo*.



## **6 SUMMARY**



## 6.1 Salicylates and HO-1

The active metabolite sodium salicylate (NaSal) of the NSAID acetylsalicylic acid (ASA) inhibits IL-4-induced P-selectin expression. In the first part of the present work we revealed that this inhibition is partly due to the ability of NaSal to induce HO-1 expression. By blocking HO-1 the inhibitory action of NaSal on IL-4 induced P-selectin expression was diminished. Furthermore, we elucidated the underlying signaling pathway of the HO-1 induction by NaSal. Salicylate was shown to increase the phosphorylation of JNK as well as the DNA-binding activity of the transcription factor AP-1 (figure 44). The causal link of these effects to the NaSal-induced induction of HO-1 expression was demonstrated by employing a JNK-inhibitor and AP-1 decoy ODN.

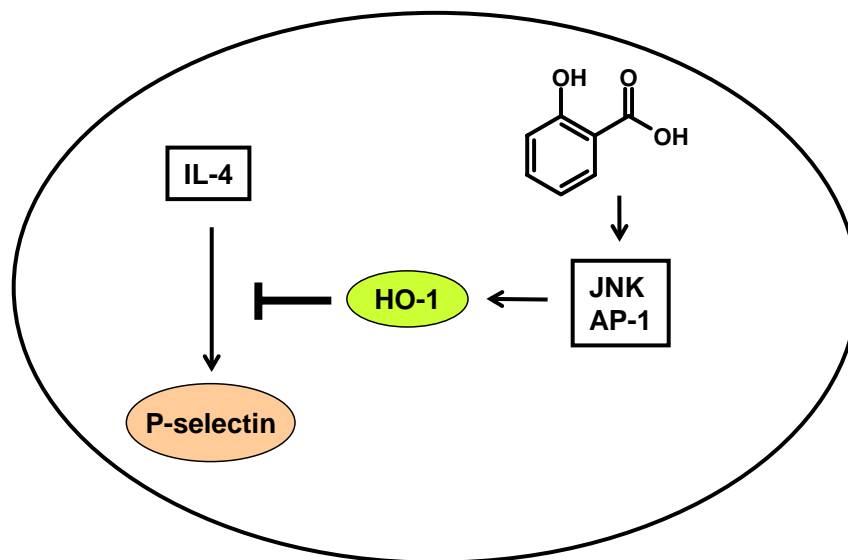


**figure 44:** Schematic diagram of the signal transduction of the HO-1-mediated inhibition of IL-4-induced P-selectin expression by salicylate. Salicylate induces HO-1 expression *via* the JNK/AP-1 pathways. This leads to a diminished induction of P-selectin expression induced by IL-4.

In summary, the findings of the present study reveal a new anti-inflammatory signal transduction mechanism for salicylate. This is in line with findings of the recent past suggesting that nonsteroidal anti-inflammatory drugs such as salicylates cause anti-inflammatory effects mostly independent of cyclooxygenase (COX) activity and prostaglandin synthesis inhibition.

## 6.2 Metalloporphyrins and caspases

In the second part of this work we report an important finding: the HO-1 inhibitors tin- and zinc(II)-protoporphyrin IX (SnPP, ZnPP) and the strong HO-1-inducer cobalt(III)-protoporphyrin IX (CoPP) inhibit caspase activity unrelated to HO-1 expression and activity *in vitro* and *in vivo*. In fact, by using recombinant caspase-3 and -8 and also by performing molecular modeling studies for caspase-3, a direct inhibition of caspase activity by the porphyrins could be demonstrated.

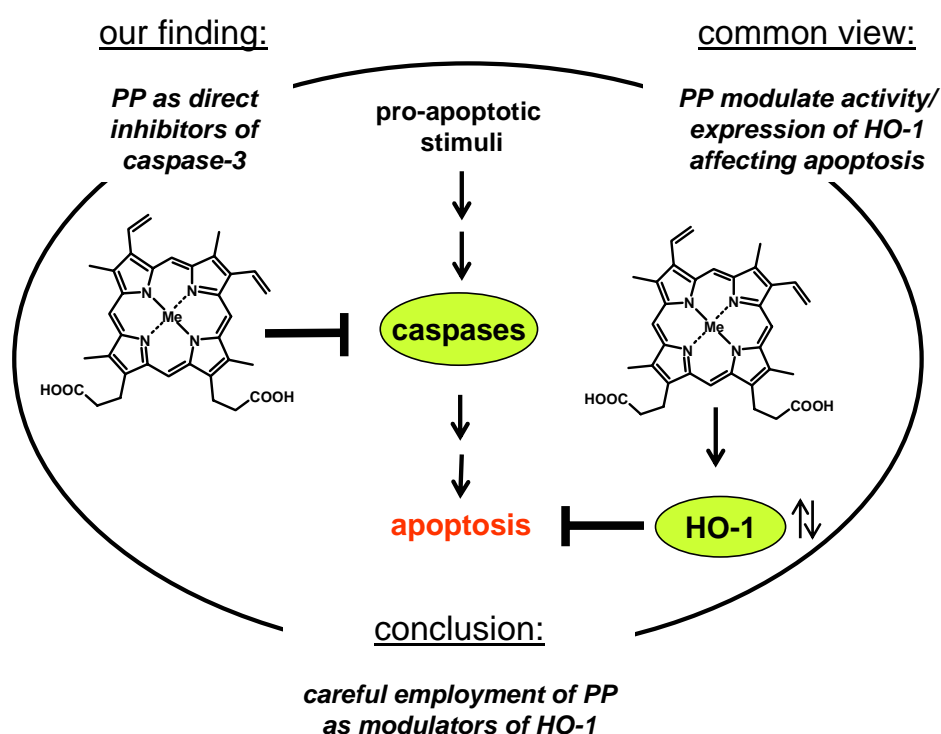


**figure 45:** Schematic model of caspase inhibition by metalloporphyrins. Besides the known mechanism of metalloporphyrins to interfere with apoptosis via HO-1 modulation, porphyrins can directly inhibit caspases after activation by pro-apoptotic stimuli.

In summary, the finding that metalloporphyrins directly inhibit caspase activity points to a novel class of caspase-inhibitors, but also requests their careful employment as modulators of the HO-system.

## **7 BIBLIOGRAPHY**



**Abramson, S. and Weissmann, G.** (1989) The mechanisms of action of nonsteroidal antiinflammatory drugs. *Clin Exp Rheumatol*; 7 Suppl 3S163-S170

**Aceves, M., Duenas, A., Gomez, C., San Vicente, E., Crespo, M.S., and Garcia-Rodriguez, C.** (2004) A new pharmacological effect of salicylates: inhibition of NFAT-dependent transcription. *J Immunol*; 173(9): 5721-5729

**Aizawa, T., Ishizaka, N., Kurokawa, K., Nagai, R., Nakajima, H., Taguchi, J., and Ohno, M.** (2001) Different effects of angiotensin II and catecholamine on renal cell apoptosis and proliferation in rats. *Kidney Int*; 59(2): 645-653

**Amann, R. and Peskar, B.A.** (2002) Anti-inflammatory effects of aspirin and sodium salicylate. *Eur J Pharmacol*; 447(1): 1-9

**Aplin, A.E., Howe, A., Alahari, S.K., and Juliano, R.L.** (1998) Signal transduction and signal modulation by cell adhesion receptors: the role of integrins, cadherins, immunoglobulin-cell adhesion molecules, and selectins. *Pharmacol Rev*; 50(2): 197-263

**April, P., Abeles, M., Baraf, H., Cohen, S., Curran, N., Doucette, M., Ekholm, B., Goldlust, B., Knee, C.M., Lee, E., and .** (1990) Does the acetyl group of aspirin contribute to the antiinflammatory efficacy of salicylic acid in the treatment of rheumatoid arthritis? *Semin Arthritis Rheum*; 19(4 Suppl 2): 20-28

**Balla, G., Jacob, H.S., Balla, J., Rosenberg, M., Nath, K., Apple, F., Eaton, J.W., and Vercellotti, G.M.** (1992) Ferritin: a cytoprotective antioxidant strategem of endothelium. *J Biol Chem*; 267(25): 18148-18153

**Balla, G., Vercellotti, G.M., Muller-Eberhard, U., Eaton, J., and Jacob, H.S.** (1991) Exposure of endothelial cells to free heme potentiates damage mediated by granulocytes and toxic oxygen species. *Lab Invest*; 64(5): 648-655

**Bayon, Y., Alonso, A., and Sanchez, C.M.** (1999) 4-trifluoromethyl derivatives of salicylate, triflusal and its main metabolite 2-hydroxy-4-trifluoromethylbenzoic acid, are potent inhibitors of nuclear factor kappaB activation. *Br J Pharmacol*; 126(6): 1359-1366

**Beri, R. and Chandra, R.** (1993) Chemistry and biology of heme. Effect of metal salts, organometals, and metalloporphyrins on heme synthesis and catabolism, with special reference to clinical implications and interactions with cytochrome P-450. *Drug Metab Rev*; 25(1-2): 49-152

**Bildner, N.** (2002) Characterization of heme oxygenase-1 induction in human endothelial cells. *Dissertation*

**Bonnett, R.** (2003) *Comprehensive Coordination Chemistry II*; Vol.9: Metal Complexes for Photodynamic Therapy. 2<sup>nd</sup> Ed., Amsterdam, NY, Elsevier Scientific Publ. Co

**Boussif, O., Lezoualc'h, F., Zanta, M.A., Mergny, M.D., Scherman, D., Demeneix, B., and Behr, J.P.** (1995) A versatile vector for gene and

oligonucleotide transfer into cells in culture and *in vivo*: polyethylenimine. *Proc Natl Acad Sci U S A*; 92(16): 7297-7301

**Bradding, P., Feather, I.H., Howarth, P.H., Mueller, R., Roberts, J.A., Britten, K., Bews, J.P., Hunt, T.C., Okayama, Y., Heusser, C.H., and .** (1992) Interleukin 4 is localized to and released by human mast cells. *J Exp Med*; 176(5): 1381-1386

**Bradford, M.M.** (1976) A rapid and sensitive method for the quantitation of microgram quantities of protein utilizing the principle of protein-dye binding. *Anal Biochem*; 72:248-254

**Brouard, S., Otterbein, L.E., Anrather, J., Tobiasch, E., Bach, F.H., Choi, A.M., and Soares, M.P.** (2000) Carbon monoxide generated by heme oxygenase 1 suppresses endothelial cell apoptosis. *J Exp Med*; 192(7): 1015-1026

**Bustin, S.A.** (2002) Quantification of mRNA using real-time reverse transcription PCR (RT-PCR): trends and problems. *J Mol Endocrinol*; 29(1): 23-39

**Chen, N., Ma, W.Y., and Dong, Z.** (2001) Inhibition of arsenite-induced apoptosis by aspirin. *Anticancer Res*; 21(5): 3247-3251

**Chiabrando, C., Castelli, M.G., Cozzi, E., Fanelli, R., Campoleoni, A., Balotta, C., Latini, R., and Garattini, S.** (1989) Antiinflammatory action of salicylates: aspirin is not a prodrug for salicylate against rat carrageenin pleurisy. *Eur J Pharmacol*; 159(3): 257-264

**Choi, B.M., Pae, H.O., Jeong, Y.R., Oh, G.S., Jun, C.D., Kim, B.R., Kim, Y.M., and Chung, H.T.** (2004) Overexpression of heme oxygenase (HO)-1 renders Jurkat T cells resistant to fas-mediated apoptosis: involvement of iron released by HO-1. *Free Radic Biol Med*; 36(7): 858-871

**Cines, D.B., Pollak, E.S., Buck, C.A., Loscalzo, J., Zimmerman, G.A., McEver, R.P., Pober, J.S., Wick, T.M., Konkle, B.A., Schwartz, B.S., Barnathan, E.S., McCrae, K.R., Hug, B.A., Schmidt, A.M., and Stern, D.M.** (1998) Endothelial cells in physiology and in the pathophysiology of vascular disorders. *Blood*; 91(10): 3527-3561

**Clark, J.E., Green, C.J., and Motterlini, R.** (1997) Involvement of the heme oxygenase-carbon monoxide pathway in keratinocyte proliferation. *Biochem Biophys Res Commun*; 241(2): 215-220

**Cohen, G.M.** (1997) Caspases: the executioners of apoptosis. *Biochem J*; 326 (Pt 1):1-16

**Collins, T., Read, M.A., Neish, A.S., Whitley, M.Z., Thanos, D., and Maniatis, T.** (1995) Transcriptional regulation of endothelial cell adhesion molecules: NF-kappa B and cytokine-inducible enhancers. *FASEB J*; 9(10): 899-909

**Cotran, R.S., Kumar, V., and Collins, T.** (1999) Pathologic Basis of Disease: Acute and chronic inflammation. 6<sup>th</sup> Ed., Philadelphia, *W.B. Saunders Company*

- De Martin, R., Hoeth, M., Hofer-Warbinek, R., and Schmid, J.A.** (2000) The transcription factor NF-kappa B and the regulation of vascular cell function. *Arterioscler Thromb Vasc Biol*; 20(11): E83-E88
- Denault, J.B. and Salvesen, G.S.** (2002) Caspases: keys in the ignition of cell death. *Chem Rev*; 102(12): 4489-4500
- Dong, Z., Huang, C., Brown, R.E., and Ma, W.Y.** (1997) Inhibition of activator protein 1 activity and neoplastic transformation by aspirin. *J Biol Chem*; 272(15): 9962-9970
- Dorman, R.B., Bajt, M.L., Farhood, A., Mayes, J., and Jaeschke, H.** (2004) Heme oxygenase-1 induction in hepatocytes and non-parenchymal cells protects against liver injury during endotoxemia. *Comp Hepatol*; 3 Suppl 1S42-
- Durante, W.** (2003) Heme oxygenase-1 in growth control and its clinical application to vascular disease. *J Cell Physiol*; 195(3): 373-382
- Earnshaw, W.C., Martins, L.M., and Kaufmann, S.H.** (1999) Mammalian caspases: structure, activation, substrates, and functions during apoptosis. *Annu Rev Biochem*; 68:383-424
- Erbacher, P., Remy, J.S., and Behr, J.P.** (1999) Gene transfer with synthetic virus-like particles *via* the integrin-mediated endocytosis pathway. *Gene Ther*; 6(1): 138-145
- Erlanson, D.A., Lam, J.W., Wiesmann, C., Luong, T.N., Simmons, R.L., DeLano, W.L., Choong, I.C., Burdett, M.T., Flanagan, W.M., Lee, D., Gordon, E.M., and O'Brien, T.** (2003) In situ assembly of enzyme inhibitors using extended tethering. *Nat Biotechnol*; 21(3): 308-314
- Fauconneau, B., Petegnief, V., Sanfeliu, C., Piriou, A., and Planas, A.M.** (2002) Induction of heat shock proteins (HSPs) by sodium arsenite in cultured astrocytes and reduction of hydrogen peroxide-induced cell death. *J Neurochem*; 83(6): 1338-1348
- Flescher, E., Ledbetter, J.A., Ogawa, N., Vela-Roch, N., Fossum, D., Dang, H., and Talal, N.** (1995) Induction of transcription factors in human T lymphocytes by aspirin-like drugs. *Cell Immunol*; 160(2): 232-239
- Fondevila, C., Shen, X.D., Tsuchiyashi, S., Yamashita, K., Csizmadia, E., Lassman, C., Busuttil, R.W., Kupiec-Weglinski, J.W., and Bach, F.H.** (2004) Biliverdin therapy protects rat livers from ischemia and reperfusion injury. *Hepatology*; 40(6): 1333-1341
- Fürst, R.** (2005) Identification of MKP-1 as a central mediator of cytoprotective effects in human endothelial cells: pathways of induction. *Dissertation*
- Galley, H.F. and Webster, N.R.** (2004) Physiology of the endothelium. *Br J Anaesth*; 93(1): 105-113

- Geng, J.G., Bevilacqua, M.P., Moore, K.L., McIntyre, T.M., Prescott, S.M., Kim, J.M., Bliss, G.A., Zimmerman, G.A., and McEver, R.P.** (1990) Rapid neutrophil adhesion to activated endothelium mediated by GMP-140. *Nature*; 343(6260): 757-760
- Gotsch, U., Jager, U., Dominis, M., and Vestweber, D.** (1994) Expression of P-selectin on endothelial cells is upregulated by LPS and TNF-alpha *in vivo*. *Cell Adhes Commun*; 2(1): 7-14
- Graham, F.L., Smiley, J., Russell, W.C., and Nairn, R.** (1977) Characteristics of a human cell line transformed by DNA from human adenovirus type 5. *J Gen Virol*; 36(1): 59-74
- Graham, F.L. and van der Eb, A.J.** (1973) A new technique for the assay of infectivity of human adenovirus 5 DNA. *Virology*; 52(2): 456-467
- Green, D.R.** (1998) Apoptotic pathways: the roads to ruin. *Cell*; 94(6): 695-698
- Grober, J.S., Bowen, B.L., Ebling, H., Athey, B., Thompson, C.B., Fox, D.A., and Stoolman, L.M.** (1993) Monocyte-endothelial adhesion in chronic rheumatoid arthritis. In situ detection of selectin and integrin-dependent interactions. *J Clin Invest*; 91(6): 2609-2619
- Grosser, N., Abate, A., Oberle, S., Vreman, H.J., Dennery, P.A., Becker, J.C., Pohle, T., Seidman, D.S., and Schroder, H.** (2003) Heme oxygenase-1 induction may explain the antioxidant profile of aspirin. *Biochem Biophys Res Commun*; 308(4): 956-960
- Gurtu, V., Kain, S.R., and Zhang, G.** (1997) Fluorometric and colorimetric detection of caspase activity associated with apoptosis. *Anal Biochem*; 251(1): 98-102
- Hamid, Q., Boguniewicz, M., and Leung, D.Y.** (1994) Differential in situ cytokine gene expression in acute versus chronic atopic dermatitis. *J Clin Invest*; 94(2): 870-876
- Hancock, W.W., Buelow, R., Sayegh, M.H., and Turka, L.A.** (1998) Antibody-induced transplant arteriosclerosis is prevented by graft expression of anti-oxidant and anti-apoptotic genes. *Nat Med*; 4(12): 1392-1396
- Hattori, R., Hamilton, K.K., Fugate, R.D., McEver, R.P., and Sims, P.J.** (1989) Stimulated secretion of endothelial von Willebrand factor is accompanied by rapid redistribution to the cell surface of the intracellular granule membrane protein GMP-140. *J Biol Chem*; 264(14): 7768-7771
- Hayashi, S., Takamiya, R., Yamaguchi, T., Matsumoto, K., Tojo, S.J., Tamatani, T., Kitajima, M., Makino, N., Ishimura, Y., and Suematsu, M.** (1999) Induction of heme oxygenase-1 suppresses venular leukocyte adhesion elicited by oxidative stress: role of bilirubin generated by the enzyme. *Circ Res*; 85(8): 663-671

- Hengartner, M.O.** (2000) The biochemistry of apoptosis. *Nature*; 407(6805): 770-776
- Huang, C., Ma, W.Y., Hanenberger, D., Cleary, M.P., Bowden, G.T., and Dong, Z.** (1997) Inhibition of ultraviolet B-induced activator protein-1 (AP-1) activity by aspirin in AP-1-luciferase transgenic mice. *J Biol Chem*; 272(42): 26325-26331
- Huang, X.L., Ling, Y.L., Ling, Y.Q., Zhou, J.L., Liu, Y., and Wang, Q.H.** (2004) Heme oxygenase-1 in cholecystokinin-octapeptide attenuated injury of pulmonary artery smooth muscle cells induced by lipopolysaccharide and its signal transduction mechanism. *World J Gastroenterol*; 10(12): 1789-1794
- Ignarro, L.J., Ballot, B., and Wood, K.S.** (1984) Regulation of soluble guanylate cyclase activity by porphyrins and metalloporphyrins. *J Biol Chem*; 259(10): 6201-6207
- Immenschuh, S. and Ramadori, G.** (2000) Gene regulation of heme oxygenase-1 as a therapeutic target. *Biochem Pharmacol*; 60(8): 1121-1128
- Ito, K., Ozasa, H., Sanada, K., and Horikawa, S.** (2000) Doxorubicin preconditioning: a protection against rat hepatic ischemia-reperfusion injury. *Hepatology*; 31(2): 416-419
- Jan, J.T., Chen, B.H., Ma, S.H., Liu, C.I., Tsai, H.P., Wu, H.C., Jiang, S.Y., Yang, K.D., and Shaio, M.F.** (2000) Potential dengue virus-triggered apoptotic pathway in human neuroblastoma cells: arachidonic acid, superoxide anion, and NF-kappaB are sequentially involved. *J Virol*; 74(18): 8680-8691
- Johnson-Tidey, R.R., McGregor, J.L., Taylor, P.R., and Poston, R.N.** (1994) Increase in the adhesion molecule P-selectin in endothelium overlying atherosclerotic plaques. Coexpression with intercellular adhesion molecule-1. *Am J Pathol*; 144(5): 952-961
- Jordan, M., Schallhorn, A., and Wurm, F.M.** (1996) Transfecting mammalian cells: optimization of critical parameters affecting calcium-phosphate precipitate formation. *Nucleic Acids Res*; 24(4): 596-601
- Jozkowicz, A. and Dulak, J.** (2003) Effects of protoporphyrins on production of nitric oxide and expression of vascular endothelial growth factor in vascular smooth muscle cells and macrophages. *Acta Biochim Pol*; 50(1): 69-79
- Kappas, A.** (2004) A method for interdicting the development of severe jaundice in newborns by inhibiting the production of bilirubin. *Pediatrics*; 113(1 Pt 1): 119-123
- Katori, M., Busuttil, R.W., and Kupiec-Weglinski, J.W.** (2002) Heme oxygenase-1 system in organ transplantation. *Transplantation*; 74(7): 905-912
- Kerr, J.F., Wyllie, A.H., and Currie, A.R.** (1972) Apoptosis: a basic biological phenomenon with wide-ranging implications in tissue kinetics. *Br J Cancer*; 26(4): 239-257

**Khew-Goodall, Y., Butcher, C.M., Litwin, M.S., Newlands, S., Korpelainen, E.I., Noack, L.M., Berndt, M.C., Lopez, A.F., Gamble, J.R., and Vadas, M.A.** (1996) Chronic expression of P-selectin on endothelial cells stimulated by the T-cell cytokine, interleukin-3. *Blood*; 87(4): 1432-1438

**Khew-Goodall, Y., Wadham, C., Stein, B.N., Gamble, J.R., and Vadas, M.A.** (1999) Stat6 activation is essential for interleukin-4 induction of P-selectin transcription in human umbilical vein endothelial cells. *Arterioscler Thromb Vasc Biol*; 19(6): 1421-1429

**Kiemer, A.K., Bildner, N., Weber, N.C., and Vollmar, A.M.** (2003) Characterization of heme oxygenase 1 (heat shock protein 32) induction by atrial natriuretic peptide in human endothelial cells. *Endocrinology*; 144(3): 802-812

**Kiemer, A.K., Weber, N.C., and Vollmar, A.M.** (2002) Induction of IkappaB: atrial natriuretic peptide as a regulator of the NF-kappaB pathway. *Biochem Biophys Res Commun*; 295(5): 1068-1076

**Kopp, E. and Ghosh, S.** (1994) Inhibition of NF-kappa B by sodium salicylate and aspirin. *Science*; 265(5174): 956-959

**Kown, M.H., Van der, S.T., Blankenberg, F.G., Hoyt, G., Berry, G.J., Tait, J.F., Strauss, H.W., and Robbins, R.C.** (2000) Zinc-mediated reduction of apoptosis in cardiac allografts. *Circulation*; 102(19 Suppl 3): III228-III232

**Labbe, R.F., Vreman, H.J., and Stevenson, D.K.** (1999) Zinc protoporphyrin: A metabolite with a mission. *Clin Chem*; 45(12): 2060-2072

**Laemmli, U.K.** (1970) Cleavage of structural proteins during the assembly of the head of bacteriophage T4. *Nature*; 227(5259): 680-685

**Lavrovsky, Y., Schwartzman, M.L., Levere, R.D., Kappas, A., and Abraham, N.G.** (1994) Identification of binding sites for transcription factors NF-kappa B and AP-2 in the promoter region of the human heme oxygenase 1 gene. *Proc Natl Acad Sci U S A*; 91(13): 5987-5991

**Lee, D., Long, S.A., Adams, J.L., Chan, G., Vaidya, K.S., Francis, T.A., and others** (2000a) Potent and selective nonpeptide inhibitors of caspases 3 and 7 inhibit apoptosis and maintain cell functionality. *J Biol Chem*; 275(21): 16007-16014

**Lee, P.J., Camhi, S.L., Chin, B.Y., Alam, J., and Choi, A.M.** (2000b) AP-1 and STAT mediate hyperoxia-induced gene transcription of heme oxygenase-1. *Am J Physiol Lung Cell Mol Physiol*; 279(1): L175-L182

**Leist, M. and Nicotera, P.** (1997) The shape of cell death. *Biochem Biophys Res Commun*; 236(1): 1-9

**Lentsch, A.B. and Ward, P.A.** (1999) Activation and regulation of NFkappaB during acute inflammation. *Clin Chem Lab Med*; 37(3): 205-208

- Li, V.G., Wang, J., Traganos, F., Kappas, A., and Abraham, N.G.** (2002) Differential effect of heme oxygenase-1 in endothelial and smooth muscle cell cycle progression. *Biochem Biophys Res Commun*; 296(5): 1077-1082
- Linden, D.J., Narasimhan, K., and Gurfel, D.** (1993) Protoporphyrins modulate voltage-gated Ca current in AtT-20 pituitary cells. *J Neurophysiol*; 70(6): 2673-2677
- Lindenblatt, N., Bordel, R., Schareck, W., Menger, M.D., and Vollmar, B.** (2004) Vascular heme oxygenase-1 induction suppresses microvascular thrombus formation *in vivo*. *Arterioscler Thromb Vasc Biol*; 24(3): 601-606
- Ludwig, S., Hoffmeyer, A., Goebeler, M., Kilian, K., Hafner, H., Neufeld, B., Han, J., and Rapp, U.R.** (1998) The stress inducer arsenite activates mitogen-activated protein kinases extracellular signal-regulated kinases 1 and 2 *via* a MAPK kinase 6/p38-dependent pathway. *J Biol Chem*; 273(4): 1917-1922
- Luo, D. and Vincent, S.R.** (1994) Metalloporphyrins inhibit nitric oxide-dependent cGMP formation *in vivo*. *Eur J Pharmacol*; 267(3): 263-267
- Lutton, J.D., Abraham, N.G., Drummond, G.S., Levere, R.D., and Kappas, A.** (1997) Zinc porphyrins: potent inhibitors of hematopoiesis in animal and human bone marrow. *Proc Natl Acad Sci U S A*; 94(4): 1432-1436
- Maines, M.D.** (1981) Zinc . protoporphyrin is a selective inhibitor of heme oxygenase activity in the neonatal rat. *Biochim Biophys Acta*; 673(3): 339-350
- Maines, M.D.** (1997) The heme oxygenase system: a regulator of second messenger gases. *Annu Rev Pharmacol Toxicol*; 37:517-554
- Maines, M.D. and Trakshel, G.M.** (1992) Differential regulation of heme oxygenase isozymes by Sn- and Zn-protoporphyrins: possible relevance to suppression of hyperbilirubinemia. *Biochim Biophys Acta*; 1131(2): 166-174
- Marin, V., Kaplanski, G., Gres, S., Farnarier, C., and Bongrand, P.** (2001) Endothelial cell culture: protocol to obtain and cultivate human umbilical endothelial cells. *J Immunol Methods*; 254(1-2): 183-190
- Marks, G.S., Brien, J.F., and Nakatsu, K.** (2003) What role does the heme--heme oxygenase--carbon monoxide system play in vasoregulation? *Am J Physiol Regul Integr Comp Physiol*; 285(3): R522-R523
- McCoubrey, W.K., Jr., Huang, T.J., and Maines, M.D.** (1997) Isolation and characterization of a cDNA from the rat brain that encodes hemoprotein heme oxygenase-3. *Eur J Biochem*; 247(2): 725-732
- McEver, R.P., Beckstead, J.H., Moore, K.L., Marshall-Carlson, L., and Bainton, D.F.** (1989) GMP-140, a platelet alpha-granule membrane protein, is also synthesized by vascular endothelial cells and is localized in Weibel-Palade bodies. *J Clin Invest*; 84(1): 92-99

- Meffert, M.K., Haley, J.E., Schuman, E.M., Schulman, H., and Madison, D.V.** (1994) Inhibition of hippocampal heme oxygenase, nitric oxide synthase, and long-term potentiation by metalloporphyrins. *Neuron*; 13(5): 1225-1233
- Menger, M.D. and Vollmar, B.** (1996) Adhesion molecules as determinants of disease: from molecular biology to surgical research. *Br J Surg*; 83(5): 588-601
- Mislick, K.A. and Baldeschwieler, J.D.** (1996) Evidence for the role of proteoglycans in cation-mediated gene transfer. *Proc Natl Acad Sci U S A*; 93(22): 12349-12354
- Morris, G.M., Goodsell, D.S., Halliday, R.S., Huey, R., Hart, W.E., Belew, R.K., and Olson, A.J.** (1999) Automated docking using a Lamarckian genetic algorithm and an empirical binding free energy function. *J Comput Chem*; 19(14): 1639-1662
- Muller, W.A.** (2003) Leukocyte-endothelial-cell interactions in leukocyte transmigration and the inflammatory response. *Trends Immunol*; 24(6): 327-334
- Murono, S., Yoshizaki, T., Sato, H., Takeshita, H., Furukawa, M., and Pagano, J.S.** (2000) Aspirin inhibits tumor cell invasiveness induced by Epstein-Barr virus latent membrane protein 1 through suppression of matrix metalloproteinase-9 expression. *Cancer Res*; 60(9): 2555-2561
- Needs, C.J. and Brooks, P.M.** (1985) Clinical pharmacokinetics of the salicylates. *Clin Pharmacokinet*; 10(2): 164-177
- Nicholson, D.W., Ali, A., Thornberry, N.A., Vaillancourt, J.P., Ding, C.K., Gallant, M., Gareau, Y., Griffin, P.R., Labelle, M., Lazebnik, Y.A., and .** (1995) Identification and inhibition of the ICE/CED-3 protease necessary for mammalian apoptosis. *Nature*; 376(6535): 37-43
- Nicotera, P. and Melino, G.** (2004) Regulation of the apoptosis-necrosis switch. *Oncogene*; 23(16): 2757-2765
- Otterbein, L.E. and Choi, A.M.** (2000) Heme oxygenase: colors of defense against cellular stress. *Am J Physiol Lung Cell Mol Physiol*; 279(6): L1029-L1037
- Otterbein, L.E., Kolls, J.K., Mantell, L.L., Cook, J.L., Alam, J., and Choi, A.M.** (1999) Exogenous administration of heme oxygenase-1 by gene transfer provides protection against hyperoxia-induced lung injury. *J Clin Invest*; 103(7): 1047-1054
- Pae, H.O., Choi, B.M., Oh, G.S., Lee, M.S., Ryu, D.G., Rhew, H.Y., Kim, Y.M., and Chung, H.T.** (2004) Roles of heme oxygenase-1 in the antiproliferative and antiapoptotic effects of nitric oxide on Jurkat T cells. *Mol Pharmacol*; 66(1): 122-128
- Pan, J. and McEver, R.P.** (1993) Characterization of the promoter for the human P-selectin gene. *J Biol Chem*; 268(30): 22600-22608

- Perez, G., Melo, M., Keegan, A.D., and Zamorano, J.** (2002) Aspirin and salicylates inhibit the IL-4- and IL-13-induced activation of STAT6. *J Immunol*; 168(3): 1428-1434
- Perry, D.K., Smyth, M.J., Stennicke, H.R., Salvesen, G.S., Duriez, P., Poirier, G.G., and Hannun, Y.A.** (1997) Zinc is a potent inhibitor of the apoptotic protease, caspase-3. A novel target for zinc in the inhibition of apoptosis. *J Biol Chem*; 272(30): 18530-18533
- Petit, A., Mwale, F., Zukor, D.J., Catelas, I., Antoniou, J., and Huk, O.L.** (2004) Effect of cobalt and chromium ions on bcl-2, bax, caspase-3, and caspase-8 expression in human U937 macrophages. *Biomaterials*; 25(11): 2013-2018
- Petrache, I., Otterbein, L.E., Alam, J., Wiegand, G.W., and Choi, A.M.** (2000) Heme oxygenase-1 inhibits TNF-alpha-induced apoptosis in cultured fibroblasts. *Am J Physiol Lung Cell Mol Physiol*; 278(2): L312-L319
- Pfaffl, M.W.** (2001) A new mathematical model for relative quantification in real-time RT-PCR. *Nucleic Acids Res*; 29(9): e45-
- Pierce, J.W., Read, M.A., Ding, H., Luscinskas, F.W., and Collins, T.** (1996) Salicylates inhibit I kappa B-alpha phosphorylation, endothelial-leukocyte adhesion molecule expression, and neutrophil transmigration. *J Immunol*; 156(10): 3961-3969
- Pileggi, A., Molano, R.D., Berney, T., Cattan, P., Vizzardelli, C., Oliver, R., Fraker, C., Ricordi, C., Pastori, R.L., Bach, F.H., and Inverardi, L.** (2001) Heme oxygenase-1 induction in islet cells results in protection from apoptosis and improved *in vivo* function after transplantation. *Diabetes*; 50(9): 1983-1991
- Pillinger, M.H., Capodici, C., Rosenthal, P., Kheterpal, N., Hanft, S., Philips, M.R., and Weissmann, G.** (1998) Modes of action of aspirin-like drugs: salicylates inhibit erk activation and integrin-dependent neutrophil adhesion. *Proc Natl Acad Sci U S A*; 95(24): 14540-14545
- Ponka, P.** (1999) Cell biology of heme. *Am J Med Sci*; 318(4): 241-256
- Poss, K.D. and Tonegawa, S.** (1997) Heme oxygenase 1 is required for mammalian iron reutilization. *Proc Natl Acad Sci U S A*; 94(20): 10919-10924
- Preston, S.J., Arnold, M.H., Beller, E.M., Brooks, P.M., and Buchanan, W.W.** (1989) Comparative analgesic and anti-inflammatory properties of sodium salicylate and acetylsalicylic acid (aspirin) in rheumatoid arthritis. *Br J Clin Pharmacol*; 27(5): 607-611
- Riedl, S.J., Renatus, M., Schwarzenbacher, R., Zhou, Q., Sun, C., Fesik, S.W., Liddington, R.C., and Salvesen, G.S.** (2001) Structural basis for the inhibition of caspase-3 by XIAP. *Cell*; 104(5): 791-800
- Riedl, S.J. and Shi, Y.** (2004) Molecular mechanisms of caspase regulation during apoptosis. *Nat Rev Mol Cell Biol*; 5(11): 897-907

**Roebuck, K.A., Carpenter, L.R., Lakshminarayanan, V., Page, S.M., Moy, J.N., and Thomas, L.L.** (1999) Stimulus-specific regulation of chemokine expression involves differential activation of the redox-responsive transcription factors AP-1 and NF-kappaB. *J Leukoc Biol*; 65(3): 291-298

**Rotonda, J., Nicholson, D.W., Fazil, K.M., Gallant, M., Gareau, Y., Labelle, M., Peterson, E.P., Rasper, D.M., Ruel, R., Vaillancourt, J.P., Thornberry, N.A., and Becker, J.W.** (1996) The three-dimensional structure of apopain/CPP32, a key mediator of apoptosis. *Nat Struct Biol*; 3(7): 619-625

**Ryter, S.W. and Tyrrell, R.M.** (2000) The heme synthesis and degradation pathways: role in oxidant sensitivity. Heme oxygenase has both pro- and antioxidant properties. *Free Radic Biol Med*; 28(2): 289-309

**Sanders, W.E., Wilson, R.W., Ballantyne, C.M., and Beaudet, A.L.** (1992) Molecular cloning and analysis of *in vivo* expression of murine P-selectin. *Blood*; 80(3): 795-800

**Sardana, M.K. and Kappas, A.** (1987) Dual control mechanism for heme oxygenase: tin(IV)-protoporphyrin potently inhibits enzyme activity while markedly increasing content of enzyme protein in liver. *Proc Natl Acad Sci U S A*; 84(8): 2464-2468

**Sass, G., Soares, M.C., Yamashita, K., Seyfried, S., Zimmermann, W.H., Eschenhagen, T., Kaczmarek, E., Ritter, T., Volk, H.D., and Tiegs, G.** (2003) Heme oxygenase-1 and its reaction product, carbon monoxide, prevent inflammation-related apoptotic liver damage in mice. *Hepatology*; 38(4): 909-918

**Sassa, S. and Nagai, T.** (1996) The role of heme in gene expression. *Int J Hematol*; 63(3): 167-178

**Schleimer, R.P., Sterbinsky, S.A., Kaiser, J., Bickel, C.A., Klunk, D.A., Tomioka, K., Newman, W., Luscinskas, F.W., Gimbrone, M.A., Jr., McIntyre, B.W., and .** (1992) IL-4 induces adherence of human eosinophils and basophils but not neutrophils to endothelium. Association with expression of VCAM-1. *J Immunol*; 148(4): 1086-1092

**Schreiber, E., Matthias, P., Muller, M.M., and Schaffner, W.** (1989) Rapid detection of octamer binding proteins with 'mini-extracts', prepared from a small number of cells. *Nucleic Acids Res*; 17(15): 6419-

**Schwenger, P., Alpert, D., Skolnik, E.Y., and Vilcek, J.** (1999) Cell-type-specific activation of c-Jun N-terminal kinase by salicylates. *J Cell Physiol*; 179(1): 109-114

**Schwenger, P., Bellosta, P., Vietor, I., Basilico, C., Skolnik, E.Y., and Vilcek, J.** (1997) Sodium salicylate induces apoptosis *via* p38 mitogen-activated protein kinase but inhibits tumor necrosis factor-induced c-Jun N-terminal kinase/stress-activated protein kinase activation. *Proc Natl Acad Sci U S A*; 94(7): 2869-2873

**Serfass, L. and Burstyn, J.N.** (1998) Effect of heme oxygenase inhibitors on soluble guanylyl cyclase activity. *Arch Biochem Biophys*; 359(1): 8-16

- Shan, Y., Pepe, J., Lambrecht, R.W., and Bonkovsky, H.L.** (2002) Mapping of the chick heme oxygenase-1 proximal promoter for responsiveness to metalloporphyrins. *Arch Biochem Biophys*; 399(2): 159-166
- Shan, Y., Pepe, J., Lu, T.H., Elbirt, K.K., Lambrecht, R.W., and Bonkovsky, H.L.** (2000) Induction of the heme oxygenase-1 gene by metalloporphyrins. *Arch Biochem Biophys*; 380(2): 219-227
- Smith, K.M. and Falk, J.E.** (1975) Porphyrins and metalloporphyrins. 2<sup>nd</sup> Ed., Amsterdam, NY, *Elsevier Scientific Publ Co*
- Soares, M.P., Lin, Y., Anrather, J., Csizmadia, E., Takigami, K., Sato, K., Grey, S.T., Colvin, R.B., Choi, A.M., Poss, K.D., and Bach, F.H.** (1998) Expression of heme oxygenase-1 can determine cardiac xenograft survival. *Nat Med*; 4(9): 1073-1077
- Springer, T.A.** (1995) Traffic signals on endothelium for lymphocyte recirculation and leukocyte emigration. *Annu Rev Physiol*; 57:827-872
- Stennicke, H.R., Ryan, C.A., and Salvesen, G.S.** (2002) Reprieval from execution: the molecular basis of caspase inhibition. *Trends Biochem Sci*; 27(2): 94-101
- Stennicke, H.R. and Salvesen, G.S.** (1997) Biochemical characteristics of caspases-3, -6, -7, and -8. *J Biol Chem*; 272(41): 25719-25723
- Symon, F.A., Walsh, G.M., Watson, S.R., and Wardlaw, A.J.** (1994) Eosinophil adhesion to nasal polyp endothelium is P-selectin-dependent. *J Exp Med*; 180(1): 371-376
- Tedder, T.F., Steeber, D.A., Chen, A., and Engel, P.** (1995) The selectins: vascular adhesion molecules. *FASEB J*; 9(10): 866-873
- Tegeder, I., Pfeilschifter, J., and Geisslinger, G.** (2001) Cyclooxygenase-independent actions of cyclooxygenase inhibitors. *FASEB J*; 15(12): 2057-2072
- Teifel, M., Heine, L.T., Milbredt, S., and Friedl, P.** (1997) Optimization of transfection of human endothelial cells. *Endothelium*; 5(1): 21-35
- Tenhunen, R., Marver, H.S., and Schmid, R.** (1968) The enzymatic conversion of heme to bilirubin by microsomal heme oxygenase. *Proc Natl Acad Sci U S A*; 61(2): 748-755
- Terry, C.M., Clikeman, J.A., Hoidal, J.R., and Callahan, K.S.** (1998) Effect of tumor necrosis factor-alpha and interleukin-1 alpha on heme oxygenase-1 expression in human endothelial cells. *Am J Physiol*; 274(3 Pt 2): H883-H891
- Thornhill, M.H., Kyan-Aung, U., and Haskard, D.O.** (1990) IL-4 increases human endothelial cell adhesiveness for T cells but not for neutrophils. *J Immunol*; 144(8): 3060-3065

- Tomita, N., Ogihara, T., and Morishita, R.** (2003) Transcription factors as molecular targets: molecular mechanisms of decoy ODN and their design. *Curr Drug Targets*; 4(8): 603-608
- Truong-Tran, A.Q., Carter, J., Ruffin, R.E., and Zalewski, P.D.** (2001) The role of zinc in caspase activation and apoptotic cell death. *Biomaterials*; 14(3-4): 315-330
- Vachharajani, T.J., Work, J., Issekutz, A.C., and Granger, D.N.** (2000) Heme oxygenase modulates selectin expression in different regional vascular beds. *Am J Physiol Heart Circ Physiol*; 278(5): H1613-H1617
- Vane, J.R.** (1971) Inhibition of prostaglandin synthesis as a mechanism of action for aspirin-like drugs. *Nat New Biol*; 231(25): 232-235
- Vane, J.R.** (2000) The fight against rheumatism: from willow bark to COX-1 sparing drugs. *J Physiol Pharmacol*; 51(4 Pt 1): 573-586
- Vartiainen, N., Goldsteins, G., Keksa-Goldsteine, V., Chan, P.H., and Koistinaho, J.** (2003) Aspirin inhibits p44/42 mitogen-activated protein kinase and is protective against hypoxia/reoxygenation neuronal damage. *Stroke*; 34(3): 752-757
- Wagener, F.A., da Silva, J.L., Farley, T., de Witte, T., Kappas, A., and Abraham, N.G.** (1999) Differential effects of heme oxygenase isoforms on heme mediation of endothelial intracellular adhesion molecule 1 expression. *J Pharmacol Exp Ther*; 291(1): 416-423
- Wagener, F.A., Volk, H.D., Willis, D., Abraham, N.G., Soares, M.P., Adema, G.J., and Figdor, C.G.** (2003) Different faces of the heme-heme oxygenase system in inflammation. *Pharmacol Rev*; 55(3): 551-571
- Weber, C., Erl, W., Pietsch, A., and Weber, P.C.** (1995) Aspirin inhibits nuclear factor-kappa B mobilization and monocyte adhesion in stimulated human endothelial cells. *Circulation*; 91(7): 1914-1917
- Weber, N.C., Blumenthal, S.B., Hartung, T., Vollmar, A.M., and Kiemer, A.K.** (2003) ANP inhibits TNF-alpha-induced endothelial MCP-1 expression--involvement of p38 MAPK and MKP-1. *J Leukoc Biol*; 74(5): 932-941
- Weller, A., Isenmann, S., and Vestweber, D.** (1992) Cloning of the mouse endothelial selectins. Expression of both E- and P-selectin is inducible by tumor necrosis factor alpha. *J Biol Chem*; 267(21): 15176-15183
- Widmann, C., Gibson, S., Jarpe, M.B., and Johnson, G.L.** (1999) Mitogen-activated protein kinase: conservation of a three-kinase module from yeast to human. *Physiol Rev*; 79(1): 143-180
- Willis, D., Moore, A.R., Frederick, R., and Willoughby, D.A.** (1996) Heme oxygenase: a novel target for the modulation of the inflammatory response. *Nat Med*; 2(1): 87-90

- Wong, C.K., Zhang, J.P., Lam, C.W., Ho, C.Y., and Hjelm, N.M.** (2000) Sodium salicylate-induced apoptosis of human peripheral blood eosinophils is independent of the activation of c-Jun N-terminal kinase and p38 mitogen-activated protein kinase. *Int Arch Allergy Immunol*; 121(1): 44-52
- Xia, L., Pan, J., Yao, L., and McEver, R.P.** (1998) A proteasome inhibitor, an antioxidant, or a salicylate, but not a glucocorticoid, blocks constitutive and cytokine-inducible expression of P-selectin in human endothelial cells. *Blood*; 91(5): 1625-1632
- Yachie, A., Niida, Y., Wada, T., Igarashi, N., Kaneda, H., Toma, T., Ohta, K., Kasahara, Y., and Koizumi, S.** (1999) Oxidative stress causes enhanced endothelial cell injury in human heme oxygenase-1 deficiency. *J Clin Invest*; 103(1): 129-135
- Yang, G., Nguyen, X., Ou, J., Rekulapelli, P., Stevenson, D.K., and Dennery, P.A.** (2001) Unique effects of zinc protoporphyrin on HO-1 induction and apoptosis. *Blood*; 97(5): 1306-1313
- Yao, L., Pan, J., Setiadi, H., Patel, K.D., and McEver, R.P.** (1996) Interleukin 4 or oncostatin M induces a prolonged increase in P-selectin mRNA and protein in human endothelial cells. *J Exp Med*; 184(1): 81-92
- Yin, M.J., Yamamoto, Y., and Gaynor, R.B.** (1998) The anti-inflammatory agents aspirin and salicylate inhibit the activity of I(kappa)B kinase-beta. *Nature*; 396(6706): 77-80
- Yoo, C.G., Lee, S., Lee, C.T., Kim, Y.W., Han, S.K., and Shim, Y.S.** (2001) Effect of acetylsalicylic acid on endogenous I kappa B kinase activity in lung epithelial cells. *Am J Physiol Lung Cell Mol Physiol*; 280(1): L3-L9
- Zbinden, P., Dobler, M., Folkers, G., and Vedani, A.** (1998) PrGen: Pseudoreceptor Modeling Using Receptor-mediated Ligand Alignment and Pharmacophore Equilibration. *Quant Struct -Act Relat*; 17(2): 122-130
- Zhang, X., Shan, P., Jiang, D., Noble, P.W., Abraham, N.G., Kappas, A., and Lee, P.J.** (2004) Small interfering RNA targeting heme oxygenase-1 enhances ischemia-reperfusion-induced lung apoptosis. *J Biol Chem*; 279(11): 10677-10684
- Zou, W., Zeng, J., Zhuo, M., Xu, W., Sun, L., Wang, J., and Liu, X.** (2002) Involvement of caspase-3 and p38 mitogen-activated protein kinase in cobalt chloride-induced apoptosis in PC12 cells. *J Neurosci Res*; 67(6): 837-843



## 8 APPENDIX



## 8.1 Abbreviations

A	Ampere
AMC	7-amino-4-methyl coumarin
AP-1	activator protein 1
APS	ammonium persulfate
ASA	acetylic salicylic acid
ATP	adenosine-5'-triphosphate
BSA	bovine serum albumine
°C	degree Celsius
CAPS	cyclohexylamino-1-propane sulfonic acid
cGMP	cyclic guanosin-5'-monophosphate
CHAPS	3-[(3-cholamidopropyl)dimethylammonio]-1-propansulfonate
CLSM	confocal laser scanning microscopy
CMV	cytomegalovirus
CoPP	cobalt(III)-protoporphyrin IX
COX	cyclooxygenase
CPRG	chlorophenolred- $\beta$ -D-galactopyranoside
dATP	2'-desoxyadenosine-5'-triphosphate
dCTP	2'-desoxycytosine-5'-triphosphate
dGTP	2'-desoxyguanosine-5'-triphosphate
DEVD	Asp-Glu-Val-Asp
DMSO	dimethylsulfoxide
dn	dominant negative
DNA	desoxyribonucleic acid
dNTP	dATP, dCTP, dGTP or dTTP
DSMZ	Deutsche Sammlung von Mikroorganismen und Zellkulturen
DTT	dithiothreitol
dTTP	2'-desoxythymidine-5'-triphosphate
dUTP	2'-desoxyuracile-5'-triphosphate
<i>E.coli</i>	<i>Escherichia coli</i>
ECs	endothelial cells

EDTA	ethylene diaminetetraacetic acid
EGF	epidermal growth factor
EGTA	ethylene-glycol-O,O'-bis-(2-amino-ethyl)-N,N,N',N',-tetraacetic acid
ELISA	enzyme-linked immunosorbent assay
EMSA	electrophoretic mobility shift assay
FAM	6-carboxyfluorescein
FasL	Fas ligand
FCS	fetal calf serum
FePP	iron(II)-protoporphyrin IX
GAPDH	glyceraldehyde-3-phosphate dehydrogenase
GFP	green fluorescent protein
GITC	guanidine isothiocyanate
GMP-140	granule membrane protein 140
h	hour
HBS	HEPES buffered saline
HEK 293	human embryonic kidney cell line 293
HEPES	N-(2-hydroxyethyl)piperazine-N'-(2-ethanesulfonic acid)
HO	heme oxygenase
HPLC	high performance liquid chromatography
HRP	horseradish peroxidase
hsp	heat shock protein
HUVEC	human umbilical vein endothelial cells
ICAM-1	intercellular adhesion molecule 1
IETD	Ile-Glu-Thr-Asp
Ig-CAM	immunoglobulin-like cell adhesion molecule
IL	interleukin
LPS	lipopolysaccharide
LTR	long terminal repeat
MAPK	mitogen activated protein kinase
MEKK	MAPK kinase kinase
min	minute
MPRE	metalloporphyrin-responsive element
mRNA	messenger RNA

---

NaSal	sodium salicylate
NF- $\kappa$ B	nuclear factor $\kappa$ B
NSAID	nonsteroidal anti-inflammatory drugs
ODN	oligodesoxynucleotides
OSM	oncostatin M
PAA	polyacrylamide
PADGEM	platelet activation dependent granule external membrane protein
PAGE	polyacrylamide gel electrophoresis
PARP	poly-ADP ribose polymerase
PBS	phosphate buffered saline
PCR	polymerase chain reaction
PEI	polyethylenimine
PMSF	phenylmethylsulfonylfluoride
POD	peroxidase
PVDF	polyvinylidenefluoride
RNA	ribonucleic acid
RNase	ribonucleases
ROS	reactive oxygen species
rRNA	ribosomal RNA
RSV	rous sarcoma virus
RT	reverse transcription
SA	salicylic acid
SDS	sodium dodecyl sulfate
SEM	standard error of mean
sGC	soluble guanylyl cyclase
SnPP	tin-protoporphyrin IX
STE	sodium chloride, Tris, EDTA buffer
SV40	simian virus 40
TAMRA	6-carboxytetramethylrhodamine
TBE	Tris, borate, EDTA buffer
TBS-T	phosphate buffered saline with Tween
TE	Tris-EDTA buffer
TEMED	N,N,N',N'-tetramethylethylenediamine

## APPENDIX

---

TNF- $\alpha$	tumor necrosis factor $\alpha$
Tris	Tris-hydroxymethyl-aminomethan
tRNA	transfer RNA
VCAM-1	vascular cell adhesion molecule 1
ZnPP	zinc(II)-protoporphyrin IX
z-VAD-fmk	N-benzyloxycarbonyl-Val-Ala-Asp-fluoromethylketone

## 8.2 Alphabetical order of companies

AGFA	Cologne, Germany
Alexis Biochemicals	Grünberg, Germany
Amersham	Braunschweig, Germany
Bachem	Heidelberg, Germany
BD Biosciences	Heidelberg, Germany
Beckmann Coulter	Krefeld, Germany
Biochrom	Berlin, Germany
Biomers	Ulm, Germany
Bio-Rad Laboratories	Munich, Germany
Biosource	Solingen, Germany
Biozol	Eching, Germany
Braun Biotech	Melsungen, Germany
Calbiochem	Schwalbach, Germany
Cambrex	Verviers, Belgium
Canberra-Packard	Dreieich, Germany
Cell Signaling	Frankfurt/Main, Germany
Clontech	Palo Alto, USA
DakoCytomation GmbH	Hamburg, Germany
Dianova	Hamburg, Germany
Eppendorf	Maintal, Germany
Fluka	Buchs, Switzerland
Fuji	Düsseldorf, Germany
Gibco/Invitrogen	Karlsruhe, Germany
Greiner	Frickenhausen, Germany
Heraeus	Hanau, Germany
Kodak	Rochester, USA
Merck-Eurolab	Munich, Germany
Millipore	Eschborn, Germany
Minerva Biolabs	Berlin, Germany
Molecular Probes/Invitrogen	Karlsruhe, Germany

## APPENDIX

---

MWG-biotech	Ebersberg, Germany
PAA Laboratories	Cölbe, Germany
PAN Biotech	Aidenbach, Germany
PE applied biosystems	Hamburg, Germany
Perkin-Elmer	Überlingen, Germany
Pharmacia Biotech	Heidelberg, Germany
Pierce	Rockford, USA
Promocell	Heidelberg, Germany
Promega	Heidelberg, Germany
Quiagen	Hilden, Germany
Roche Diagnostics	Mannheim, Germany
Roth	Karlsruhe, Germany
Santa Cruz	Heidelberg, Germany
Sigma-Aldrich	Taufkirchen, Germany
Stratagene	Heidelberg, Germany
Stressgen	San Diego, USA
Takara Bio Inc.	Shiga, Japan
Tecan	Crailsheim, Germany
TPP	Trasadingen, Switzerland
Upstate/Biomol	Hamburg, Germany
USB	Cleveland, USA
Zeiss	Oberkochen, Germany

## 8.3 Publications

### 8.3.1 Poster presentations

Blumenthal SB, Kiemer AK, Vollmar AM. Metallo-porphyrines are able to inactivate caspase-3.

45<sup>th</sup> Spring Meeting of the Deutsche Gesellschaft für experimentelle und klinische Pharmakologie und Toxikologie, March 9-11, 2004, Germany.

*Naunyn Schmiedebergs Arch Pharmacol. 2004;369Suppl1:R121*

Kiemer AK, Bildner N, Blumenthal SB, Vollmar AM. Aspirin induces HO-1 in human endothelial cells. Experimental Biology 2003 Annual Meeting, April 11-15, 2003, San Diego, CA, USA.

*FASEB J. 2003; 17(4)*

### 8.3.2 Original Publications

Kiemer AK, Blumenthal SB, Zahler S, Vollmar AM. Heme oxygenase-1: a novel anti-inflammatory target of salicylates in the endothelium

*Manuscript in preparation.*

Blumenthal SB, Kiemer AK, Tiegs G, Seyfried S, Höltje M, Brandt B, Höltje H, Zahler S, Vollmar AM. Metalloporphyrins inactivate Caspase-3 and -8.

*FASEB J, in press.*

Weber NC, Blumenthal SB, Hartung T, Vollmar AM, Kiemer AK. ANP inhibits TNF-alpha-induced endothelial MCP-1 expression - involvement of p38 MAPK and MKP-1.

*J Leukoc Biol.* 2003 Nov;74(5):932-41. Epub 2003 Aug 11.

## 8.4 Curriculum Vitae

### Persönliche Daten

Name:	Blumenthal
Vornamen:	Signe Birgitta
Geburtstag:	23. September 1976
Geburtsort:	München
Staatsangehörigkeit:	deutsch
Familienstand:	ledig

### Hochschule

seit 01/2002	Dissertation zum Dr. rer. Nat in der Arbeitsgruppe von PD Dr. Alexandra K. Kiemer am Lehrstuhl Pharmazeutische Biologie von Frau Prof. Dr. Angelika M. Vollmar, Department Pharmazie, Ludwig-Maximilians-Universität München
Mai 1996 – Okt. 2000	Studium der Pharmazie an der Ludwig-Maximilians-Universität München
Okt. 2000	2. Teil der Pharmazeutischen Prüfung
Aug. 1998	1. Teil der Pharmazeutischen Prüfung
Nov. 1995 – Feb. 1996	Studium der Chemie an der Leopold-Franzens-Universität Innsbruck, Österreich

### Schule

Sept. 1986 – Juli 1995	Gymnasium Vaterstetten
Sept. 1982 – Juli 1986	Grundschule Vaterstetten

**Berufsausbildung und praktische Erfahrungen**

Feb. 2002	3. Teil der Pharmazeutischen Prüfung und Approbation als Apothekerin
Mai 2001 – Nov. 2001	Pharmaziepraktikum an der Universität in Uppsala, Schweden am Lehrstuhl Pharmazeutische Biowissenschaften, Department Biological Research on Drug Dependence von Herrn Prof. Dr. Fred Nyberg
Nov. 2000 – April 2001	Pharmaziepraktikum bei Herrn Dr. Ingolf Ipach, Apotheke am Bahnhof, Vaterstetten
Nov. 1996 – Okt. 1999	Merck-Schuchhardt & Co KG, Hohenbrunn bei München  Administration von Sicherheitsdatenblättern für Chemikalien
März 1997	Famulatur bei Frau Dr. Silke Barfod, Kristall-Apotheke, München
Sept. 1996	Famulatur bei Herrn Dr. Dierk Scheel, Hof-, Stadt- und Rats-Apotheke, Flensburg

## 8.5 Acknowledgements

At first I would like to sincerely thank Prof. Dr. Angelika M. Vollmar for giving me the opportunity to perform this interesting work in her research group. Her trust, encouragement, and continuous and generous support throughout the last years have been very helpful and motivating for me.

I am very grateful to Prof. Dr. Alexandra K. Kiemer for her advice, support, and for always being available for proof-readings and inspiring discussions.

Special thanks go to my thesis committee, especially to Prof. Dr. Ernst Wagner for being co-referee of this work.

I would also like to thank PD Dr. Stefan Zahler for his experienced advice and friendly help, and for proof-reading this work.

Many thanks to Dr. Monika Höltje, Birte Brandt, and Prof. Dr. Hans-Dieter Höltje (Heinrich-Heine-University Düsseldorf) for kindly performing the molecular modeling studies, and to Stefan Seyfried and Prof. Dr. Gisa Tiegs (University of Erlangen-Nuremberg) for kind contribution of the *in vivo* data.

A huge and warm thank you goes to my Dr. "Hasi" Robert Fürst for the awesome and fun time in and outside the lab. I am deeply grateful for his close friendship and for being always on cordial terms for all my moods. I would also like to sincerely thank Melanie Keller, Dr. Stefanie Kulhanek-Heinze, Florian Hoffmann, and Dr. Guido Jürgenliemk for the numerous amusing breaks, great laughs, dubious jokes, and for their friendship. Many thanks to the team of the B 4.074 lab

Elisabeth Grieblinger, Sylvia Bächer, and Anja Koltermann for spending such a pleasant lab time with me and for putting up with our musical taste. A very special thank you to Dr. Rainer Samtleben for sharing his wisdom and experiences and for always having a word of encouragement. Thanks to all former and current members of the PBIII-team, Dr. Anke Förnges, Dr. Nicole Bildner, Florian Hoffmann, Anita Rudy, Dr. Nicole Barth, Dr. Rainer Samtleben, and Uschi Kollmansberger for the great fun and teamwork throughout the student courses. A lot of thanks to Thomas & Thomas for always making me laugh, and a special thank you to Thomas Roos for always helping out with advice about IT issues. Many thanks to Dr. Nicole Barth for helping me to understand the mysteries of real-time PCR. I would also like to thank Brigitte Weiss, Cornelia Niemann, Hanna Stöckl, Rita Socher, and Elfriede Eppinger for helpful technical assistance and kind support. A very big thank you to all members of the research group of Prof. Vollmar for an enjoyable, pleasant, and motivating atmosphere in the group.

After all I want to express my deepest gratitude to my family for their constant encouragement, to my friends simply for being my friends, and to Richard for his calmness and caring support. Thank you so much.